

**MODELING OF TUMOR GROWTH AND
OPTIMIZATION OF THERAPEUTIC PROTOCOL
DESIGN**

KANCHI LAKSHMI KIRAN

B.E.(Hons), National Institute of Technology, Durgapur, India

**A THESIS SUBMITTED
FOR THE DEGREE OF DOCTOR OF PHILOSOPHY
DEPARTMENT OF CHEMICAL & BIOMOLECULAR ENGINEERING
NATIONAL UNIVERSITY OF SINGAPORE**

2011

ACKNOWLEDGMENTS

Firstly, I would like to thank my parents for their love and affection, valuable teachings and their perseverance in making me a responsible global citizen. My parents have been the prime force behind my achievements. I want to dedicate this work to my parents. I am thankful to my brothers, uncle and my late grandparents for their love, concrete support and encouragement.

I am very lucky to be part of the group “Informatics Process Control Unit (IPCU)” under the supervision of Dr. Lakshminarayanan Samavedham (Laksh). I would like to thank Dr. Laksh not only for introducing me to an interesting research discipline but also for his support, encouragement, and mentorship. During my PhD, I was given complete freedom which provided me more opportunities to learn and cherish various phases of my graduate student life. I was allowed to teach graduate and undergraduate students, mentor final year projects of undergraduate students, attend and organize conferences and meetings and lead the activities of Graduate Students Association (GSA). My journey of PhD at NUS has been very adventurous and I feel it is like swimming in an ocean rather than swimming in a pool. I have got everlasting recipe from the thoughtful discussions with Dr. Laksh on several topics for leading a fruitful life.

I would like to thank my senior IPCU members - Balaji, Raghu, Sreenu, Sundar for sharing their invaluable experiences and for their motivation during the budding stage of my PhD which accelerated my research progress. Also, I would like to thank my contemporary IPCU members - Abhay, Naviyn, Logu, Karthik, May Su, Prem, Manoj, Vaibhav, Krishna, Pavan, Kalyan for their professional comments and critique. I carry with me a lot of happy memories of the IPCU lab.

I would like to thank the department for giving me an opportunity to serve as the President of GSA - ChBE. I also would like to extend my sincere thanks to GSA committee members - Sudhir, Sundaramoorthy, Suresh, Abhay, Sadegh, Naviyn, Logu, Hanifa, Vasanth, Niranjani, Shreenath, Anoop, Ajitha, Vamsi, Anji, Srivatsan and Vignesh for their support, cooperation and hope on me as a leader. Moreover, I want to thank all other friends from NUS for their help.

I would like to thank Prof. Farooq and Prof. Feng Si-Shen for their constructive comments and suggestions on my PhD qualifying report and presentation. I also want to thank Prof. Krantz, Dr. Rudiyanto Gunawan, Prof. Rangaiah at NUS, Singapore and Prof. Sundarmoorthy at Pondicherry Engineering college, India for their help and encouragement.

I wish to thank Prof. Vito Quaranta, Vanderbilt University for providing me an opportunity to deliver an invited lecture at Vanderbilt Ingram Cancer Centre, Vanderbilt University.

I would like to thank administrative staff and lab officers of the department for their help during my PhD.

Last but not least, I am very grateful to NUS for providing me precious moments, financial support and a platform for participating in various global programs which led to my allround development.

TABLE OF CONTENTS

	Page
Summary	viii
List of Tables	x
List of Figures	xi
Abbreviations	xiv
Nomenclature	xv
1 Introduction	1
1.1 Motivation	1
1.1.1 Role of process systems engineering in cancer therapy . . .	3
1.2 Cancer statistics	5
1.3 What is cancer ?	6
1.3.1 Different stages of tumor growth	8
1.4 Clinical phases	8
1.4.1 Cancer detection	9
1.4.2 Cancer diagnosis	9
1.4.3 Cancer therapy	10
1.4.4 Emerging and targeted therapies	11
1.5 Our focus - avascular tumor growth	13
1.6 Contributions	14
1.7 Thesis organization	15
2 Literature review	17
2.1 Mathematical modeling of cancer growth	17
2.2 Continuum models	20
2.2.1 Homogenous models	21
2.2.2 Heterogenous models	23
2.2.3 Spatio-temporal models	24
2.2.4 Discrete and hybrid models	32

	Page
2.2.5 Model calibration	33
2.3 Tumor and its interaction with immune system	34
2.3.1 Tumor-immune models	37
2.4 Model-based design of treatment protocols of cancer therapy . . .	38
2.4.1 Pharmacokinetic and pharmacodynamic modeling	39
2.4.2 Optimal control theory (OCT)	40
2.4.3 Description of optimization problem formulation using cancer therapy models	42
2.5 Challenges in the model-based applications	44
2.5.1 Description of the strategy implemented in this thesis work	45
3 Mathematical modeling of avascular tumor growth based on dif- fusion of nutrients and its validation	47
3.1 Introduction	47
3.2 The proposed model	48
3.2.1 Model equations	50
3.3 Model solution	52
3.3.1 Non-dimensionalization of equations	52
3.3.2 Numerical procedure	53
3.4 Model validation and discussion	54
3.4.1 Validation with <i>in vitro</i> data (Freyer and Sutherland, 1986 <i>b</i>)	54
3.4.2 Validation with <i>in vitro</i> data (Sutherland et al., 1986) . . .	59
3.4.3 Comparison with Casciari et al. (1992) model	64
3.4.4 Comparison with parameters of Gompertzian relation based on experimental data (Burton, 1966)	65
3.5 Conclusions	66
4 Sequential scheduling of cancer immunotherapy and chemother- apy using multi-objective optimization	67
4.1 Introduction	67
4.2 Mathematical model	68
4.3 Multi-objective optimization	71
4.3.1 Non-domination set (Pareto set)	72
4.3.2 NSGA-II	72

	Page
4.3.3 Post-Pareto-optimality analysis	74
4.4 Problem formulation	75
4.4.1 Non-dimensionalization	78
4.5 Results and discussion	78
4.5.1 Case 1: Chemotherapy	78
4.5.2 Case 2: Immune-chemo combination therapy	83
4.6 Conclusions	87
5 Model-based sensitivity analysis and reactive scheduling of dendritic cell therapy	89
5.1 Introduction	89
5.1.1 Dendritic cell therapy	90
5.2 Scheduling under uncertainty	91
5.3 Mathematical model	92
5.4 Global sensitivity analysis	94
5.4.1 Theoretical formulation of HDMR	96
5.4.2 RS-HDMR	97
5.5 Results and discussion	99
5.5.1 Uncertainty and sensitivity analysis using HDMR	99
5.5.2 Validation of HDMR results using reactive scheduling	102
5.5.3 Comparison between nominal and reactive schedule for cases 1-3	103
5.5.4 Reactive scheduling of combination therapy and dendritic cell therapy	106
5.6 Conclusions	110
6 Application of scaling and sensitivity analysis for tumor-immune model reduction	112
6.1 Introduction	112
6.2 Mathematical model	113
6.3 Scaling analysis	115
6.3.1 Algorithm	116
6.3.2 Reduced model	117
6.4 Global sensitivity analysis for correlated inputs	120

	Page
6.5 Results and discussion	123
6.5.1 Comparison between original model and reduced model via theoretical identifiability analysis	123
6.5.2 Sensitive parametric groups based on global sensitivity analysis	126
6.5.3 Comparison between original model and reduced model - Pa- rameter estimation	130
6.6 Conclusions	133
7 Population based optimal experimental design in cancer diagnosis and chemotherapy - <i>in silico</i> analysis	135
7.1 Introduction	135
7.2 Mathematical model	138
7.3 Population-based studies	139
7.3.1 Optimal design of experiments for cancer diagnosis	139
7.3.2 Optimal design of chemotherapeutic protocol and post-therapy analysis	144
7.4 Conclusions	150
8 Conclusions and recommendations for future work	152
8.1 Conclusions	152
8.2 Recommendations for future work	157
8.2.1 Validation of the tumor growth models	157
8.2.2 Model-based therapeutic design	157
8.2.3 Multiscale modeling	158
8.2.4 Statistical analysis using clinical data of cancer	162
References	164
Appendix	180
Publications & Presentations	181
Curriculum Vitae	183

SUMMARY

Cancer is a leading fatal disease with millions of people falling victim to it every year. Indeed, the figures are alarming and increasing significantly with each passing year. Cancer is a complex disease characterized by uncontrolled and unregulated growth of cells in the body. Cancer growth can be broadly classified into three stages namely, avascular, angiogenesis and metastasis based on their location and extent of spread in the body. Mechanisms of cancer growth have been poorly understood thus far and considerable resources have been committed to elucidate these mechanisms and arrive at effective therapeutic strategies that have minimal side effects. Mathematical modeling can help in the modeling of cancer mechanisms, to propose and validate hypothesis and to develop therapeutic protocols. This research intends to contribute to this important area of cancer modeling and treatment.

Among these stages, study of avascular stage is quite relevant to the present trend of technology development. Many mathematical models have been developed to comprehend the avascular tumor growth, but the availability of a compendious model is still elusive. This thesis proposes a simple mechanistic model to explain the phenomenon of tumor growth observed from the multicellular tumor spheroid experiments. The main processes incorporated in the mechanistic model for the avascular tumor growth are diffusion of nutrients through the tumor from the microenvironment, consumption rate of the nutrients by the cells in the tumor and cell death by apoptosis and necrosis.

Chemotherapy and immunotherapy are the main focus of this thesis - tumor growth models are integrated with the pharmacokinetic and pharmacodynamic models of therapeutic drugs. The integrated model is used to optimize the therapeutic interventions in order to kill the tumor cells and avert the catastrophic side effects

by effectively leveraging multi-objective optimization and control methods. Furthermore, scaling and sensitivity analysis are applied on the tumor-immune models to screen the dominating mechanisms affecting the tumor growth. Then, the dominant mechanisms are used to test out the aspects of inpatient and outpatient variability. Application of reactive scheduling approach is addressed to nullify the effects of inpatient variability on the therapeutic outcome. Similarly, population-based simulation studies are carried out to design diagnostic and therapeutic protocols and to find the parametric combinations that determine the treatment outcome.

Overall, this thesis showcases the utility and ability of process systems engineering approaches in improving the cancer diagnosis and treatment.

LIST OF TABLES

Table	Page
1.1 Differences between benign and malignant tumors	7
3.1 Parameter values	55
3.2 Maximum volume of multicellular tumor spheroids at different concentrations	58
3.3 Values of the parameter k_1 of Gompertzian empirical relation	65
4.1 Parameter values (Kuznetsov et al., 1994; Martin, 1992)	70
5.1 Parameter values (Piccoli and Castiglione, 2006)	95
5.2 Parameter bounds	99
5.3 Variation of accuracy with sample size and relative error	101
5.4 Parameter ranking (R)	101
5.5 Variation of key parameters	107
6.1 Parameter values	116
6.2 Parametric groups	118
6.3 Values of dimensionless coefficients	119
6.4 Scale factors of rate of change of the scaled states	119
6.5 Relative importance of parameter groups (Π_i) based on S_{p_j} using HDMR model	128
6.6 Structural sensitivity indices ($S_{p_j}^a$) for the key parameters	128
6.7 Comparison of confidence regions between original and reduced models	132
6.8 Closeness between parameter estimates and “true” values	132

LIST OF FIGURES

Figure	Page
1.1 Change in death rates of different diseases in US from 1950 to 2003	4
1.2 Clinical phases of cancer treatment	9
2.1 Publications on tumor microenvironment during 1995-2008	18
2.2 Different spatial scales in tumor growth studies	20
2.3 Classification of tumor growth models	21
2.4 Functional models	24
2.5 Classification of immune actions	35
2.6 Description of different immune actions	37
2.7 Metrics of PK-PD modeling	41
2.8 Strategy followed in this thesis	46
3.1 Different zones in avascular tumor growth	48
3.2 Tumor growth curves of simulated and experimental data at 16.5 $mmol/L$ glucose and 0.28 $mmol/L$ oxygen	56
3.3 Quiescent and necrotic radius at different tumor radius during its growth at 16.5 $mmol/L$ glucose and 0.28 $mmol/L$ oxygen	56
3.4 Tumor growth curves of simulated and experimental data at 16.5 $mmol/L$ glucose and 0.07 $mmol/L$ oxygen	57
3.5 Quiescent and necrotic radius at different tumor radius during its growth at 16.5 $mmol/L$ glucose and 0.07 $mmol/L$ oxygen	57
3.6 Profile of partial pressure of oxygen (PO_2) in the HT29 spheroids when its diameter is 1039 μm	60
3.7 Profile of partial pressure of oxygen (PO_2) in the HT29 spheroids when its diameter is 1116 μm	60
3.8 Profile of partial pressure of oxygen (PO_2) in the HT29 spheroids when its diameter is 1169 μm	61
3.9 Profile of partial pressure of oxygen (PO_2) in the HT29 spheroids when its diameter is 1415 μm	61
3.10 Profile of partial pressure of oxygen (PO_2) in the HT29 spheroids when its diameter is 2077 μm	62

Figure	Page
3.11 Profile of partial pressure of oxygen (PO_2) in the HT29 spheroids when its diameter is $2156 \mu m$	62
3.12 Profile of partial pressure of oxygen (PO_2) in the HT29 spheroids when its diameter is $2314 \mu m$	63
3.13 Variation of partial pressure of oxygen (PO_2) at the centre of the HT29 spheroids with the increase in its diameter	63
3.14 Comparison between the proposed model and Casciari et al. (1992) model on the basis of variation of oxygen concentration at the centre of the EMT6/Ro spheroids with the increase in its diameter	64
4.1 Schematic representation of NSGA-II	73
4.2 L_2 norm method	74
4.3 Schematic representation of the problem	75
4.4 Comparison between original and non-dimensionalized model	79
4.5 Algorithm to find the optimal compromise solution	79
4.6 Pareto solutions for the problem formulation for case 1 (i.e. only chemotherapy)	80
4.7 Comparison of evolution of states between cluster 1 and cluster 2	81
4.8 Evolution of states corresponding to the proposed treatment protocol of doxorubicin	81
4.9 Reduced representation of Pareto solutions for the problem formulation for case 2 (i.e. combination therapy)	84
4.10 Treatment protocol corresponding to the proposed combination therapy	85
4.11 Evolution of states corresponding to the proposed combination therapy	85
4.12 Comparison of tumor relapse time between the proposed chemotherapy and the proposed combination therapy	86
5.1 Dendritic cell/Vaccine therapy	90
5.2 Comparison between nominal and reactive schedule when parameters are not varied	104
5.3 Comparison between nominal and reactive schedule when key parameters are varied	104
5.4 Comparison between nominal and reactive schedule when non-key parameters are varied	105
5.5 Comparison of α value for the three cases	105

Figure	Page
5.6 Evolution of tumor for different therapy cases	109
5.7 Reactive schedule of dendritic cell therapy	109
5.8 Comparison of total dosage between reactive scheduling and nominal scheduling	110
6.1 Sequential methodology	113
6.2 Comparison of evolution of states between original model and reduced model	120
6.3 Sensitivity indices of the parametric groups	126
6.4 Patterns of HDMR component functions with the variations in key parameters. X-axis: Scaled key parameter values, Y-axis: Scaled values of the component functions	129
7.1 Determination of diagnostic protocol (D_i) for a patient population based on information index (I_i) evaluated using the mathematical model	137
7.2 Post - therapy analysis using statistical modeling to find the rules determining the therapeutic effect on a patient	137
7.3 Pareto solution (problem formulation A) corresponding to population based design of diagnostic protocol	143
7.4 Proposed sampling times of tumor, CD8+ T-cells and interleukin during diagnosis	143
7.5 Pareto solution (problem formulation B) corresponding to population based design of treatment protocol	146
7.6 Proposed treatment protocol for the considered patient cohort	148
7.7 Tumor evolution in different patients	148
7.8 Rules to determine the success of proposed treatment protocol on the population	149
8.1 Application of this thesis work in the clinical practice	156
8.2 A multiscale framework for comprehending cancer using OMICS data	161
8.3 Identification of diagnostic features and the prediction of therapeutic design using clinical data	162

ABBREVIATIONS

DZM	Different zone model
MZM	Mixed zone model
MCTS	Multicellular tumor spheroids
MAT	Monoclonal antibody therapy
ACT	Adoptive-cell-transfer therapy
AUC	Area under the curve
PK	Pharmacokinetic
PD	Pharmacodynamic
OMM	Oxygen microelectrode measurements
MOO	Multi-objective optimization
GA	Genetic algorithm
NSGA	Non-dominated sorting genetic algorithm
TRT	Tumor relapse time
DC	Dendritic cells
DCV	Dendritic cell vaccine
GSA	Global sensitivity analysis
VBM	Variance based methods
HDMR	High dimensional model reduction
EFAST	Extended fourier amplitude sensitivity tests
RS-HDMR	Random sampling - High dimensional model reduction
FIM	Fisher information matrix

NOMENCLATURE

Chapter 2

N	Tumor cells
N_0	Initial number of tumor cells
k	Proliferation rate constant
θ	Carrying capacity of tumor size
α	Parameter which determines whether the saturated tumor size is attained quickly or slowly
P, Q, D	Densities of proliferating cells, quiescent cells, dead cells
k_{pp}	Proliferation rate of proliferating cells
$k_{pq}, k_{qp}, k_{pd}, k_{qd}$	Transformation rate constant
λ	Decay rate of dead cells
$C_i(r, t)$	Concentration distribution of the diffusible chemicals
$R(t)$	The position of the outer tumor radius
$R_q(t)$	The locus of the boundary separating proliferating and quiescent cells
$R_n(t)$	The locus of the boundary separating quiescent and necrotic cells
D_i	Diffusion coefficient
ϕ_i	Volume fraction of cell type in a given phase
v_i	Velocity of cell type in a given phase
$\lambda_i(\phi_i, C_i)$	Chemical and phase dependent production
$C(t)$	Therapeutic drug
$X(t)$	State variables
$U(t)$	input or control or manipulated variables

Chapter 3

$C_i(t)$	Concentration of nutrients (Oxygen or Glucose)
$R(t)$	The position of the outer tumor radius
$R_q(t)$	The locus of the boundary separating proliferating and quiescent cells
$R_n(t)$	The locus of the boundary separating quiescent and necrotic cells
A	Proliferation rate constant
A_p	Apoptosis rate constant
N_e	Necrotic rate constant
$C_{i\infty}$	Concentration of the nutrient at the tumor surface
D_1	Diffusivity of glucose
C_{1c}	Critical concentration of glucose
μ_1	Maximum consumption rate of glucose
K_1	Michaelis-Menten constant for glucose
D_2	Diffusivity of oxygen
C_{2c}	Critical concentration of oxygen
μ_2	Maximum consumption rate of oxygen
K_2	Michaelis-Menten constant for oxygen
ν	Volume of the tumor
ν_0	Initial volume of the tumor
k_1, k_2	Gompertzian parameters

Chapter 4

$E(t)$	Effector cells
$T(t)$	Tumor cells
$M(t)$	Chemotherapeutic drug
N	Number of therapeutic interventions
t_f	Stipulated course period

N_e Number of interventions of effector cells

Chapter 5

$H(t)$ Helper T-cells

$C(t)$ Cytotoxic T-cells

$M(t)$ Tumor cells

$D(t)$ Dendritic cells

$I(t)$ Interleukin

V_f Variance of the model output

V_i, V_{ij} Partial variances of the inputs

S_i, S_{ij} Sensitivity indices

G Model output

P Parameter set

u_1 Input rate of dendritic cells

u_2 Input rate of interleukin

Chapter 6 & 7

T Tumor cells

N Natural killer cells

L Cytotoxic T-cells

C Circulating lymphocytes

I Interleukin

M Doxorubicin

U Input rate of doxorubicin

O Model output

G_i Sensitivity matrix

J_c Joint confidence interval

ψ_1 Significance level

Π_i Parametric groups

α_i time derivative scale factors

T_s, N_s, L_s, C_s, M_s Scale factors

n_{P1}, n_{P2} population size

Chapter 1

INTRODUCTION

'Growth for the sake of growth is the ideology of the cancer cell.'

- Edward Abbey

1.1 Motivation

The global challenge driving the oncology community is to understand and exploit the complex nature of cancer growth to discover specific diagnostic indices and treatment protocols for anti-cancer drugs. This challenge demands conducting laboratory and clinical experiments for the collection of informative data. The aggregated knowledge from the experiments and clinical experiences must then be translated into promising therapies and used in P4 (preventive, proactive, participatory and personalized) medicine. Presently, cancer diagnostic and treatment protocols are suggested based on the knowledge generated from clinical trials involving particular cohort of patients, but are applied on other patient groups as well (Kleinsmith, 2005). Also, for a given treatment protocol only few patients may be cured and others may not. Variability in patient outcomes is one of the practical challenges of the existing and emerging therapeutic protocols. Variability can be broadly classified as interpatient and inpatient variability. Interpatient variability is the difference in effect of therapy (target or side effects) on different patients. On the other hand, inpatient variability is the variations that occur in a given patient during the treatment course. In fact, it is necessary to know the reason behind the variability of the effect of diagnostic and treatment protocols on the patients, so that the protocols can be tailored appropriately to individual patients or patient

groups. It is to be noted that experiments that can elucidate the reasons for inter- and inpatient variability are costly and time-consuming. The objectives of any therapy are to minimize the total number of cancer cells by maintaining it below the lethal level while minimizing the side effects. Keeping this in view, the main challenge is to find a way for the clinical implementation of novel and combinatorial therapies. FDA approval is needed before any clinical implementation - the whole process of discovery, laboratory trials and approval can take several years. According to recent studies, the cost involved in the research and development of a new drug for Food and Drug Administration (FDA) approval is between US \$ 500 million and US \$ 800 million and the development time is around 10-12 years. For example, Dendreon took around 18 years to get FDA's approval and around US \$ 750 million was invested. A lot of *in vitro/in vivo* experiments should be performed to clear the different phases of FDA approval and understand the side effects, efficacy and the variability of the therapy (Lord and Ashworth, 2010). In this context, *in silico* (computer) based tools may help to investigate the fundamentals of cancer growth and unique features of a given therapy and its protocols. Even FDA has recognized and encouraged the population based pharmacokinetic and pharmacodynamic modeling studies to ease the approval of new drugs with lesser number of experiments. In this regard, Gatenby (1998) states that 'recent research in tumor biology, particularly that using new techniques from molecular biology, has produced information at an explosive pace. Yet, a conceptual framework within which all these new (and old data) can be fitted is lacking'. Gatenby and Gawlinski (2003) stress the point that clinical oncologists and tumor biologists possess virtually no comprehensive theoretical model to serve as a framework for understanding, organizing and applying the data and emphasize the need to develop mechanistic models that provide real insights into critical parameters that control system dynamics. Murray (2002) states that 'the goal is to develop models which capture the essence of various interactions allowing their outcome to be more fully understood'. Tiina et al. (2007) presented the results of a search in the PubMed bibliographic database which shows

that, out of 1.5 million papers in the area of cancer research, approximately 5% are related to mathematical modeling. According to Byrne (1999), effective and efficient treatment modalities can be developed by identifying the mechanisms which control the cancer growth. Thus, once we understand the mechanism, the key components of it can be modified to eliminate (or reduce pain arising from) the disease. This state of knowledge may be possibly reached through laboratory experiments alone, but at the cost of infinite time and numerous (replicated) experiments. However, the achievement of this goal can be speeded up through the application of process systems engineering techniques (Mathematical modeling, Control theory and Optimization) to describe different aspects of solid tumor growth in the absence or presence of anti-cancer agents. This implies that sound and robust tools are essential in order to investigate the fundamentals of cancer growth and unique features of a given therapy and its protocols.

1.1.1 Role of process systems engineering in cancer therapy

Mathematical modeling and simulation is a versatile tool in comprehending the system behavior and has been used for different applications in natural science and engineering disciplines (Quarteroni, 2009). A mathematical model is an abstraction of a process system. It is composed of model equations and parameters. Usually, available experimental data is used for estimating the model parameters and for validating its prognostic ability. Then, parametric analysis (sensitivity analysis with respect to parameters) of the model is performed to understand the domain and variations of the system behavior with the variation in the parameters (Rodrigues and Minceva, 2005). With understanding of the system and a valid model, one can pursue model based process control and optimization (Edgar et al., 2001). In a similar fashion, the applications of the tumor growth modeling are many (Deisboeck et al., 2009). Firstly, cancer growth can be predicted and the main parameters responsible for it can be better understood. Secondly, these models can be combined

with pharmacokinetic and pharmacodynamic models of the therapeutic agents to study their impact on cancer growth (Quaranta et al., 2005). Thus, the combination model can serve as a decision-making tool for planning and scheduling of the different therapies. In addition, interpatient and inpatient variability scenarios can be imitated by perturbing the parameters and optimization techniques can be used to schedule a therapy accordingly. Modeling and *in silico* experiments can provide new insights and offer different possibilities to understand and treat cancer. Experimentalists and clinicians are becoming increasingly aware of the role of mathematical modeling and its value-addition along with medical techniques and experimental approaches in order to accelerate our understanding in distinguishing various possible mechanisms responsible for the tumor growth (Friedrich et al., 2007; Gottfried et al., 2006; Kunz-Schughart et al., 1998; Kunz-Schughart, 1999; Oswald et al., 2007).

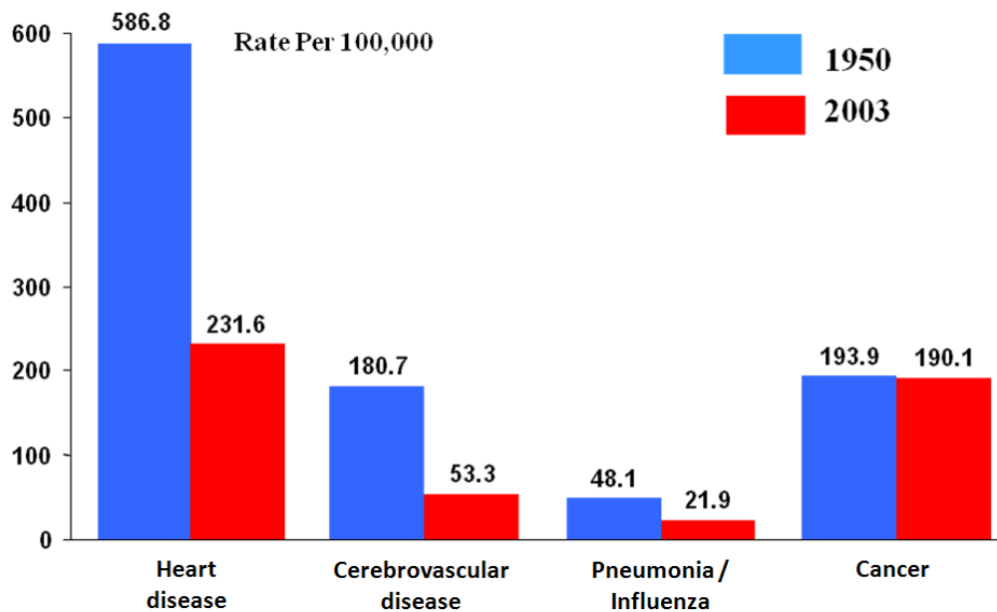


Fig. 1.1. Change in death rates of different diseases in US from 1950 to 2003

1.2 Cancer statistics

The word Cancer (meaning “crab” in Latin) was introduced by Hippocrates in the 5th century BC to explain a group of diseases resulting from the abnormal growth and spread of tissues to the other parts of the body and ultimately proving fatal. Even though cancer has subsisted for a very long time, its existence is noticeably increasing during the last 50 years. As of now, the probability that a randomly selected person will get cancer has almost doubled when compared to 1950s (Klein-smith, 2005). Cancer stands next only to heart disease in the list of most fatal diseases in the world. From Figure 1.1, it is obvious that the decrease in death rate of cancer patients over the years 1950-2003 has been minimal as compared to other major diseases. Cancer related deaths have been escalating meteorically - according to the World Health Organization (WHO), 7.6 million people died of cancer (out of 58 million deaths overall) in 2008. They speculated that cancer deaths will increase to 18% and 50% by 2015 and 2030 respectively. Recently, the American Cancer Society (ACS) reported that around 1.6 million new cancer cases and 0.6 million cancer death cases occurred in the US in 2009. According to another report on worldwide cancer rates by the WHO’s International Agency for Research on Cancer (IARC), North America leads the world in the rate of cancers diagnosed in adults, followed closely by Western Europe, Australia and New Zealand. In Britain, it was estimated using 2008 data that more than one in three were expected to develop the disease over their survival period ¹. According to Cancer Council Australia, around 114,000 new cases of cancer were diagnosed in Australia in 2010 and it was estimated that one in two Australians will be diagnosed of cancer by the age of 85. Cancer deaths in Singapore reflected the global trend (27.1% of total deaths) during the period 1998-2002 and approximately 49,400 new cases of cancer were diagnosed during the period 2005-2009 ². The reasons for such alarming trends include the

¹<http://info.cancerresearchuk.org/cancerstats/incidence/risk/>

²http://www.nrdo.gov.sg/uploadedFiles/NRDO/Cancer_Trends_Report%20.05-09.pdf

non-availability of definite therapy for all types of cancer and the indeterminate nature of the existing therapies for patients with same type of cancer.

The above mentioned figures have drawn the attention of researchers to understand the mechanism of cancer and come out with better therapies. In this effort, remarkable progress has been made in the past few decades in uncovering some of the cellular and molecular mechanisms leading to cancer and the cumulative information reveal that around 100 types of cancer exist. Their names are distinguished from one another on the basis of its location and the cell type involved. Based on the gravity of the cancer problem, Perumpanani (1996) remarks that ‘the research community has taken on the challenge posed by cancer on a war-footing and this has in recent years resulted in an explosion in our understanding of cancer’. Some researchers claim that the analysis of cancer mechanisms has enhanced our understanding of the normal cells (Alberts et al., 2002; Kleinsmith, 2005). This may lead to many fundamental discoveries in cell biology and broadly benefit the various fields of medicine. Despite the advances made in the understanding of cancer and mechanisms, much remains to be done before the deaths of millions of people due to cancer can be reduced. One main challenge is to be able to understand and exploit the complex nature and multiple stages of tumor growth. Another challenge is to conduct the right laboratory and bedside experiments to collect useful data to extract information regarding the mechanisms of cancer cell behavior.

1.3 What is cancer ?

Cancer is the uncontrolled proliferation of abnormal cells of any tissue or organ in the human body. An abnormal cancer cell evolves from the normal cell due to accumulation of DNA damage - this DNA damage (i.e. genetic mutations in pieces of DNA) makes the cell immortal. The genes transferred from the parents might carry with them an inherent risk or susceptibility to cancer. When such a “normal” but

Table 1.1
Differences between benign and malignant tumors

Trait	Benign	Malignant
Nuclear size	Small	Large
Ratio of nuclear size to cytoplasmic volume	Low	High
Nuclear shape	Regular	Pleomorphic (irregular shape)
Mitotic index	Low	High
Tissue organization	Normal	Disorganized
Differentiation	Well differentiated	Poorly differentiated
Tumor boundary	Well defined	Poorly defined

“risk prone” cell is exposed to external factors such as UV radiation, carcinogenic chemicals etc., it could undergo a series of genetic mutations and transform into a cancerous cell. Mutations cause the cell to evade cell death and grow improperly with or without growth signals from the environment (Hanahan and Weinberg, 2000; Martins et al., 2007). Once the cancer cell is formed, it searches for nutrients from the nearby tissues and proliferates rapidly compared to the adjacent normal cells (Tiina et al., 2007). The induced mutation by the external factors not only enhances the proliferation rate of the cells but also decreases its death rate by down-regulating and up-regulating the tumor suppressor genes and oncogenes respectively (Hanahan and Weinberg, 2000). Over time, this results in the formation of a clump of cells known as neoplasm or tumor. Tumor growth is based upon conditions like tumor location, cell type, and nutrient supply. On the basis of the growth pattern, tumors are classified into two fundamental groups. One group is *benign tumors* whose growth is narrowed to a local area and are composed of well-differentiated cells. The other one is *malignant tumors* which can invade the nearby tissues, migrate to other parts of the body and their cells are poorly differentiated. The differences in the microscopic appearance of the *benign* and *malignant* tumors are tabulated in Table 1.1.

1.3.1 Different stages of tumor growth

Generally, the overall cancer growth is categorized into three stages namely avascular, angiogenesis and metastasis (Tiina et al., 2007). In avascular stage, the tumor growth is localized and nutrients are consumed from the nearby tissues. At this stage, the tumor is known as benign tumor as it is not life-threatening and its growth rate is usually slower than that in the other two later stages. Initially, avascular tumors get adequate nutrients and the cells flourish. As time proceeds, the avascular tumor growth rate reduces and reaches saturation size due to insufficient nutrition supply to the innermost cells in the tumor. Then, the nutrient-deficient tumor cells signal the nearby blood vessels about their nutrient requirement leading to the second stage called angiogenesis. Consequently, the tumor develops association with the blood vessels in its proximity. Subsequently, the tumor cells loosen and the cell debris flows through the connected blood vessels. The tumor cells can thus migrate from their origin to the other parts of the body resulting in the final stage called metastasis. After metastasis, the patient will be left with multiple tumors in the body (Kleinsmith, 2005), because the migrated cancer cells invade the other parts of the body via repetition of the above mentioned growth phases. At the angiogenesis and metastasis stage, the tumor grows very randomly as well as rapidly and is quite malignant. Treatment, at this stage, becomes quite complicated and often unfruitful. Hence, the early detection of tumor in avascular stage enables cancer cure with higher probability.

1.4 Clinical phases

The common phases any cancer patient undergoes are detection, diagnosis and administration of therapy (Figure 1.2). A multidisciplinary team comprising of specialized clinicians, pathologists, radiologists, pharmacists, nurses, general practi-



Fig. 1.2. Clinical phases of cancer treatment

tioners is involved in the different phases (Airley, 2009). Experts advise for regular screening tests, so that any cancer (if present) can be detected at an early stage.

1.4.1 Cancer detection

There are various detection routes for different cancers which are broadly classified as physical examination tests, laboratory tests, imaging techniques and visual examination test. Physical examination tests include extraction of cells from the tumor site (e.g. pap smear for cervical cancer). Imaging techniques such as mammography, magnetic resonance imaging, ultrasonography, positron emission tomography are generally used to detect breast tumor. In some of these techniques, high energy radiations are employed to generate pictures of internal tissues and facilitating the recognition of the abnormal tissue region(s). Similarly, in the laboratory tests, cancer prone proteins are measured from the blood sample (e.g. the concentration of prostate-specific antigen (PSA) for prostate cancer). In the visual examination such as colonoscopy for colorectal cancer, a slender, flexible and optical fibre tube is inserted in the region and devices attached to the tube are used to visualize and locate the abnormal tissues (Airley, 2009; Kleinsmith, 2005).

1.4.2 Cancer diagnosis

Detection procedures address the sign of cancer. However, the positive results in the detection step do not mean the presence of cancer. Hence, they are followed by diagnostic examinations for the confirmation of cancer. Diagnosis also includes

quantification of cancer characteristics. In this regard, it requires the biopsy specimen extracted from the tumor site. Microscopic and pathological studies are performed to grade the tumor based on distinctive features such as cell morphology, mitotic index and doubling time. Mitotic index indicates the percentage of dividing cells whereas doubling time implies the rate of division. Further, the tumor staging is determined based on different criteria: (a) the size of the localized tumor and its spread to the nearby tissues, (b) the extent of spread to the regional lymph nodes and (c) the extent of spread to the distant parts (metastasis). This kind of staging is known as TNM staging where T, N, M stands for tumor, lymph node and metastasis respectively. Additionally, biochemical tests of the molecular components of the cells may figure out gene or proteins expressed in the tumor which will serve as biomarkers or prognostic indicators. For example, estrogen receptor is an indicator of breast cancer prognosis. The information about tumor grading, staging concluded from pathological and radiological data, patient's blood cell count and his/her historical health record, are referred for suggesting a particular therapy or combination of therapies. Then, it is the role of oncology pharmacists to monitor and prepare the therapy. Presently, they use their clinical and pharmaceutical expertise in designing the treatment plan for an individual. The freedom of attempting intuitive ideas regarding therapeutic inputs in designing cancer therapy is very less and it demands foolproof evidence owing to ethical constraints.

1.4.3 Cancer therapy

Research efforts over the last hundred years has resulted in the development of many treatment modalities. The most common of these are surgery, chemotherapy, radiation therapy, and immunotherapy (Airley, 2009; Kleinsmith, 2005). However, there is no specific therapy for treating all forms of cancer and each therapy has its own advantages and deficiencies. As a rule, surgery is preferred to remove the tumors provided its location permits surgical intervention. However, all cancer cells

cannot be removed by surgery and hence surgery is usually followed or substituted by chemotherapy and/or radiation therapy. Among these two, chemotherapy is better than radiation therapy because it is a systemic therapy. In systemic therapies, drug circulates in the blood stream and not only kills the residual cancer cells at the tumor site but also annihilates migrated cancer cells. On the contrary, radiation therapy is a localized therapy which is a better option in the early stages of cancer (Shepard et al., 1999). In general, most of the patients undergo chemotherapy at some stage of their treatment. Chemotherapy is administered as a course in cycles based on the health condition of the patient rather than as a one-shot treatment (Airley, 2009). This serves to lessen its side effects and to accomplish the goal of the chemotherapy. The principle of chemotherapy is to recognize and attack the rapidly proliferating cells by restraining DNA replication and by rupturing their DNA. Consequently, it may also damage normal cells that are fast proliferating by nature (e.g. blood cells, cells lining the intestines, colon, cells inside the mouth and throat, cells in hair follicles). Yet another problem is that some cancer cells may acquire mutations which make them resistant to chemotherapy drugs. In this case, even the few drug resistant cancer cells may lead to the invasive growth of the tumor. The side effects of chemotherapy can sometimes be worse than the disease itself. Thus, only chemotherapy as an adjuvant therapy after surgery or as a prime therapy, may not eradicate the tumor completely and may lead to serious side effects. One solution to this challenging issue is the application of combination therapy. In this regard, combining chemotherapy with emerging and targeted therapies such as immunotherapy can be a promising and synergistic option to treat many cancer types (Gabrilovich, 2007; Lake and Robinson, 2005).

1.4.4 Emerging and targeted therapies

Surgery, radiation therapy and chemotherapy either alone or in various combinations are successful only when the tumor is identified in the initial stages. But,

still there are some cancers (pancreas, liver or lungs) which are detected only at their aggressive stages. Now, cancer scientists are putting lot of efforts in developing novel and effective treatment strategies with higher selectivity such that only cancer cells are targeted while sparing the normal cells. Thus, these therapies are known as targeted therapies. These include immunotherapy, gene therapy, and viral therapy. In immunotherapy, the main idea is to identify and extract or engineer the immune cells which are cytotoxic to tumor cells to improve the selectivity and cytotoxicity. Some forms of immunotherapy are Bacillus Calmette-Guerin (BCG) (Bunimovich-Mendrazitsky et al., 2007), cytokine therapy, adoptive cell transfer therapy. In BCG therapy, bacteria are injected into the patients to provoke the immune system and eliminate tumor cells. The success of BCG therapy has been notable in the treatment of early stage bladder cancer. Similarly, in cytokine therapy, cytokines (proteins) are used to stimulate the immune response. This will be discussed elaboratively in the following chapter. Gene therapy exploits the role of oncogenes and tumor suppressor genes in cancer development based on discoveries over the past two decades. In gene therapy, the defective genes are replaced by the normal genes (Mesri et al., 2001). In one form of gene therapy, viruses containing the normal copy of p53 gene (tumor suppressor gene) in their DNA are used to replace the defective p53 gene. Alternatively, in viral therapy, viruses are engineered to recognize the cells with defective p53 gene and kill them. This process is known as lysis. ONYX-015 is one such engineered adenovirus, which replicates swiftly in the defective p53 gene cells and eventually activates the immune response (Zurakowski and Wodarz, 2007). However, these emerging therapies are still in their early phases and demand the computational modeling support to test different hypothesis and expedite the clinical implementation procedures.

1.5 Our focus - avascular tumor growth

There are many reasons for concentrating on avascular tumor growth. The first motivation is the increasing awareness of cancer among people. In the past, cancer was often recognized only at the later stages. But nowadays, based on the health history of their immediate family members, and due to better awareness programs, people become cautious and undergo regular health checkups. Governments, in developing countries, also organize mass health check and screening campaigns. If anything, people will undergo more regular, frequent and possibly cheaper health scans in the future. Thus, diseases such as cancer may be detected earlier rather than later. The second motivation is provided by the advancements in the biomedical field over the past 30 years (Preziosi, 2003), and sophistication of experimental approaches such as imaging and gene sequencing. These advanced techniques can locate tumors even when their size is very small (in the order of $100 \mu m$). As a result, data corresponding to avascular tumor growth should not be a constraining factor in its modeling. Note, however, that it does not mean that avascular stage is the most important. In fact, from a clinical point of view, angiogenesis and metastasis are of equal (if not more) significance and modeling of these stages is also important for designing cancer therapies. As a starting point to comprehend the complexity of all stages of cancer, it will be better to start with a study of the avascular tumor growth study. While avascular tumor growth is simple to model mathematically, it also contains many of the phenomena that are similar to the case of vascular models. Moreover, the reproducibility of experiments with avascular tumor growth is better than with vascular tumors. The experiments of avascular tumor growth can also be done *in vitro* in the form of multicellular tumor spheroids (MCTS) which are quite cheap relative to animal experiments (Freyer, 1988; Freyer and Sutherland, 1986*b,a*; Kunz-Schughart et al., 1998; Kunz-Schughart, 1999; Hlatky et al., 1988*a*; Marusic et al., 1994; Maruic et al., 1994; Mueller-Klieser, 1997, 1987; Oswald et al., 2007). Therefore, the modeling of avascular tumor can be helpful

in making predictions and designing experiments on the advanced stages of cancer as well (Tiina et al., 2007). Research in cancer biology related to avascular tumor growth has provided a vast amount of data through *in vitro* (Freyer, 1988; Freyer and Sutherland, 1986*b,a*) and *in vivo* experiments (Marusic et al., 1994) of different cancer cell lines. Despite this, an appropriate mechanism-based mathematical model for illustrating the tumor growth remains elusive. In the avascular stage, the tumor growth involves the formation of three zones, namely proliferation zone, quiescent zone and necrotic zone. Eventually, in the avascular stage, the tumor reaches a steady size. The cause for the attainment of steady state by the tumor has been hypothesized in different ways. The study of tumor growth and its use for the development of cancer therapies is therefore an important area of research. Its valuable outcomes can provide a helping hand in enhancing the quality of life and increase life span of the cancer patients resulting in social and economic benefits to the world.

1.6 Contributions

The thesis work seeks to address the following issues in the field of *in silico* cancer research.

1. **Mathematical Modeling:** In this research, a mechanistic model is developed for predicting the avascular tumor growth based on microenvironment conditions (moving boundary problem). This work can be useful for tumor pathologists who may wish to categorize the tumor cells into either benign or malignant by estimating the model parameters using tumor growth data.
2. **Optimization, Control:** Tumor growth models are integrated with the pharmacokinetic and pharmacodynamic models of cancer therapeutics and an optimization problem keeping in view the objectives of tumor reduction and

minimization of side effects is formulated. Then, multi-objective stochastic optimization is applied to design an optimal treatment plan.

3. Model reduction, Sensitivity analysis: Many of the unresolved issues in the medical field remain so because they are not data rich. This makes it very difficult to estimate model parameters precisely. Hence, model simplification is an important step in model-based practical applications. In this work, a tumor-immune model is reduced and sensitivity analysis is performed to find the influential parametric groups. This facilitates the use of model based experimental design to design experiments and help experimentalists to generate informative data.
4. Data driven analysis: The main idea is to mimic a veteran oncologist in suggesting standard treatment plan for the cancer patients by employing quantitative approaches. “Patients” are generated by varying the sensitive parameters of the model. The average therapeutic protocol for the generated patient cohort for a given therapy is determined by framing an optimization problem with suitable objectives and constraints. The obtained optimal treatment planning is applied on these patients to study its effect on the tumor evolution during the therapeutic horizon. Later, data driven techniques are used to derive “rules” based on key parameter values that can help predicting success of the therapy on future patients.

1.7 Thesis organization

The second chapter describes different categories of mathematical models used for tumor growth analysis and emphasizes the utility of optimal control theory in designing cancer therapy protocols. Also, the challenges that can be addressed using PSE methodologies and tools are highlighted. In Chapter 3, a new mechanistic model for avascular tumor growth is proposed based on the hypothesis of diffusion

and consumption of nutrients. The proposed model is also validated with data from multicellular tumor spheroid experiments. The application of multi-objective optimization in the sequential scheduling of chemotherapy and immunotherapy for a given “patient” (a tumor-immune-chemo model with known parameters) is the subject of Chapter 4. Chapter 5 is devoted to the issue of inpatient variability and its effect on the treatment outcomes. Particularly, it focuses on the scheduling of dendritic cell therapy under uncertainty using reactive scheduling strategy. The interesting question of quantification of variability using sensitivity analysis is also visited. Chapter 6 projects the usefulness of model reduction in promoting model-based approaches in clinical settings. Model reduction using scaling and sensitivity analysis is exemplified with an example of tumor-immune model. Chapter 7 addresses population based studies (interpatient variability) using reduced tumor-immune model (from Chapter 6) to design diagnostic and therapeutic protocols. Parametric combinations that determine the treatment outcome are also uncovered using a classification tool. In the final chapter (Chapter 8), the key conclusions of the thesis are summarized along with recommendations for future work.

Chapter 2

LITERATURE REVIEW

‘Imagination is more important than knowledge.’

- Albert Einstein

In this chapter, the main focus is on the description of different classes and subclasses of tumor growth models. Models depicting the interaction between tumor cells and immune system are discussed by elaborating on the different mechanisms of immune action. Development of treatment protocols using the combination of tumor growth and pharmacokinetic-pharmacodynamic models is presented. The challenges in deriving ideas from mathematical modeling techniques for clinical implementation are briefly discussed.

2.1 Mathematical modeling of cancer growth

Cancer research is a very good example of multidisciplinary team that includes biologists, clinicians, oncologists, pharmacists, general practitioners, radiologists, mathematicians and engineers. The role of mathematicians and engineers in cancer has been realized only in the recent years even though many mathematical models were developed to expound tumor growth in the last few decades (Anderson and Quaranta, 2008; Byrne, 2010). At the same time, Figure 2.1 shows the increasing trend of number of research articles in the field of tumor microenvironment over the 1995-2008 period (Witz, 2009). According to Anderson and Quaranta (2008), the proposed models can be broadly classified as continuum, discrete and hybrid models based on the scales of the mechanism of interest. Traditionally, tissue and

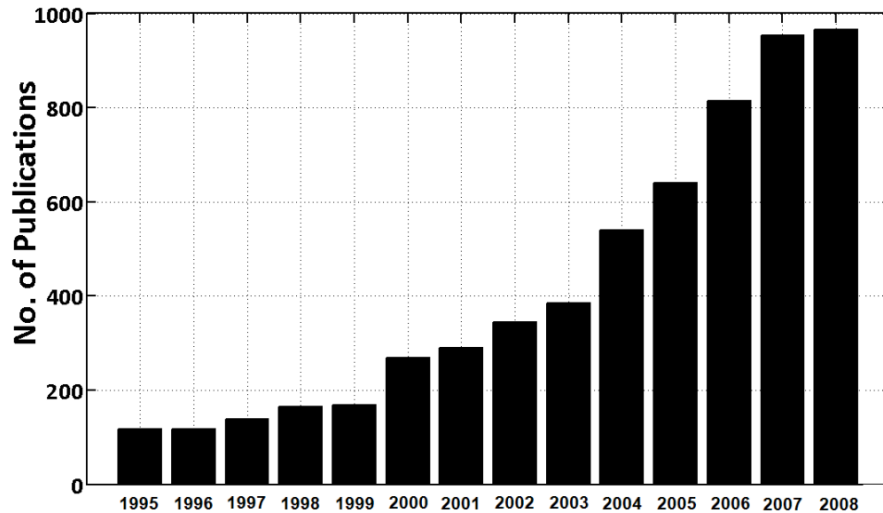


Fig. 2.1. Publications on tumor microenvironment during 1995-2008

cell scale phenomena are studied using continuum and discrete models respectively. Then, hybrid models are introduced in order to understand the effect of cell scale phenomena on the tissue scale. Each type of model has its own advantages and disadvantages.

There are many review articles which provide comprehensive details on the chronological development of mathematical models that deal with different stages of cancer growth (Araujo and McElwain, 2004; Bellomo, Angelis and Preziosi, 2003; Byrne et al., 2006; Lowengrub et al., 2010; Sanga et al., 2007, 2006; Tiina et al., 2007). Araujo and McElwain (2004) presented a comprehensive discussion on the history of studies related to solid tumor growth, illustrating the role of mathematical modeling approaches from the early decades of twentieth century to the present time. This review projected a proper balance between the mathematical models and experimental investigations which have been carried over these years. Such a comprehensive review covering theoretical and experimental domain is indeed useful; otherwise, the mathematical models have no utility by themselves. Overall, their work provided a glimpse on the status and achievements of mathematical modeling of both avascular and vascular tumor growth. It included the models of avascular tumors, multicellu-

lar spheroids, models of tumor invasion and metastasis, as well as that of vascular tumor. Thus, this review provides a general idea of models for tumor growth. The review by Tiina et al. (2007) concentrated exclusively on the models of avascular tumor growth. It discussed the broad classification of the avascular tumor growth models into continuum mathematical models and discrete cell population models. Tiina et al. (2007) pointed out the fact that the hitherto developed mathematical models were very simple as they focused on certain general processes (diffusion of nutrients) that did not fully account for the complexity of the biology and biochemistry of the avascular tumor growth. Another encouraging view from the authors is that mathematical modeling has two-fold applications in cancer biology. On one hand, they can be applied for the verification of hypotheses as suggested by the experimentalist and on the other hand, they provide a framework for predicting the outcomes of other intuitive ideas. They highlighted the impact of mathematical modeling in tumor biology by considering an example under the category of continuum model. This review also included the theory of multiphase models, tissue mechanics models, and discrete models. According to Tiina et al. (2007), the motivation for the discrete models is the advances in biotechnology which makes it feasible to capture data related to phenomena occurring at mesoscopic and microscopic levels (Figure 2.2). This cellular level knowledge is used to obtain information about the macroscale phenomena of tumor growth by using multiscale modeling. Similarly, Lowengrub et al. (2010) have provided a broad classification of models. Specifically, this work has focused on the continuum models, their analysis and model calibration using clinical data to predict tumor morphology and growth. However, the complexity of the models increases significantly by incorporating the updated knowledge of cancer biology at different scales.

By raising this issue of model complexity, Tiina et al. (2007) introduced the parameterization of the models as an important challenge. A well-parameterized model implies that, only from the knowledge of parameter values, we should be able to differentiate the variations in the system behavior. As a simple example, based

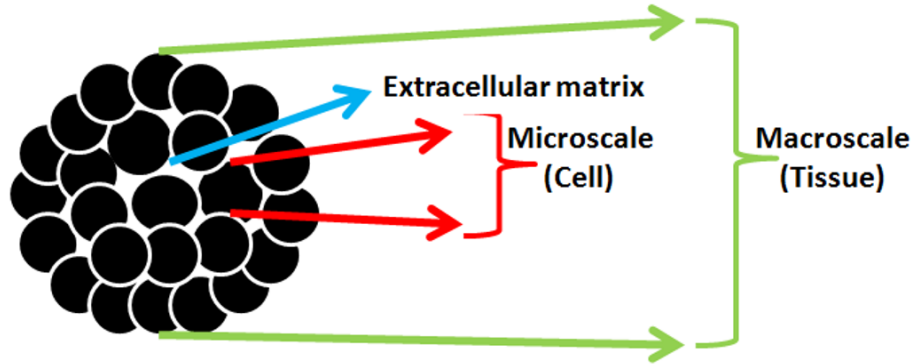


Fig. 2.2. Different spatial scales in tumor growth studies

on the value of Reynolds number (Re), we are able to conclude the characteristics of the flow of a Newtonian fluid through a circular pipe such as laminar ($Re < 2100$) or turbulent ($Re > 2100$). Thus, better parameterized models are the models where the parameters have physical meaning. The key message is that simpler and better parameterized mechanistic models are required and are important as compared to other models that just fit the data.

2.2 Continuum models

Continuum modeling approach is very convenient to study large scale systems. Continuum models are useful once a cell is already transformed to a cancerous cell after undergoing mutations in its genetic code. Tumors are considered as collection of cells in continuum models in which they are described as density or volume fraction of cells. Experimentally, it is observed that transformation in the tumor occur as it progresses and results in the formation of different regions. In continuum models, the rules are framed for different regions of the tumor but not for each and every cell. Thus, individual cells in the tumor cannot be tracked separately. They are usually, described using ordinary, partial differential and integro-differential equations and detail explanation is provided in the later part. The main advantage is that continuum models have fewer parameters and they can be easily estimated from the

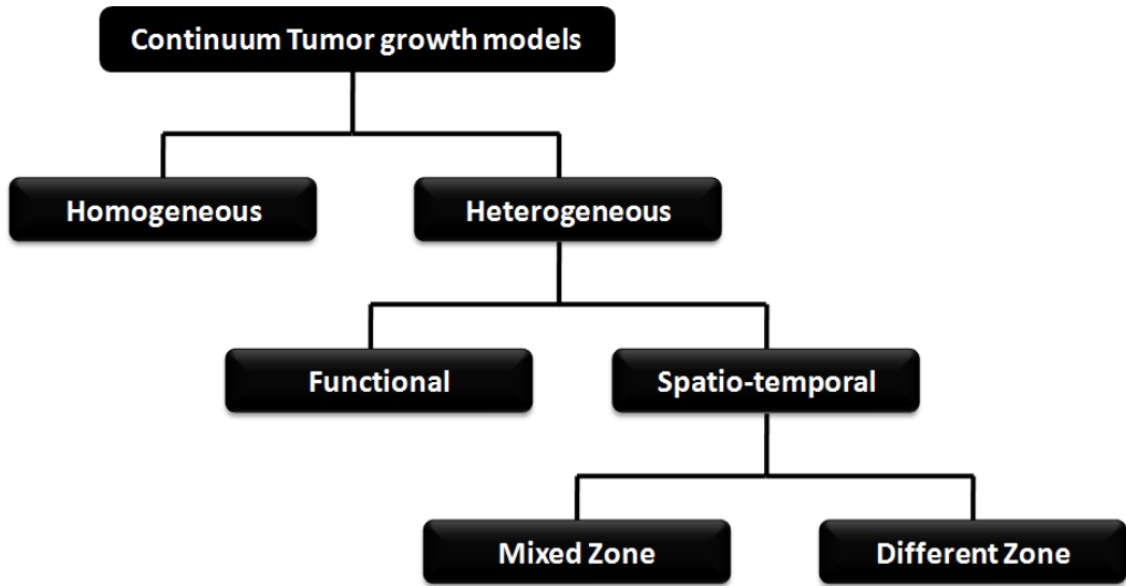


Fig. 2.3. Classification of tumor growth models

available experimental model system like multicellular tumor spheroids. Continuum models are quite relevant to quantify the macroscale tumor behaviour.

Another review chapter by Byrne in Preziosi (2003) is mainly based on earlier valuable contributions (Byrne, 1999, 1997; Byrne and Chaplain, 1998, 1996, 1995; Byrne and Gourley, 1997). This review further narrowed down to the continuum models of the avascular tumor growth. Continuum models for avascular tumor growth can be further classified into two categories: homogeneous and heterogeneous models (see Figure 2.3). These are explained in the next section.

2.2.1 Homogenous models

Homogenous models are those in which all the tumor cells are assumed to be alike and they ignore the spatial effects in explaining the growth dynamics of the tumor growth. These are the earliest models and are formulated as system of differential equations. All homogeneous models are empirical (e.g. exponential model, logistic model, Gompertzian model). These models are data-specific and are unable to shed

light on the inherent mechanisms governing the tumor cells because they are built by data-fitting of *in vitro* and *in vivo* experimental results. Marusic et al. (1994) used the *in vitro* data of multicellular tumor spheroids available for 15 different cell lines (Freyer, 1988) to test several empirical models. *In vivo* tumor growth data obtained by injecting tumor cells from two of the above mentioned cell lines into athymic mice were used to test different empirical models (Marusic et al., 1994). The exponential growth model is the simplest homogenous model in which the total number of cells in the solid tumor increases exponentially with time. In this model, all cells are assumed to receive the nutrients and other growth factors abundantly. This model is quite precise in representing the very early growth of the tumor and is given by Equations (2.1) and (2.2):

$$\frac{dN}{dt} = kN, \quad \text{with } N(t = 0) = N_0, \quad (2.1)$$

$$N(t) = N_0 e^{kt} \quad (2.2)$$

where, $k > 0$ is the net rate at which the cells proliferate, and N_0 represents the initial number of the tumor cells. The exponential model does not capture the decreased growth rate of tumor cells and their attainment of final saturation which are obtained from the *in vitro* and *in vivo* experiments. The decrease in growth rates and final saturation happen because, with the increase in the tumor size, all cells will not have access to same amount of nutrients and growth factors. In order to capture the saturation of tumor size a generalized empirical model is given by Equations (2.3) and (2.4):

$$\frac{dN}{dt} = \frac{k}{\alpha} N \left[1 - \left(\frac{N}{\theta} \right)^\alpha \right], \quad \text{with } N(t = 0) = N_0, \quad (2.3)$$

$$N(t) = \theta \left(\frac{N_0^\alpha}{N_0^\alpha + (\theta^\alpha - N_0^\alpha) e^{-kt}} \right) \quad (2.4)$$

where, θ is the carrying capacity of tumor size and α is a parameter which determines whether the saturated tumor size is attained quickly or slowly. When $\alpha = 1$, the model is called the logistic growth model and when $\alpha \rightarrow 0^+$, the model is called the Gompertzian growth model. In this way many empirical models were fitted to the experimental data, but the parameters of the models could always be related to exact phenomenon of the tumor growth.

2.2.2 Heterogenous models

Functional models are also called as compartmental models or spatially averaged models and they assume that different cell types are in different compartments based on cell kinetics (Preziosi, 2003). Cell kinetics is the transformation of a cell from one phase to another phase depending on the environmental conditions. Based on the availability of nutrients and activity of the cells, there are three types of cells namely proliferating cells, quiescent cells and necrotic cells. Usually, the outer layer of tumor consists of proliferating cells, as they will be getting sufficient nutrients. The cells in the inner layer next to proliferation zone are called the quiescent cells. Quiescent cells do not proliferate but they are alive, because the quantum of nutrient supply reaching them is just able to keep them alive. The innermost zone of the tumor consists of necrotic cells which are dead due to the inadequacy of nutrients. In Piantadosi (1985), the transition between the resting and growing cells is expressed in terms of ordinary differential equations. Furthermore, the model assumes that production of the growing fraction and loss fraction from the resting fraction of cell population follows first order kinetics. Garner et al. (2006) analyzed a simple cell population model to study the long-term behavior of quiescent and proliferating cells. An example of the functional model is shown below (Figure 2.4) for different types of tumor cells.

$$\frac{dP}{dt} = (k_{pp} - k_{pq} - k_{pd})P + k_{qp}Q \quad (2.5)$$

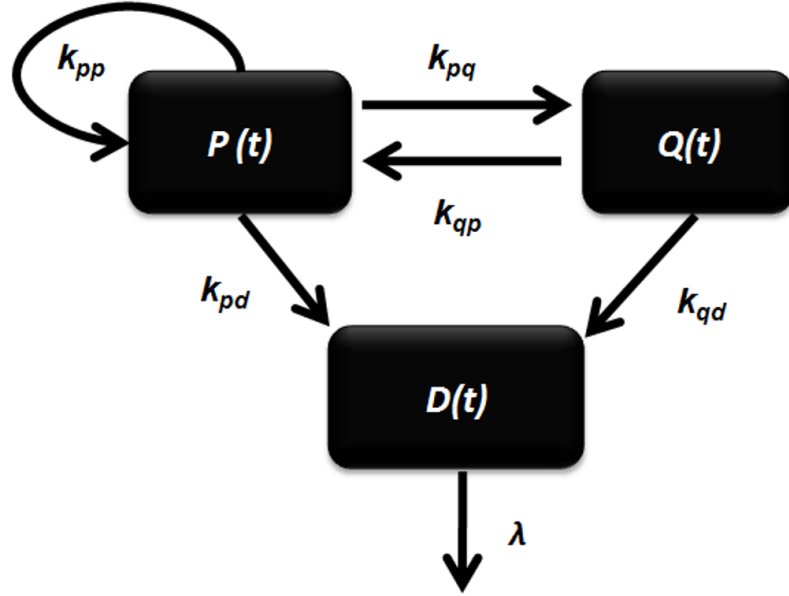


Fig. 2.4. Functional models

$$\frac{dQ}{dt} = k_{pq}P - (k_{qp} + k_{qd})Q, \quad (2.6)$$

$$\frac{dD}{dt} = k_{pd}P + k_{qd}Q - \lambda D \quad (2.7)$$

$P(0) = p_0$, $Q(0) = q_0$, $D(0) = d_0$ where P , Q , D are the densities of proliferating cells, quiescent cells, dead cells respectively and p_0 , q_0 , d_0 are their initial conditions. Although these functional models neglect the spatial effects, they provide insight into the overall growth dynamics of solid tumors. These models can be used for estimating the kinetic parameters from experimental data and to study the response of different therapeutic agents.

2.2.3 Spatio-temporal models

The next class in the heterogeneous model family is spatio-temporal models which relate the variations of different cell types in space and time with nutrient variation. The spatio-temporal models can be further sub-divided into different zone model (DZM) and mixed zone model (MZM). DZM is based on the notion that different types of cells are present in the separate regions of the tumor and they

are separated by boundaries. The goal, then, is to find the position of the interface between the regions spatially and temporally on the basis of the nutrient levels. The motivation for DZMs was from the idea of biologists which focused on the effect of the tumor growth due to variations in the composition of the medium surrounding the tumors. The main measurements made by the biologists in these experiments are: radii of the tumors over time, nutrient distribution within the tumors and the ratio of the radii of different zones in the tumor. Thus, the key variables in these types of models are: $R(t)$, the position of the outer tumor radius of the assumed radially symmetric tumor; $C_i(r, t)$, the concentration distribution of the diffusible chemical (this may be nutrients, anti-cancer drugs, growth inhibitors); $R_q(t)$, the locus of the boundary separating proliferating and quiescent cells; and $R_n(t)$, the locus of the boundary separating the quiescent and necrotic cells. Since the tumor size changes with time, the domains on which the model is formulated also changes and this problem falls in the category of moving boundary problems. The simplest DZM which explains the growth of a radially symmetric, avascular tumor include equations governing the evolution of the important diffusible chemicals $C_i(r, t)$, the outer tumor radius $R(t)$, and the quiescent and necrotic radii $R_q(t)$ and $R_n(t)$. The principle of mass balance is used to derive equations for $C_i(r, t)$ and $R(t)$ where as $R_q(t)$ and $R_n(t)$ are based on the assumption that quiescent and necrotic zone formation is the result of concentration of chemicals (mainly the growth factors) falling below their threshold values. The model equations are stated in both words and in mathematics to clearly emphasize the connection between the underlying physical assumptions and the mathematical formulation.

The chemical concentration, $C_i(r, t)$

$$\left(\begin{array}{c} \text{rate of change of} \\ \text{chemical concentration} \end{array} \right) = \left(\begin{array}{c} \text{flux due to} \\ \text{diffusion} \end{array} \right) - \left(\begin{array}{c} \text{rate of chemical} \\ \text{consumption} \end{array} \right)$$

$$\frac{\partial C_i}{\partial t} = \frac{D_i}{r^2} \frac{\partial}{\partial r} \left(r^2 \frac{\partial C_i}{\partial r} \right) - \Gamma(C_i, R, R_q, R_n) \quad (2.8)$$

In Equation (2.8), D_i denotes the assumed constant diffusion coefficient of the chemical i and $\Gamma(C_i, R, R_q, R_n)$ denotes its rate of consumption or production. In reality, $\Gamma(C_i, R, R_q, R_n)$ is a nonlinear function that depends on the type of cell line and the chemical of interest. In order to observe the behavior of the model, sometimes, only vital chemicals are considered and it is also assumed that their consumption rate is constant or follows some typical trends (Michaelis - Menten).

The outer tumor radius, $R(t)$

$$\begin{pmatrix} \text{rate of change of} \\ \text{tumor volume} \end{pmatrix} = \begin{pmatrix} \text{total rate of cell} \\ \text{proliferation} \end{pmatrix} - \begin{pmatrix} \text{total rate of} \\ \text{cell death} \end{pmatrix}$$

$$\frac{1}{3} \frac{d}{dt} (R^3) = R^2 \frac{dR}{dt} = \int_0^R S(c, R, R_q, R_n) r^2 dr - \int_0^R N(c, R, R_q, R_n) r^2 dr \quad (2.9)$$

In Equation (2.9), $S(c, R, R_q, R_n)$ and $N(c, R, R_q, R_n)$ denote respectively the rates of cell proliferation and cell decay within the tumor. Cell proliferation rate is assumed constant in many cases to make the model simpler, but in reality, it may depend on the local concentration of the nutrients. The total death rate is assumed to be the combination of apoptosis and necrosis. Apoptosis occurs in the quiescent and proliferating zones and necrosis result from the deprivation of the nutrients in the necrotic zone.

The contributions of Burton (1966) and Greenspan (1972) are deemed as pioneering studies in the development of heterogeneous models. These two seminal works in the field of modeling of avascular tumor growth has been quoted extensively and form the basis for most of the future works. According to Burton (1966), the tumor growth decrease happens because of the formation of the necrotic region which is

based on the concentration of oxygen in the solid tumor. The model assumes that the tumor is spherical in shape, and diffusion is the only mode for the transport of oxygen to all cells in the tumor and the consumption rate of oxygen per unit volume of the tumor tissue is constant. Then, this diffusion based model was solved and an analytical relation between the critical radius, necrotic radius and tumor radius was derived. Critical radius is the tumor radius at which the necrotic region begins to form at its centre. An empirical fitting of the Gompertzian relation to this analytical equation was done. The author observed that the fit is good over a range of 100 fold increase in tumor size and matches closely with the experimental results based on the 18 different types of the tumors. The best part of this work is the ability of the model to predict without any reference to physiological parameters of the tumor. However, there is a drawback in this work; the analytical relation was based on the assumption that, the concentration gradient of oxygen is zero everywhere in the necrotic zone which is not always the case (Casciari et al., 1992). In Greenspan (1972), the author developed a model of tumor growth based on diffusion and incorporated different hypotheses to model the internal processes responsible for the tumor growth. The main assumptions are:

1. Disintegration of necrotic cells into a number of chemical compounds and their role in inhibiting the mitosis of cancer cells (transforming of proliferating cells to quiescent cells).
2. Surface tension among living cancer cells maintain a compact and solid mass and it is responsible for the inward motion of cells from the outer region to compensate the loss due to the disintegration of necrotic cells.
3. The loss of necrotic core is proportional to its volume
4. All living cells are identical and are analogous to incompressible fluid as they assumed that the density of cells is the same everywhere in the tumor.

5. The proliferation rate of cell volume by mitosis is based on the concentration of the nutrients and the chemicals produced by the necrotic region.

The theory of Greenspan (1972) considered two different possibilities responsible for the introduction of inhibitory factors. The first one is a chemical inhibitor that is the product of necrosis resulting from the insufficient nutrient supply. The second possibility is purely based on the products of the metabolic processes of the living cells. Based on these assumptions, the author has analyzed tumor growth retardation due to necrosis and waste products and finally concluded that these analyses can be related to experimental observations based on the onset of necrosis. The work of Greenspan (1972) proved to be the main impetus for the theory of growth inhibitory factors in later works (Adam and Maggelakis, 1989; Adam, 1987*a,b*, 1986; Glass, 1973; Shymko and Glass, 1976). But these models neglected the cell volume loss due to necrosis. In Glass (1973), they considered the chalone mechanism to illustrate the growth retardation of the tumor. Chalones are the mitotic inhibitors which are partially responsible for the controlled replication of the cells. They further assumed that the production of chalone was uniform throughout the tissue, which then diffuse and decay. Shymko and Glass (1976) extended this hypothesis to higher dimensions and endeavored to study the effect of different geometries on the pattern and the stability of growth. Then, Adam (1989, 1988, 1987*a,b*, 1986) improved the idea of Glass (1973) by regarding the spatially non-uniform inhibitor production, different geometries and validating with experimental results of Folkman and Hochberg (1973). In addition to non-uniform inhibitor production, a new model by Chaplain et al. (1994) introduced a nonlinear, spatially dependent diffusion coefficient to explain the diffusion of a growth inhibitory factor. The results from this model were shown to be compatible with the experimental findings over the profiles of the growth inhibitory factors.

The extended work of Burton (1966) and Greenspan (1972) by Deakin (1975) argued that the rate of oxygen consumption cannot be uniform throughout the tumor. This argument was based on the experimental evidence from Sutherland and Durand (1973). Deakin (1975) considered that the oxygen consumption is proportional to the oxygen concentration but considered the non-uniformity of oxygen only to the viable rim thickness. Later McElwain and Ponzio (1977) investigated the effects of this non-uniformity and produced three different phases in the tumor development.

Another important contribution of Sutherland and Durand (1973) is the observation of dormancy of multicellular spheroids without the formation of necrotic region. This issue was further emphasized by the results of Durand (1976). The additional cell loss mechanism is noticed as apoptosis (Kerr, 1971; Kerr et al., 1972) and the model by McElwain and Morris (1978) was the first work to include it. A blended model was introduced based on the propositions of these works (Deakin, 1975; Greenspan, 1972; McElwain and Ponzio, 1977). According to the review paper Tiina et al. (2007), the model proposed by Casciari et al. (1992) is a “breakthrough” example of mathematical modeling in tumor biology. This work provided the impetus to study the effect of concentration gradients of multiple nutrients such as oxygen, glucose, lactate ions, carbon dioxide, bicarbonate ions, chlorine ions and hydrogen ions and their varying consumption rates. It also included the effect of the waste products of the metabolism. The main assumption of the model is that cellular metabolism and cell growth rates are mainly dependent on the local concentration of oxygen, glucose concentration and extracellular pH. The authors have used empirical expressions for the consumption rate of oxygen and glucose and the cell proliferation rate based on the experimental data. Moreover, they assumed that the necrotic zone formation is based on the critical concentration of glucose. This model was validated with published data of EMT6/Ro spheroids in terms of oxygen and glucose profiles at the centre of the tumor and their consumption rates. The model showed a good fit when the spheroid growth data is below $700 \mu m$. The

model was quite successful in predicting the viable rim thickness at particular conditions. The authors finally suggest that other factors like cell-cell contact effects may be used to explain the tumor growth. Despite these improved aspects, their model did not include apoptosis. In the paper Busini et al. (2007), a comprehensive mechanistic model comprising the main processes related to tumor growth like nutrient consumption, mitosis, apoptosis and necrosis was discussed. The model was represented in population balance equations and was combined with the drug models. Their solution was validated with both *in vitro* and *in vivo* results. The shortcoming of this work is that it did not include the quiescent zone formation.

There are some works which have emphasized on the effect of acidosis on tumor growth (Gatenby and Gawlinski, 2003, 1996; Gatenby et al., 2006; Smallbone et al., 2005). The hypothesis in the literature is that the transformation of cells from proliferating to quiescent or necrotic is attributed to the acidic environment (lower pH value)(Vaupel et al., 1989). In the hypoxic conditions (oxygen deficient), glycolytic phenotype is observed where glucose is metabolized via glycolysis or anaerobic respiration and produces lactic acid. There is also a theory known as Warburg effect which states that the tumor cells adopt glycolysis pathway for glucose metabolism even in the normoxic conditions. Based on these theories, acidosis is included in the continuum models by the considering the variation of H^+ ion concentration in the tumor. Other modeling works found consistency with experimental observations about the correlation of apoptotic pathways in the normal cells near the tumor with the acidic environment (Gatenby and Gawlinski, 1996). In contrast, the MZMs suggest that the regions of different types of cells are not separated sharply, but gradually. Thus, MZM aims to find spatial and temporal variation of the number of cells of different types per unit volume of the tumor. These models come under the category of multiphase models (Ambrosi and Preziosi, 2002; Breward et al., 2003, 2002).

$$\frac{\partial \phi_i}{\partial t} + \nabla \cdot (v_i \phi_i) = \nabla \cdot (D_i \nabla \phi_i) + \lambda_i(\phi_i, C_i) - \mu_i(\phi_i, C_i) \quad (2.10)$$

where, for different phase (cell type) 'i', ϕ_i is the volume fraction ($\sum_i \phi_i = 1$), v_i is the velocity, D_i is the random motility or diffusion, $\lambda_i(\phi_i, C_i)$ is the chemical and phase dependent production, and $\mu_i(\phi_i, C_i)$ is the chemical and phase dependent degradation/death. The first MZM was probably suggested by Ward and King (1997). Unlike DZMs, this model does not consider different layers for different type of cells in the avascular tumor. Instead, it presumes a mixture of live and dead cells and describes the variation of live cell density and dead cell density with the variation of the nutrients. DZMs have considered the *a priori* knowledge of tumor structure with three different regions. According to Ward and King (1997) the structure of different regions of tumor growth should not be assumed but it should be produced from the solutions of the models. In this paper, the authors proposed a model without any such presumptions about the tumor structure in the form of a system of partial differential equations to describe the growth of an avascular tumor spheroid. Moreover, the authors also performed asymptotic analysis (effects of limiting values of parameters) in order to distinguish the exponential growth phase and retardation growth phase of the tumor. This model was then extended by the inclusion of pharmacokinetics and pharmacodynamics of the diffusible drug and its effects were compared between the multicellular spheroids and the monolayer cases. Another example of MZM is the model by Sherratt and Chaplain (2001). According to them, most of the previous models developed were based on *in vitro* experiments on multicellular spheroids. Consequently, this model is inclined towards representing *in vivo* phenomena rather than *in vitro* and considers the nutrient source as nearby tissues. In addition, the model also included the concept of cell movement reflecting the contact inhibition of migration. Similarly, the work by Breward et al. (2002) considered two phase model to describe the avascular tumor growth which was further advanced by accounting for ATP production from energy metabolism in the models of multicellular tumor spheroids (Bertuzzi et al., 2007; Venkatasubramanian et al., 2006). There are other good examples of MZM (Tindall and Please, 2007; Tindall et al., 2008). In Tindall and Please (2007), effects of cell cycle dynamics

was considered and their main focus was on two different conditions of chemotactic responses of proliferating cells and quiescent cells to the external nutrient supply and their effects on the tumor structure. They extended this work in Tindall et al. (2008) to study the formation of necrotic region in avascular tumors and analytically proved that necrotic core is correlated with low levels of nutrient concentration.

2.2.4 Discrete and hybrid models

Discrete modeling focuses on tracking and updating the state of individual cells which are guided by specific biophysical rules. Framing of these rules is a challenging task that demands a lot of experimental analyses related to inter and intracellular events (e.g. biochemical pathways, cell cycle) controlling the cell survival and death. However, discrete modeling will be very useful for studying the mechanisms such as nutrient consumption, cell division, interaction with the microenvironment (growth factors, extracellular matrix, and immune system) and the progressive steps of transformation of a normal cell to a cancer cell. In short, discrete models characterize the state of the cells based on the microenvironment conditions. Some of the review works are given here (Abbott et al., 2006; Drasdo et al., 2007; Anderson and Quaranta, 2008; Araujo and McElwain, 2004; Byrne et al., 2006; Deisboeck et al., 2009; Lowengrub et al., 2010; Moreira and Deutsch, 2002; Quaranta et al., 2008, 2005).

Hybrid modeling is also known as multiscale modeling. It is the combination of both continuum and discrete models. These models attempt to provide comprehensive explanation of the tumor growth on the basis of the mutual information transfer between sub-cellular, cellular and tumor scales (Bellomo, Angelis and Preziosi, 2003; Kim and Stolarska, 2007; Martins et al., 2007; Stolarska et al., 2009; Weinan et al., 2007). Consequently, it helps to relate the mishappenings at the cell level to the aggressiveness and morphology of the tumor. In the hybrid approaches of tumor modeling, the diffusion of nutrients is explained by the continuum models and the

cell state is defined by the discrete model based on the local concentration of the nutrients. As a result, the computational cost for both discrete model simulation and hybrid model simulation increases significantly with the increase in number of cells.

Some works have used continuum and discrete models to compare the tumor evolution using multicellular tumor spheroids (Byrne and Drasdo, 2009; Schaller and Meyer-Hermann, 2006). Eventually, they concluded that continuum models are simple and suitable enough to use for predicting the tumor growth. However, the discrete or hybrid models might be necessary to understand microscale mechanisms taking place in the cells (Schaller and Meyer-Hermann, 2006).

2.2.5 Model calibration

The parameters of the model play a vital role in predicting the outputs of interest through simulations. In the field of tumor growth modeling, the parameters are obtained in different ways. The parameters are estimated from the tumor growth data gathered from *in vivo*, *in vitro* experiments and magnetic resonance images (MRI). *In vivo* studies are done using DNA transfection methods. In these methods, DNA of the tumor cell is transfected into normal cells to transform them to tumor cells followed by injecting them into laboratory mice (Kleinsmith, 2005). However, this is an arduous procedure and requires the modification of the mice subjects by knocking out some genes to nullify the effect of immune system on tumor growth. On the other hand, conventional suspension and monolayer *in vitro* experiments do not exactly represent the tumor growth. Therefore, alternatively, multicellular tumor spheroid experiments (MCTS) are preferred as a model experimental system for avascular tumor (LaRue et al., 1998; Kunz-Schughart, 1999; Kunz-Schughart et al., 1998; Mueller-Klieser, 1997). MCTS replicates the three dimensional network of cell-cell and cell-matrix interactions. This experimental methodology was adapted

in the area of cancer research by Sutherland and coworkers in 1971. Initially, this methodology was aimed to be applied to radiobiology. However, later, it was employed to a significant level in the fields of biomedical research and basic cell biology. They are used to study the effect of local microenvironments on cellular growth, cell-cell contact, cell metabolism, cell cycle regulation, cell doubling time, the effect of epigenetic factors in controlling radiation survival, DNA repair process, quiescent cell formation and cell survival under hypoxic conditions (Mueller-Klieser, 1987). In addition, MCTS has contributed to the comprehension of therapeutic response of the cells and in screening the mechanistic studies of drug penetration, binding and innovative therapeutic strategies such as combination therapy and the evaluation of toxic effects on the normal cells. Tumor heterogeneity (proliferating, quiescent and necrotic cells) is also reflected from these experiments. Even though, tumor cell type-dependent variations are seen in spheroid growth, the physiological parameters derived from MCTS are general in nature. Despite the above, MCTS has secured little success in the clinical implementation for testing the drugs on the tumor material extracted from the patients. This could be due to the reason that the growth characteristics of cancer cells might vary in different stages.

2.3 Tumor and its interaction with immune system

The main function of the immune system is to fight against the abnormal changes in the body, and the successful functioning of it lies in its ability to distinguish the “self” and “non-self” based on the self marking molecules. The immune system recognizes the abnormality with the help of antigens presented by the injured or abnormal cells. If the immune system exhibits a response based on the antigen recognition, then antigens are called immunogenic. According to immunosurveillance theory by Lewis Thomas (Ichim, 2005): “Effector cells of the immune system actively patrol the body to identify and eradicate incipient tumor cells”. Tumors are also classified as immunogenic and non-immunogenic. Immunogenic tumors are

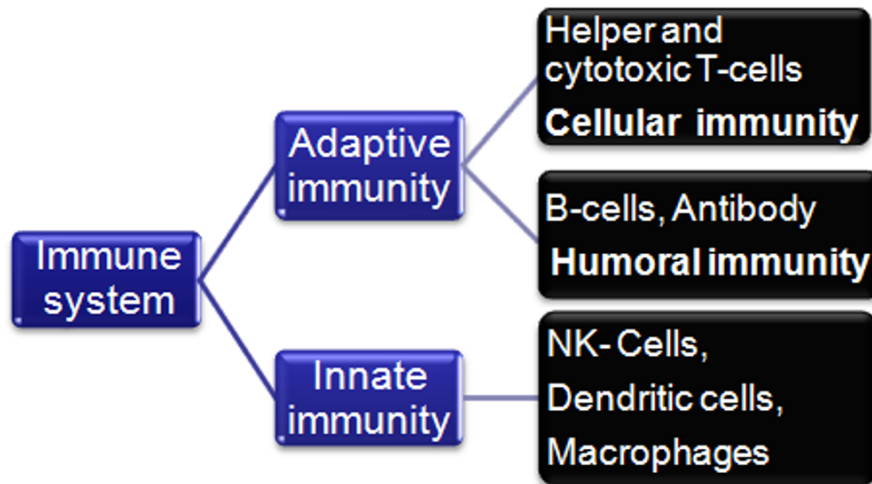


Fig. 2.5. Classification of immune actions

those which are recognized by the immune cells in the human body. But not all antigens are immunogenic. Before studying the tumor-immune interactions, we can take a brief look at the mechanisms of the immune system. In this regard, the review paper by Adam et al. (2003) provides a comprehensive discussion on the immune response in cancer.

In our body, the immune action is carried out by specialized cells called lymphocytes which are mostly present in the blood. The common lymphocytes are macrophages, dendritic cells, natural killer (NK) cells, lymphokine activated killer (LAK) cells, B-cells and T-cells. Immune response is categorized as natural immunity, humoral immunity and cellular immunity based on the lymphocytes (Figure 2.5). Macrophages, dendritic cells, natural killer cells are responsible for natural immunity, in which these cells directly attack the infected cells (cancer cell) and act as antigen presenting cells (APC). Antigen is an agent which can easily be recognized by immune cells. Thus, APC highlights the infected cells and alerts the T-cells for further action against the infected cells. In humoral immunity, antibodies produced by B-cells encounters the infected cells. Each B-cell has a specific antibody of a particular shape. The concept of antibody-antigen interaction resembles the mechanism of lock and key. When the shape of an antibody of a B-cell matches exactly

with the shape of the antigen corresponding to the infected cells, B-cell proliferates and produces plasma cells which actively secrete the antibodies. These antibodies neutralize the activity of the infected cell by inhibiting their cell division process, by producing a lethal group of enzymes called complement and by opsonization. In opsonization, antibodies coat the infected cells in order to make them easily recognizable by the killer lymphocytes. This process is known as antibody dependent cell-mediated cytotoxicity. In cellular immunity, the key players are T-cells which are further classified as helper T-cells (CD4+) and cytotoxic T-cells (CD8+). Helper T-cells gets activated by the natural immune cells and regulates the production of the cytokines. Cytokines are the proteins which keep the momentum of all the immune cells as per their requirement. Interleukins and interferons are regarded as the important cytokines to fulfill the immune action. Cytotoxic T-cells directly attack the infected cells after its activation by the cytokines.

Cancer immunotherapy is broadly classified into different schemes - monoclonal antibody therapy (MAT), adoptive-cell-transfer therapy (ACT), vaccine therapy and interleukin therapy (Figure 2.6). The common aspect of all schemes of immunotherapy is to enhance the immunogenicity of the individual. Immunogenicity is the ability of the immune system to recognize tumor cells. MAT is based on the mechanism of humoral immunity while others are based on cellular immunity. In MAT, antibodies are produced in large quantities using hybridoma technology and injected into the patient. In ACT, tumor infiltrating lymphocytes exhibiting the anti-tumor activity are found. They are then isolated and cultured in larger quantities in the presence of cytokines (interleukin) and injected back to the patient (Dudley et al., 2002; Dudley and Rosenberg, 2003). In vaccine therapy, APCs are engineered externally to recognize the tumor associated antigens and trigger the cellular mediated immunity. At present, extensive clinical studies are being done on dendritic cell therapy (Aarntzen et al., 2008; Ballestrero et al., 2008; Banchereau

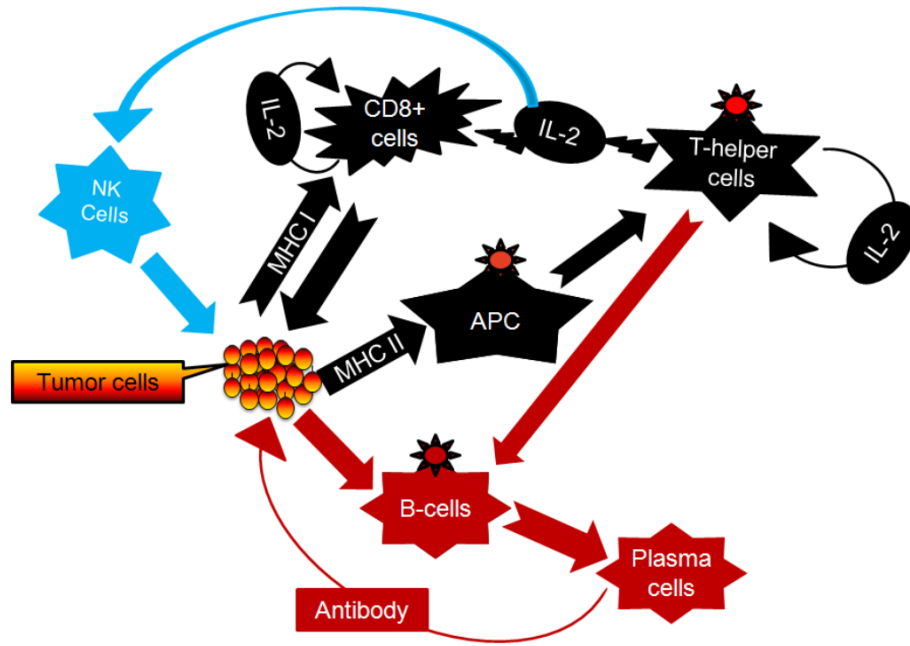


Fig. 2.6. Description of different immune actions

et al., 2001; Dhodapkar et al., 1999; Jacobs et al., 2009; Svane et al., 2003; Vuylsteke et al., 2006; Ludewig and Hoffman, 2005).

2.3.1 Tumor-immune models

Many tumor-immune interaction models have been developed and some of the review works are Bellomo, Bellouquid and De Angelis (2003); Bellomo and Preziosi (2000). They can be classified on the basis of immune cells interaction and model type (e.g. functional and spatio-temporal) models). In the first type of classification there are two categories of models. In the first category, all types of immune cells are included as one ensemble called as effector cells (Joshi et al., 2009; Kirschner and Panetta, 1998; Kuznetsov and Knott, 2001; Kuznetsov et al., 1994). Contrastingly, in the second category of models, the kinetics and interaction of different immune cells and their activation by cytokines is studied (Cappuccio et al., 2007; Castiglione and Piccoli, 2007, 2006; De Boer and Hogeweg, 1986; Pappalardo et al., 2005; de Pillis et al., 2009, 2006, 2005; Castiglione et al., 2004; Piccoli and Cas-

tiglione, 2006; Szymanska, 2003). In some models, phenomena such as sneaking through and tumor dormancy are introduced - these models account for situations where the tumor camouflages the immune system. The only model in which the parameters are estimated using experimental data is that of Kuznetsov et al. (1994) and it was further extended by distinguishing the action of different immune cells. The aforementioned tumour-immune models are functional type, where spatial variations of immune cells are neglected. There are some works which considered spatio-temporal tumour-immune models and solved using lattice fixed discrete models such as cellular automata (Mallet and De Pillis, 2006).

2.4 Model-based design of treatment protocols of cancer therapy

The field of mathematical modeling of anticancer therapies has witnessed several contributions over the past four decades (Eisen, 1979; Swan, 1990; Martin, 1992; Swan, 1995; Swierniak et al., 2009). A recent review on modeling as a tool for planning cancer therapies by Swierniak et al. (2009) focuses majorly on optimization of cell cycle phase-specific chemotherapy, anti-angiogenic therapy and the effect of drug resistance. Cell cycle phase models are the compartmental models where the compartments indicate different phases of the cell cycle (Agur et al., 1988; Panetta and Adam, 1995; Gardner, 2000; Dua et al., 2008). The review also briefly addresses the strategies of optimal control such as bang-bang control and singular control in the model-based cancer therapy with age structured models accounting for kinetic heterogeneity of cancer cells. Eventually, this work stresses on multiscale models and its utility in realizing personalized therapy as a reality. Another mini-review (Gardner and Fernandes, 2003) was on computational assistance as new tools for chemotherapy. It discussed about the issues associated with the application of optimal control theory to cancer chemotherapy. This work also highlights examples (Panetta and Fister, 2000; Swierniak et al., 1996) to depict the variations of the

sub-optimal or optimal solutions with different problem formulations and model simplification strategies. Gardner and Fernandes (2003) also summarize the advantages and disadvantages of computational tools such as OncoTCap developed by Day and colleagues at the University of Pittsburgh Cancer Institute¹ and KITT - Kinetically tailored treatment (Gardner, 2002). These models include the complex interactions involved in the tumor growth, the effect of cell cycle phase specific drugs, effect of cell cycle phase non-specific cytostatic drugs and the phenomenon of drug resistance. These simulators are used to analyze different phenomena and therapy schedules of drugs with individual patient kinetic parameters as inputs (estimated from the tumor biopsy tests). Finally, Gardner and Fernandes (2003), also emphasize on the need for validation of the simulators with individual patient data so as to open avenues for promising and individual therapies.

2.4.1 Pharmacokinetic and pharmacodynamic modeling

Pharmacokinetics (PK) is the study of the flow of a drug in the body which includes the mechanisms of absorption, distribution, metabolism, excretion and liberation of the drug. Hence the pharmacokinetic models describe the relationship between the dosage and the concentration of the drug in the blood after its administration (Swierniak et al., 2009). There are different routes of drug administration (oral, intravenous, intramuscular, peritoneal) and the route employed decides the structure of the PK models. The common parameters in these models are volume of distribution, clearance rate, and biological half life. The PK models can be classified as non-compartmental model (same as non-parametric models) and compartmental models (functional models) (Holford et al., 2010). In non-compartmental analysis, blood/plasma samples are collected at some regulated intervals to estimate the total drug exposure by estimating the area under the curve of drug concentration-time graph. Compartmental models are kinetic models which are used to predict the

¹[http:// www.oncotcap.pitt.edu/2000](http://www.oncotcap.pitt.edu/2000)

drug concentration over time. Thus, non-compartment models are model independent while compartment models are model dependent. Compartmental models are further divided into single and multiple compartmental models. In single compartment models, the whole body is assumed to be homogeneous, without any variations in the drug penetration in different tissues. Conversely, in multiple compartment models, the variations of the drug in different tissues are considered. Pharmacodynamics (PD) is the study of the biochemical and physiological effects of the drug on the target (microorganisms, tumor cells) and other organs of the body. Thus, pharmacodynamic models quantify therapeutic and toxic effects. For example, the effect of the drug on tumor and normal cells corresponds to therapeutic and toxic effects respectively. The important parameters of pharmacodynamic representations are half maximal inhibitory concentration (IC_{50}) and half maximal effective concentration (EC_{50}). Also PK-PD models differ from each other based on the model structures (linear and nonlinear). Overall, PK-PD model simulation is helpful in order to understand the drug concentration, answer the practical issues faced by the clinicians and to design the treatment protocols. The metrics used to evaluate the drug activity are area under the curve (AUC , see definition in Equation (2.11)), maximum (C_{max}) and minimum (C_{min}) concentration of drug for a given dosage (Figure 2.7). In short, PK is what the body does to the drug and PD is what the drug does to the body.

$$AUC = \int_0^t C(t) dt \quad (2.11)$$

2.4.2 Optimal control theory (OCT)

OCT is a mature discipline with numerous applications in both science and engineering disciplines for deriving control policies. Its importance and usage in biomedical domain is increasing (Nof and Parker, 2009). OCT deals with finding a control law or trajectory of the decision variables such that a specific optimality

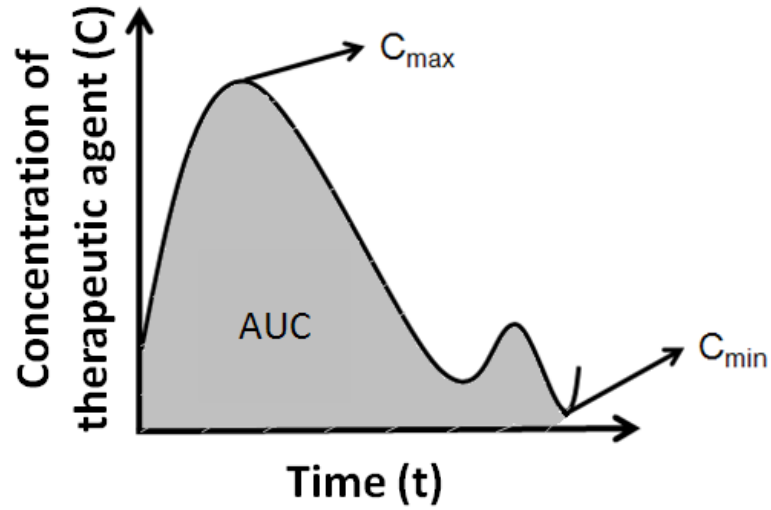


Fig. 2.7. Metrics of PK-PD modeling

criterion is achieved. In terms of cancer therapy, the control law is related to the intervention times and dosage of the drug such that tumor is completely eliminated and side effects due to the drug is minimized. The control problem includes cost function(s) (objective(s) (J)) which are a function of state variables ($X(t)$), input or control or manipulated variables ($U(t)$) as shown in Equation (2.12). Thus, an optimal control problem is a set of system equations describing the control actions for minimizing or maximizing the cost functions. The independent variable is time (t), t_o is the initial time and t_f is the final time. The terms Φ and L given in Equation (2.12) represent the endpoint cost and Lagrangian respectively. Equation (2.13) represents the dynamic model of the real system. And b in Equation (2.14) corresponds to equality and inequality constraints on state variables, input variables and time to be considered while proposing a control law.

Elements of the optimal control problem

Objectives:

$$J = \Phi(x(t_0), t_0, x(t_f), t_f) + \int_{t_0}^{t_f} L(x(t), u(t), t) dt \quad (2.12)$$

Dynamic model:

$$\dot{\mathbf{x}}(t) = f(\mathbf{x}(t), \mathbf{u}(t), t) \quad (2.13)$$

Constraints:

$$b(\mathbf{x}(t), \mathbf{u}(t), t) \leq 0 \quad (2.14)$$

The state variables in the context of cancer therapy are the density of cells (cancer cells, normal cells, immune cells) and the concentration of therapeutic agents. The input variables denote the therapeutic dosages. The cost functions include minimization of tumor burden (area under the curve of tumor evolution), final tumor size, maximum tumor size and minimization of therapeutic burden (area under the curve of concentration of therapeutic agent) and cumulative dosage rate of therapeutic agent for a given time horizon. The usual decision variables are type of therapy, time of intervention, dosage rate and duration of therapeutic intervention. The constraints are on the drug dosage rate, maximum and minimum concentration of the drug in the body during the treatment course. Particularly, many domain problems relevant to cancer therapy were formulated and solved using OCT. These include Swan (1986, 1990, 1995), Murray (1990*a,b*), Martin (1992), Iliadis and Barbolosi (2000), Barbolosi and Iliadis (2001), Parker and Doyle (2001), Matveev and Savkin (2002), de Pillis and Radunskaya (2003), Piccoli and Castiglione (2006), Cappuccio et al. (2007), Castiglione and Piccoli (2007), de Pillis et al. (2007), Ledzewicz and Schttler (2007), Dua et al. (2008) and Chareyron and Alamir (2009). Often, these optimal control problems are nonlinear and hence numerical techniques are employed for solving them.

2.4.3 Description of optimization problem formulation using cancer therapy models

Broadly, cancer therapy models are characterized based on tumor stage, type of therapies (surgery, radiation therapy, chemotherapy, immunotherapy, viral ther-

apy), and models used for tumor growth and PK-PD of the drugs. In the model based therapeutic design, until now, optimal control theory was fully exploited in order to address the scheduling of therapies using a therapeutic agent (Barbolosi and Iliadis, 2001; Cappuccio et al., 2007; Dua et al., 2008; Ghaffari and Naserifar, 2010; Harrold and Parker, 2009; Martin, 1992; Swan, 1995) and combination of therapeutic agents (Chareyron and Alamir, 2009; de Pillis et al., 2006; Tse et al., 2007; Kiran et al., 2009). In the above work, tumor growth, pharmacokinetic, pharmacodynamic models were coupled and optimization of the therapy with objectives, constraints and decision variables on tumor cells, normal cells and therapeutic agents was demonstrated. The formulated optimization problem was solved using different algorithms like gradient based methods, evolutionary methods (genetic algorithm, particle swarm optimization, differential evolution, simulated annealing etc.).

One major focus of the above-mentioned work was on the formulation of objectives and constraints so as to achieve better solutions (Gardner and Fernandes, 2003). Depending on how one formulates the objectives, one may have a single or multi-objective optimization problem. However, as mentioned before, scheduling cancer therapy usually involves multiple objectives such as the need to shrink tumor growth and avoidance of treatment side effects. In some of the previous work (Dua et al., 2008), different objectives related to the tumor cells and therapeutics was combined into a single objective. In such a strategy, the assignment of weights to the different objectives is an intricate issue. Often, in such cases, the problem is solved repeatedly by varying the weightage of objectives to find the best solution using gradient based methods and evolutionary algorithms. Such a strategy can be time-consuming. On the other hand, very little work has been done using multi-objective optimization strategy where the problem is solved by considering all the objectives for sets of solutions (Pareto set)(McCall et al., 2007; Kiran et al., 2009; Kiran and Lakshminarayanan, 2009). Multi-objective optimization enables the understanding of the therapeutic consequences and provides a chance to choose a solution from the Pareto set as per the requirements of the decision maker. The selection of the

solution from the Pareto set may not always be straightforward - a systematic post analysis of the Pareto set is essential in order to choose an appropriate solution. The chosen solution is called as optimal compromised solution, because the optimal solution for one objective may not be the optimal solution for the other objective(s). Thus, the post-Pareto-optimality analysis facilitates the decision making process.

2.5 Challenges in the model-based applications

There are some challenging aspects that need to be addressed before using tumor growth models in actual practice. Mathematical models can become highly complex by integrating all the knowledge on cell and tissue acquired by biologists relating to the tumor growth phenomenon. In general, complexity can be related to the model structure, the number of parameters in the model and their order of magnitude, nonlinearity in parameters/states, practical constraints in measurement times and in manipulating the input variables, magnitude and character of measurement errors etc (Sun, 2006; Sun and Hahn, 2006). These reasons necessitate more tumor size measurements to estimate parameters with acceptable precision. Often, however, the availability of tumor size data for a given patient is quite limited. In such cases, the precise estimation of all the patient parameters can become quite difficult. In some of the earlier work, non-dimensionalization strategy was used to ease numerical solution of the models (Kirschner and Panetta, 1998; Kuznetsov et al., 1994; de Pillis et al., 2006; Ward and King, 1997). However, the theoretical implications of parametric groups were not highlighted. Even the parametric sensitivity on the output of interest is studied using one parameter at a time (OAT) method (Kirschner and Panetta, 1998; Kuznetsov et al., 1994; de Pillis et al., 2009, 2006, 2005).

The main drawback of the existing tumor growth models is that some of them are too simple while some are too complex to explain the mechanism of the nutrients effect on tumor growth. Model validation, an important feature in the model building process is found to be missing for some theoretical models in the literature.

Another important challenge in the case of mechanistic tumor model is that the tumor size varies with time; consequently, the position of the tumor surface changes. This is known as free boundary problems. The numerical solution for free boundary problems is very challenging as they involve solving of partial differential equations where the spatial domain is not fixed.

Model reduction is an important issue for modeling based practical applications (Sun, 2006; Sun and Hahn, 2006). In doing so, care should be taken to avoid the loss of information in the process of model reduction. Scaling and sensitivity analysis can be used for model reduction. With reduced models, the computational time taken for model simulation may be significantly reduced. Reduction in time for a single simulation may not seem to be very significant. However, if one resorts to optimization of inputs or performs parameter estimation where the model may be simulated a few thousand times, the savings in time can be quite significant and useful. Then, global sensitivity analysis of the reduced model will help to unearth the key parameters of the model. Similarly, model reduction will definitely be an impetus for employing physiological models in clinical practice. The information extracted about the key parameters in the model can be further utilized in formulating diagnostic and treatment protocols for patients or patient cohorts.

2.5.1 Description of the strategy implemented in this thesis work

A schematic representation of the strategy employed in this thesis work is shown in Figure 2.8. The models in this thesis work are chosen based on the situation as follows. Spatio-temporal models are used for comprehending the mechanism of the tumor growth phenomenon. On the other hand, functional models are considered for designing cancer treatment protocols for patients and patient cohorts. After the first step of mathematical model selection, the parameters are taken from the literature. Then, the raw models are subjected to a *priori* model analysis to reduce the model and facilitate the application of effective numerical procedures. Then,

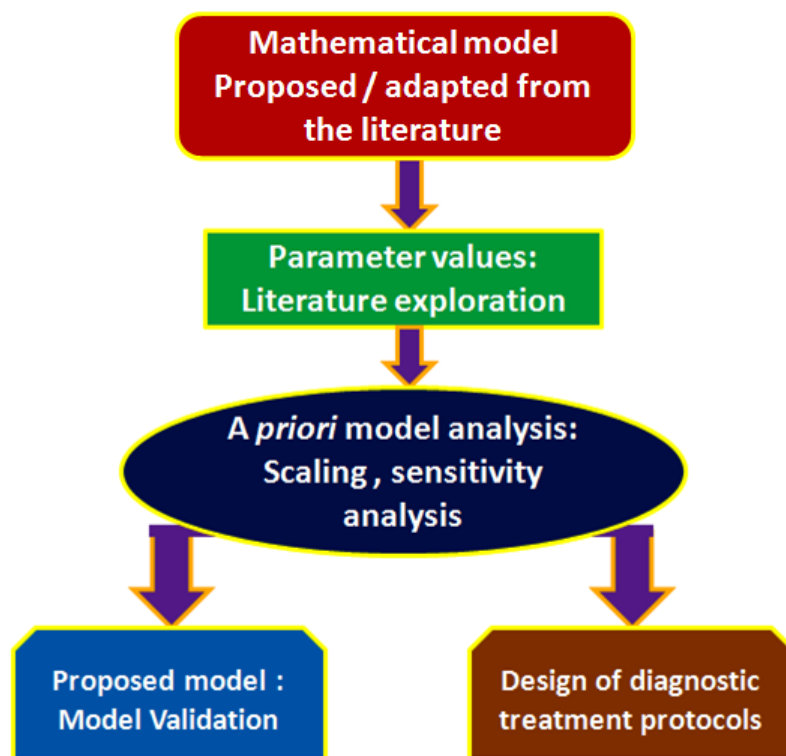


Fig. 2.8. Strategy followed in this thesis

the reduced models are used to formulate optimization problems for realistically - considered applications. The aim of the thesis is to develop simulation based tumor growth studies that might be decision-support tools for the clinicians and oncological pharmacists.

Chapter 3

MATHEMATICAL MODELING OF AVASCULAR TUMOR GROWTH BASED ON DIFFUSION OF NUTRIENTS AND ITS VALIDATION

'All models are wrong, but some are useful.'

- George E P Box

3.1 Introduction

In this chapter, a mathematical model based on the diffusion of nutrients is developed by considering the physiological changes accompanying the growth of avascular tumor. Avascular tumor growth involves the formation of three different zones namely proliferation, quiescent and necrotic zones. The main processes on which avascular tumor growth depends are: (i) diffusion of nutrients through the tumor from the contiguous tissues, (ii) consumption rate of the nutrients by the cells in the tumor and (iii) cell death by apoptosis and necrosis. In the model, it is assumed that the tumor is spherical and the principal nutrients responsible for its growth are oxygen and glucose. By solving for the concentration profiles using the proposed model which describes the above processes, the radii of the quiescent and necrotic zones as well as that of the tumor are computed. The proposed model is also validated using *in vitro* tumor growth data and Gompertzian empirical relationship parameters available in the literature. The model is shown to be successful in capturing the saturated volume of the avascular tumor for different nutrient con-

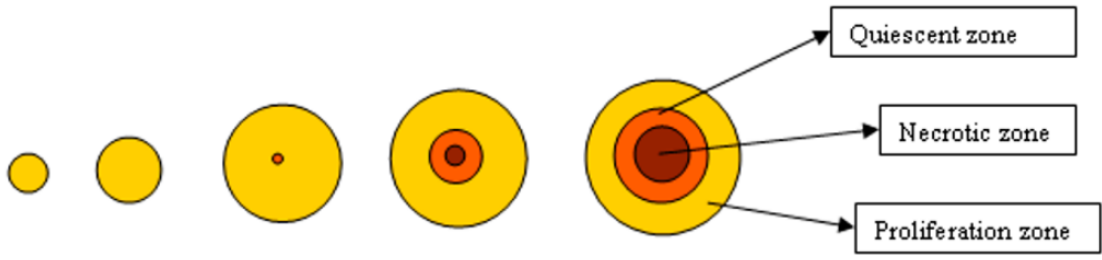


Fig. 3.1. Different zones in avascular tumor growth

centrations at the tumor surface and the concentration profiles of the nutrients in the tumor.

3.2 The proposed model

The meaning of different zone model (DZM) and mixed zone model (MZM) is same as discussed in the previous chapter. In practical terms there is no significant difference between the DZMs and MZMs - the results from MZM almost resembles the pattern of DZM proving that proliferating cells are at the outer rim, necrotic cells are at the centre and quiescent cells in between (see Figure 3.1). Although spatial-temporal models are mechanistic, some models do not include apoptosis (Burton, 1966; Casciari et al., 1992), quiescence (Busini et al., 2007) or the multi-nutrient effect (Burton, 1966; Casciari et al., 1992). Besides this, some models are not validated with any experimental results (Greenspan, 1972; Tindall and Please, 2007; Ward and King, 1997). Based on the assumption that the tumor cells transform to necrotic cells only when the nutrient concentrations are below their critical values and the presence of apoptotic dead cells is very negligible (implying that there would be no dead cells in the outer region), a new DZM is proposed. The proposed model is also validated with the *in vitro* experimental results provided by Freyer and Sutherland (1986b) and Gompertzian empirical relation.

A simple DZM that incorporates the key mechanisms occurring in the tumor is presented in this chapter. The mechanisms are nutrient diffusion, nutrient consumption, and cell death processes (apoptosis and necrosis). The proposed model also includes the quiescent region along with proliferation and necrotic region, which has been neglected in most of the previous models. In quiescent region, tumor cells neither proliferate nor die. Though the different regions have been incorporated in the model, it is assumed that the size of proliferating cells, quiescent cells and necrotic cells are the same. The model assumes a spherical shape for the tumor and ignores the extracellular matrix in between the cells.

The vital nutrients for cell proliferation in the tumor are glucose and oxygen. The diffusion coefficients and surface concentration of these nutrients are assumed constant. Initially, all cells in the tumor are proliferative as adequate nutrients diffuse from the surrounding tissue to each and every cell. Consequently, the tumor grows exponentially. As time proceeds, the total radius of the tumor increases and concentration of nutrients decreases in the central part of the tumor and, at a certain time, the nutrients reach critical concentration. Once the first nutrient attains its critical concentration at the centre, quiescent region appears in the tumor. In the quiescent region, the cells will neither proliferate nor die. Similarly, necrotic region starts when the second nutrient achieves its critical concentration at the centre. In the necrotic region, cells die due to shortage of both the nutrients (Hlatky et al., 1988a). Therefore, the position of quiescent radius and necrotic radius is decided by the value of critical concentration of first nutrient and second nutrient respectively. Actually, any of the nutrients can be the first nutrient or second nutrient; it all depends on the concentration of the nutrients at the tumor surface, their diffusivity, critical concentration and consumption rate. With further increase in tumor radius, the quiescent and necrotic radii increase as well. The tumor radius reaches a steady state value when the quiescent region and necrotic region engulfs most of the total tumor region. In addition to necrosis (Byrne and Chaplain, 1998, 1996; Tindall

et al., 2008), there is natural cell death process (known as apoptosis) where cells in the proliferating region die because of age factor. McElwain and Morris (1978) assumed that apoptosis is the only cell loss mechanism in their model. Necrosis is characterized by the membrane damage and energy depletion while apoptosis is the result of genetic changes in the cell (Bell et al., 2001). Therefore, total death rate of cells in the tumor is the sum of necrosis rate and apoptosis rate and this is reflected in our model. However, to keep the model complexity within manageable limits, it is assumed that the degradation of necrotic and apoptotic cells will not affect the diffusion and consumption rate of the nutrients.

3.2.1 Model equations

As discussed above, the diffusion and consumption of the nutrients are captured in Equations (3.1) and (3.2) to give the spatial and temporal variation of the nutrients. Many models based on single nutrient (Burton, 1966; Casciari et al., 1992; Ward and King, 1997) and multiple nutrients did use the quasi-steady-state form of Equation (3.1) or (3.2) , because the time taken for diffusion is very less than the time taken for tumor growth. Moreover, it is considered that the nutrient consumption follows Michaelis-Menten type of kinetics with fixed values for its parameters. Equation (3.2) implies that there is no nutrient consumption in the necrotic zone.

$$\left(\begin{array}{c} \text{rate of change of} \\ \text{nutrient concentration} \end{array} \right) = \left(\begin{array}{c} \text{flux due to} \\ \text{diffusion} \end{array} \right) - \left(\begin{array}{c} \text{rate of nutrient} \\ \text{consumption} \end{array} \right)$$

If ($C_i \geq$ critical concentration of all the nutrients (oxygen and glucose))

$$\frac{\partial C_i}{\partial t} = \frac{D_i}{r^2} \frac{\partial}{\partial r} \left(r^2 \frac{\partial C_i}{\partial r} \right) - \left(\frac{\mu_i C_i}{K_i + C_i} \right) \quad (3.1)$$

else

$$\frac{\partial C_i}{\partial t} = \frac{D_i}{r^2} \frac{\partial}{\partial r} \left(r^2 \frac{\partial C_i}{\partial r} \right) \quad (3.2)$$

where, r is the radial position in the tumor; $i = 1$ and $i = 2$ represents glucose and oxygen respectively. Equations (3.3) through (3.5) give the temporal variation of the tumor radius at the different stages of tumor growth. These equations include decay rate of dead cells based on apoptosis as well as necrosis. The apoptosis-based dead cells decay at a rate proportional to the volume of the viable zone (proliferation and quiescent), whereas necrosis based dead cells decay at a rate proportional to the volume of the necrotic zone. As stated earlier, the model assumes that decayed cells do not affect the diffusion and consumption of the nutrients.

The outer tumor radius, $R(t)$

$$\left(\begin{array}{c} \text{rate of change of} \\ \text{volume of tumor} \end{array} \right) = \left(\begin{array}{c} \text{total rate of cell} \\ \text{proliferation} \end{array} \right) - \left(\begin{array}{c} \text{total decay rate of} \\ \text{dead cells} \end{array} \right)$$

First stage (all cells are in proliferation zone; $R_q = 0, R_n = 0$)

$$3R^2 \frac{dR}{dt} = A(R^3) - A_p(R^3) \quad (3.3)$$

Second stage, (appearance of quiescent zone $R_q > 0, R_n = 0$)

$$3R^2 \frac{dR}{dt} = A(R^3 - R_q^3) - (A_p R^3) \quad (3.4)$$

Third stage (appearance of necrotic zone appears $R_q > R_n, R_n > 0$)

$$3R^2 \frac{dR}{dt} = A(R^3 - R_q^3) - (A_p(R^3 - R_n^3)) - (N_e R_n^3) \quad (3.5)$$

where, $R_n(t)$ is the radial position of the outer radius of necrotic zone from the tumor centre, $R_q(t)$ is the radial position of the outer radius of quiescent zone from

the tumor centre, A is proliferation rate constant, A_p is apoptosis rate constant, N_e is necrosis rate constant.

Equations (3.1) to (3.5) must be solved to get $R(t)$, $R_q(t)$ and $R_n(t)$. The solution of these equations is non-trivial because of the dependence of $R(t)$, $R_q(t)$ and $R_n(t)$ on the location of the critical concentration of the nutrients in the tumor. Section 3.3 presents the details on the model solution. The initial conditions and the boundary conditions of the model are as shown below.

Initial conditions (at $t = 0$)

$R = r_p$ (the initial tumor radius in the experimental data of Freyer and Sutherland (1986b))

$C_i = C_{i\infty}$ at all r

Boundary conditions

at $r = R$

$C_i = C_{i\infty}$ where $C_{i\infty}$ is concentration of the nutrient at the tumor surface

at $r = 0$

$\frac{\partial C_i}{\partial r} = 0$ (because of symmetry assumption)

3.3 Model solution

3.3.1 Non-dimensionalization of equations

Let

$$C_i^* = \frac{C_i}{C_{1\infty}}, \quad r^* = \frac{r}{R}$$

where, $C_{1\infty}$ is concentration of glucose at the tumor surface, which is considered as reference concentration and $R(t)$ represents tumor radius at any time

$$\frac{\partial C_i^*}{\partial t} = \frac{D_i}{R^2} \frac{\partial}{\partial r^*} \left(r^{*2} \frac{\partial C_i^*}{\partial r^*} \right) - \left(\frac{\mu_i C_i^*}{K_i + C_i^* C_{1\infty}} \right) \tag{3.6}$$

3.3.2 Numerical procedure

For non-dimensionalization, one can choose either $C_{1\infty}$ or $C_{2\infty}$ as the reference concentration. Here, $C_{1\infty}$ has been chosen as reference concentration, because $C_{1\infty}$ is greater than $C_{2\infty}$. Therefore, the solution of dimensionless concentrations of oxygen and glucose is always bounded between 0 and 1. The non-dimensionalized partial differential equation (3.6) and the outer tumor radius equations (Equation (3.3) to (3.5) as appropriate) are solved to get the tumor radius at different times. Equation (3.6) can be transformed to a set of ordinary differential equations and solved using the “Method of lines” (Lee and Schiesser, 2003). In this method, the spatial derivatives are transformed to algebraic form by using a finite difference approximation of required accuracy. The set of ordinary differential equations can be solved as initial value problems using MATLAB (Shampine, 1994). Note that the number of finite difference points is fixed along the tumor radius.

Nutrient concentrations, tumor radius, necrotic zone radius and quiescent zone radius are functions of time. However, there are no equations available for the temporal variation of necrotic zone radius and quiescent zone radius. Therefore, the number of unknowns (5) are more than the number of equations (3). In order to deal with this scenario, the equations are solved for short time intervals by assuming necrotic zone radius (R_n) and quiescent zone radius (R_q) as piecewise constant. The question is: what would be the range of the time interval over which the radii of the necrotic zone and quiescent zone may be considered as constant? It is known that cells take a few hours to several days for completing a cell cycle (Kleinsmith, 2005). Therefore, it is logical to proceed with the proposition that time interval may be based upon the duration of cell cycle. Thus, the cell cycle theory informs that noticeable growth of tumor radius is seen after every few hours to days. Therefore, the following solution strategy is devised. Initially, quiescent and necrotic zones do not exist. $R_q(0)$ and $R_n(0)$ are therefore taken as zero. The equations are solved

for a 3 hour horizon (say from $t = 0$ to $t = 3$ hours). At the end of 3 hours, the concentration profile of glucose and oxygen are examined in order to locate R_q and R_n corresponding to their critical concentrations. Then, the obtained values of R_q and R_n are substituted in the appropriate outer tumor radius equations (one of Equations (3.3) to (3.5)) based on the tumor stage and simulated for next 3 hours. These solution steps are repeated for the next block of 3 hours using appropriate initial conditions for the state variables until the tumor radius attains a steady state value.

3.4 Model validation and discussion

Model validation is a very crucial and essential part of mathematical modeling. In this work, the model is validated with the available *in vitro* results in the literature and with a well known empirical relation related to tumor growth called Gompertzian relation (Burton, 1966). The values of the model parameters and their references are presented in Table 3.1. These parameters are either measured directly (diffusivities, critical concentration of the nutrients, maximum consumption rates) or estimated (Michaelis-Menten constants, proliferation rate constant, apoptosis rate constant, necrotic rate constant) by fitting to a model. Note that the validation data sets are independent from data sets that were used to derive the model parameters summarized in Table 3.1. Thus, the proposed model has been subjected to stringent tests as reported below.

3.4.1 Validation with *in vitro* data (Freyer and Sutherland, 1986b)

In Freyer and Sutherland (1986b), EMT6/Ro mouse mammary carcinoma cell spheroids were cultured in suspension in either 0.28 *mmol/L* or 0.07 *mmol/L* oxygen and 16.5, 5.5, 1.7, 0.8 *mmol/L* glucose to study the effects of glucose and oxygen on spheroid growth. They determined the value of mean size of a spheroid population

Table 3.1
Parameter values

Symbols	Quantity	Value	Units
D_1	Diffusivity of glucose (Casciari et al., 1988)	1.1×10^{-6}	cm^2/s
C_{1c}	Critical concentration of glucose (Hlatky et al., 1988b)	7.7×10^{-6}	$mole/cm^3$
μ_1	Maximum consumption rate of glucose (Casciari et al., 1992)	4×10^{-8}	$mole/cm^3.s$
K_1	Michaelis-Menten constant for glucose (Casciari et al., 1992)	4×10^{-8}	$mole/cm^3$
D_2	Diffusivity of oxygen (Mueller-Klieser and Sutherland, 1985)	1.82×10^{-5}	cm^2/s
C_{2c}	Critical concentration of oxygen (Jiang et al., 2005)	2×10^{-8}	$mole/cm^3$
μ_2	Maximum consumption rate of oxygen (Casciari et al., 1992)	1.43916×10^{-8}	$mole/cm^3.s$
K_2	Michaelis-Menten constant for oxygen (Casciari et al., 1992)	4.640×10^{-9}	$mole/cm^3$
A	Proliferation rate constant Burton (1966)	0.12 – 5.2	1/day
A_p	Apoptosis rate constant (Busini et al., 2007)	1.5×10^{-6}	1/hour
N_e	Necrosis rate constant (Busini et al., 2007)	1.36×10^{-2}	1/hour

by measuring the two orthogonal diameters on each of 50 spheroids using an inverted microscope fitted with a calibrated eyepiece reticule. Using the above data, they evaluated the total spheroid volume variation with time for 28 days, maximum volume of the tumor, exponential doubling time and tumor diameter at the onset of necrosis for different media conditions.

Simulated growth curve was obtained from the proposed model using the parameter values in Table 3.1. Figure 3.2 shows the simulated growth curve of the tumor for 28 days in comparison with the experimental data when the glucose and oxygen concentrations in the media are 16.5 $mmol/L$ and 0.28 $mmol/L$ respectively. There is a high degree of agreement between the simulated growth curve and the

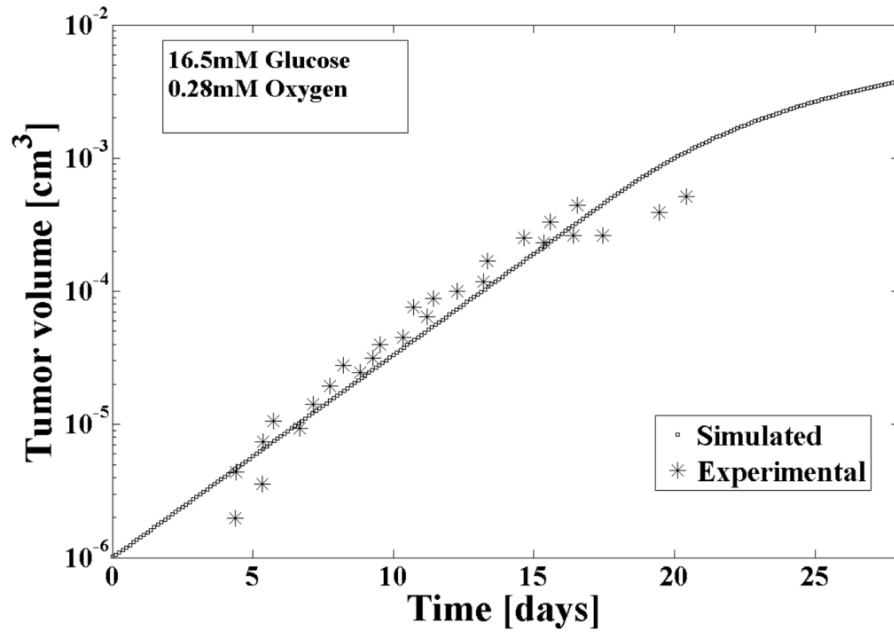


Fig. 3.2. Tumor growth curves of simulated and experimental data at 16.5 mmol/L glucose and 0.28 mmol/L oxygen

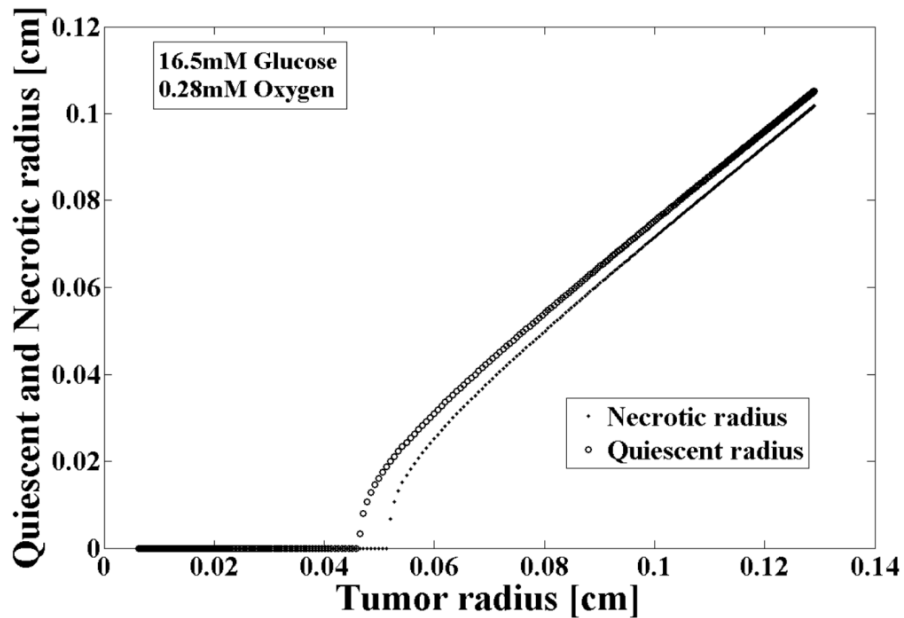


Fig. 3.3. Quiescent and necrotic radius at different tumor radius during its growth at 16.5 mmol/L glucose and 0.28 mmol/L oxygen

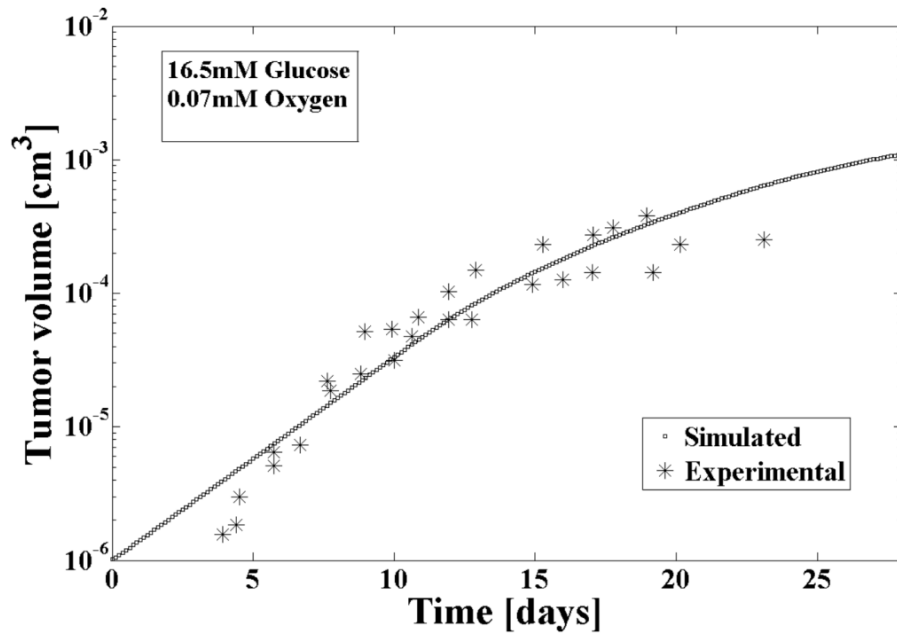


Fig. 3.4. Tumor growth curves of simulated and experimental data at 16.5 $mmol/L$ glucose and 0.07 $mmol/L$ oxygen

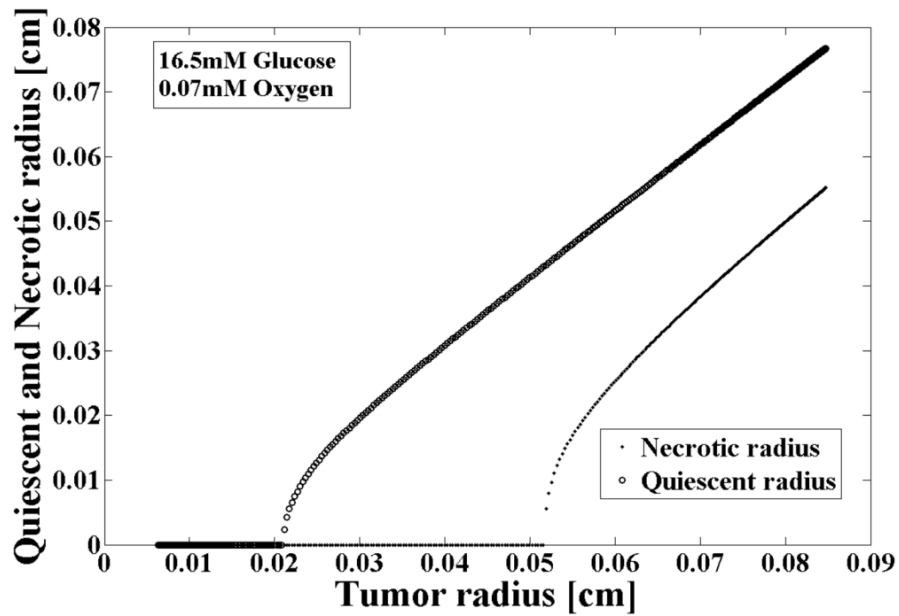


Fig. 3.5. Quiescent and necrotic radius at different tumor radius during its growth at 16.5 $mmol/L$ glucose and 0.07 $mmol/L$ oxygen

Table 3.2
Maximum volume of multicellular tumor spheroids at different concentrations

External oxygen concentration (<i>mmol/L</i>) ^a	External glucose concentration (<i>mmol/L</i>) ^a	Maximum volume (<i>cm</i> ³) ^a	Maximum volume (<i>cm</i> ³) ^b
0.28	16.5	4.4×10^{-2c}	9×10^{-3}
	5.5	1.1×10^{-2c}	3.2×10^{-3}
	1.7	8.3×10^{-4}	1.1×10^{-3}
	0.8	8.3×10^{-4}	4.54×10^{-4}
0.07	16.5	7.7×10^{-3}	2.6×10^{-3}
	5.5	6.1×10^{-4}	6.99×10^{-4}
	1.7	1.5×10^{-4}	1.56×10^{-4}
	0.8	7.8×10^{-5}	4.48×10^{-5}

^a Freyer and Sutherland (1986)

^b Proposed model

^c Extrapolated values (experimental)

experimental data. The simulated curve shows that once the quiescent and necrotic zones are formed in the tumor, the tumor growth retards and reaches a final state (see Figure 3.2 for $t > 25$ days). In addition, the proposed model was able to locate the position of outer radius of the quiescent and necrotic zones as shown in Figure 3.3. The tumor diameter at the onset of necrosis is almost the same as that of the estimated value (0.0516 cm) in Freyer and Sutherland (1986*b*). In order to test the prognostic ability of the model, the simulated results are verified with the experimental data, when the oxygen concentration is changed to 0.07 *mmol/L*. These results are shown in Figures 3.4 and 3.5 respectively. It is seen that the tumor diameter at the onset of necrosis (0.0510 cm) is in good agreement with the value given in Freyer and Sutherland (1986*b*). Table 3.2 shows the comparison between simulated values and the experimental values of the maximum volume of the tumor for different combinations of glucose and oxygen concentrations. The experimental values (3rd column) are from Freyer and Sutherland (1986*b*). The agreement between the experimental values and our model predictions (4th column) is very good. Interestingly, it is observed from Table 3.2 that for a given concentration of oxygen,

the maximum volume of the tumor increases with the increase in the concentration of glucose. The reason is that, if the nutrient concentration at the tumor surface were increased, the nutrient takes longer time to reach its critical value at the tumor centre and, over the same time, the tumor radius would have increased to a higher value.

3.4.2 Validation with *in vitro* data (Sutherland et al., 1986)

In Sutherland et al. (1986), oxygenation and development of necrosis in spheroids of HT29 cell line of colon adenocarcinoma was compared with Co112 cell line. Initially HT29 cell spheroids were cultured in an ambience of DMEM furnished with 10% fetal bovine serum and after five days the medium was further equilibrated with 5% CO_2 (v/v) and air. These conditions maintained the concentration of glucose and partial pressure of oxygen at 25 $mmol/L$ and 141 mm of Hg respectively at the surface of the spheroids. During the growth, the partial pressure of oxygen $P(O_2)$ in the spheroids was determined by the oxygen microelectrode measurements (OMM). In the process of culturing of HT29 spheroids, they have shown the variation of profiles of oxygen concentration inside the spheroids for different sizes of HT29 spheroids with the help of OMM. In this work, the proposed model is validated with these experimental results by considering the same ambient conditions. Figures 3.6-3.13 show the comparison between the model and the experimental results. The model is able to predict the decreasing trend of the oxygen concentration from the surface of the spheroids to the centre. Moreover, the model captures the thickness of the viable rim of the spheroids to be 0.02531 cm , when the diameter of the spheroid is 1.415 cm , which is close to the experimental value (0.0225 cm). However, in Figures 3.6-3.12, it is observed that the model predictions deviate from the experimental values at the surface of the spheroids. The reason is that the model assumes the concentration of the nutrients at the surface to be constant and their values are the same as in the medium. In contrast, in the experiments, there is a concentration

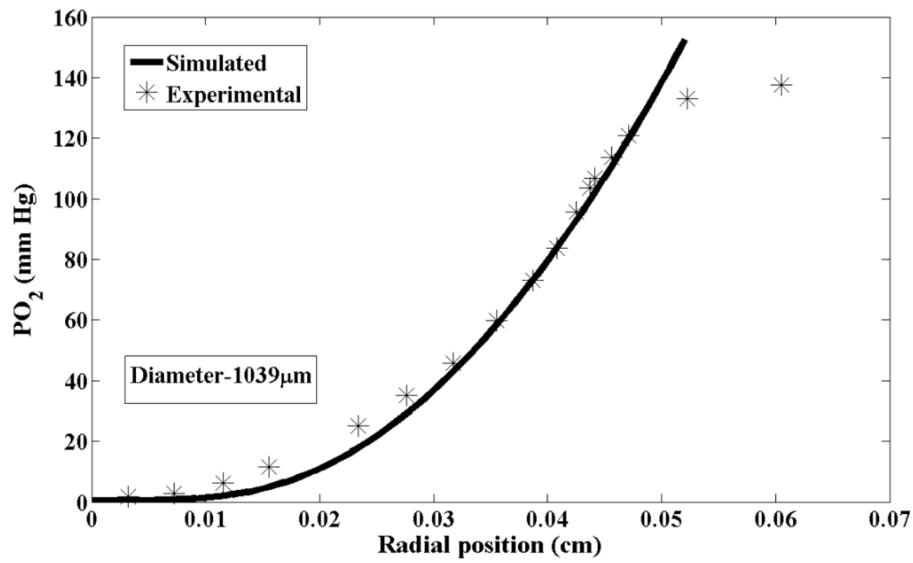


Fig. 3.6. Profile of partial pressure of oxygen (PO_2) in the HT29 spheroids when its diameter is 1039 μm

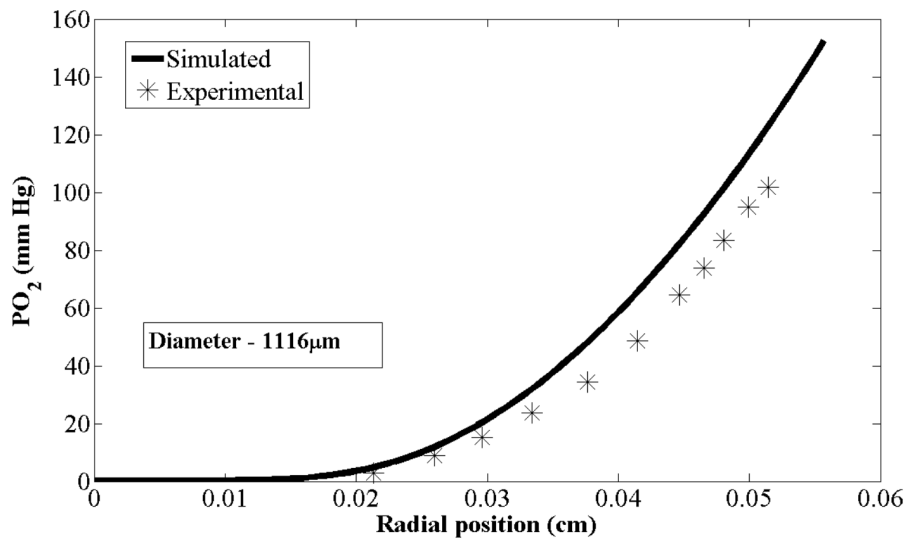


Fig. 3.7. Profile of partial pressure of oxygen (PO_2) in the HT29 spheroids when its diameter is 1116 μm

gradient of the nutrients from the bulk medium to the surface. This also implies that the deviation of the model will be more when the diameter of the spheroids is very small and this is seen clearly in Figure 3.13.

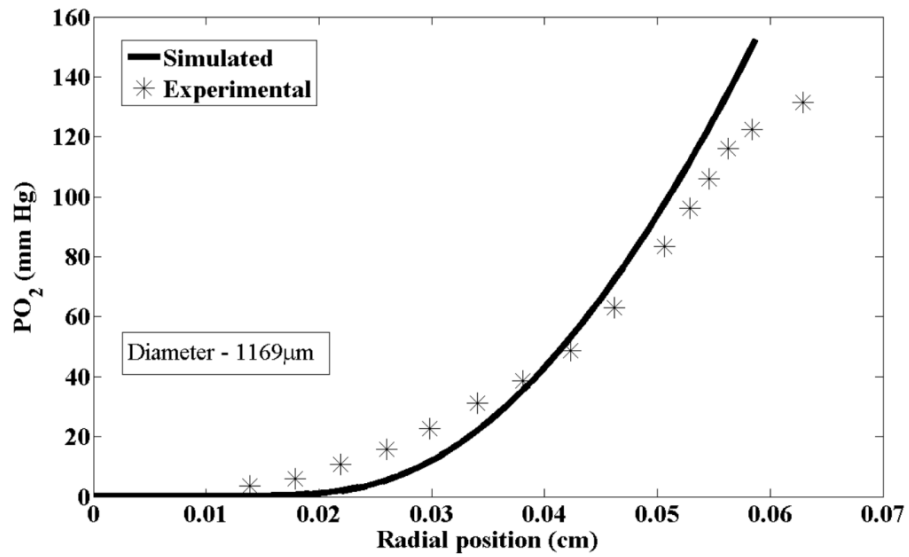


Fig. 3.8. Profile of partial pressure of oxygen (PO_2) in the HT29 spheroids when its diameter is 1169 μm

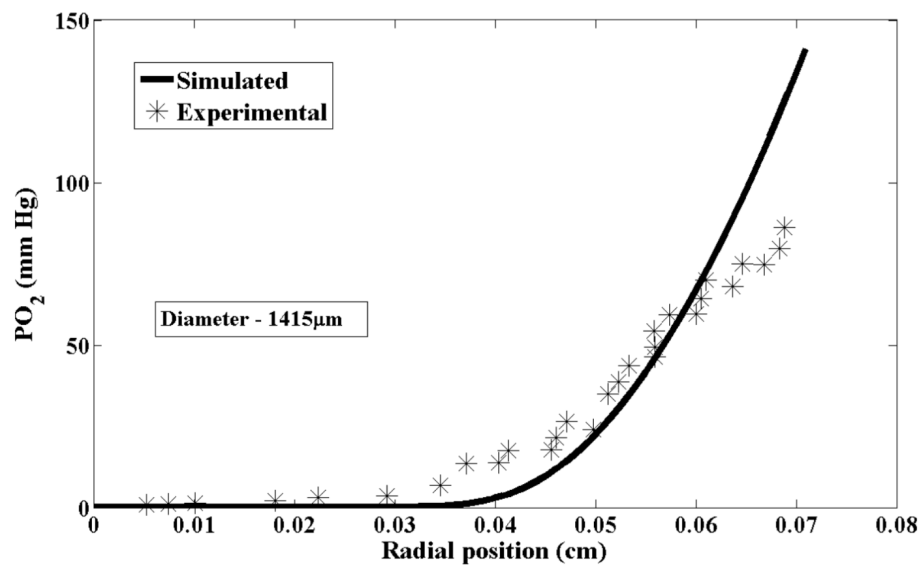


Fig. 3.9. Profile of partial pressure of oxygen (PO_2) in the HT29 spheroids when its diameter is 1415 μm

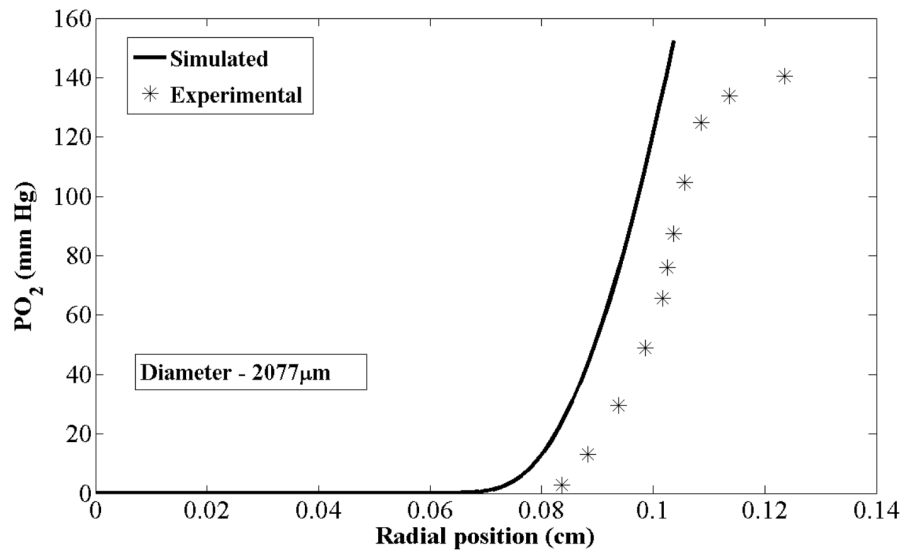


Fig. 3.10. Profile of partial pressure of oxygen (PO_2) in the HT29 spheroids when its diameter is $2077\mu m$

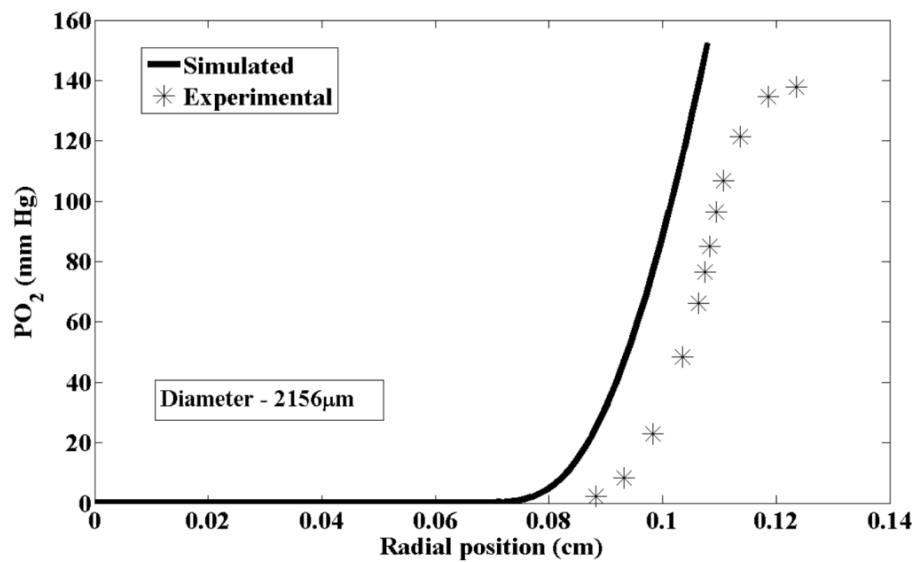


Fig. 3.11. Profile of partial pressure of oxygen (PO_2) in the HT29 spheroids when its diameter is $2156\mu m$

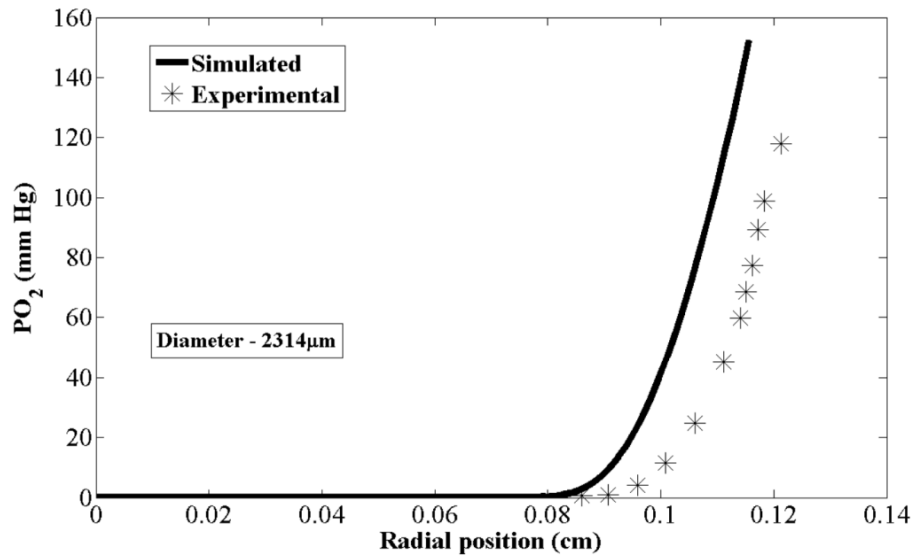


Fig. 3.12. Profile of partial pressure of oxygen (PO_2) in the HT29 spheroids when its diameter is $2314 \mu m$

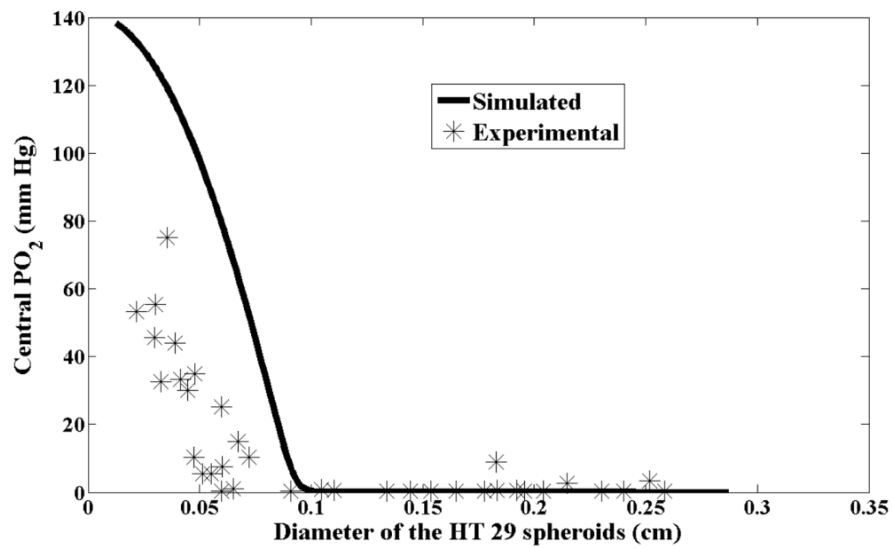


Fig. 3.13. Variation of partial pressure of oxygen (PO_2) at the centre of the HT29 spheroids with the increase in its diameter

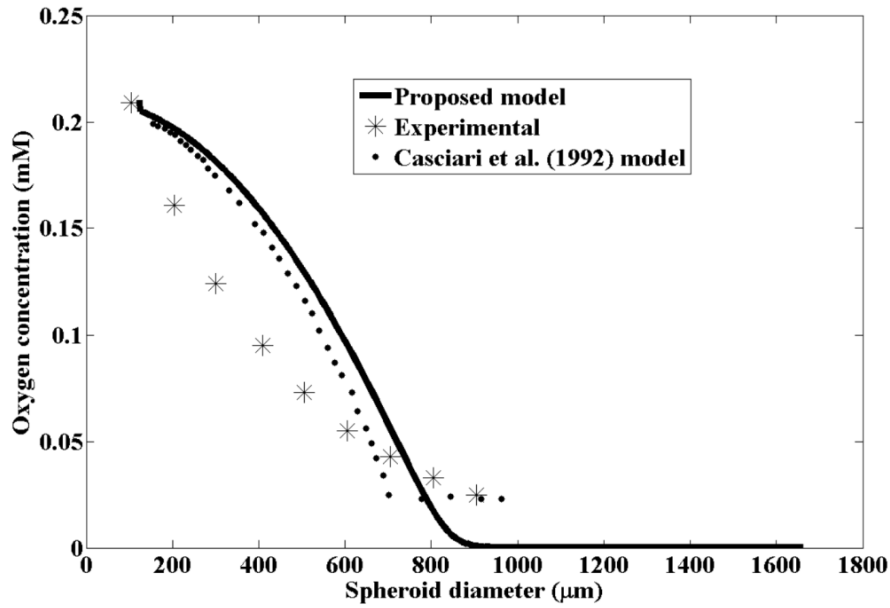


Fig. 3.14. Comparison between the proposed model and Casciari et al. (1992) model on the basis of variation of oxygen concentration at the centre of the EMT6/Ro spheroids with the increase in its diameter

3.4.3 Comparison with Casciari et al. (1992) model

Casciari et al. (1992) validated their model with the experiment results of Mueller-Klieser and Sutherland (1982), where EMT6/Ro spheroids were cultured in 500 ml Bellco flasks containing 300 ml BME with 15% fetal bovine serum, 0.21 mmol/L oxygen and 5.5 mmol/L glucose. The proposed model is now tested with the same experimental results - the result is shown in Figure 3.14. The discrepancy between the model and the experimental results at the lower spheroid diameter is due to assumption that the concentration of nutrients at the surface is equal to that in the bulk medium. However, the model is able to capture the decreasing nature of the oxygen concentration at the centre even for spheroid diameter beyond 700 μm as in the experimental results, which is not seen in the Casciari et al. (1992) model. Note that the proposed model is simpler than the Casciari et al. (1992) model but can provide better representation of the experimental data in some regions.

Table 3.3
Values of the parameter k_1 of Gompertzian empirical relation

External oxygen concentration (mmol/L)	External glucose concentration (mmol/L)	k_1 (1/day)
0.28	16.5	9.12
	5.5	7.86
	1.7	8.1
	0.8	6.56
0.07	16.5	7.03
	5.5	5.05
	1.7	6.28
	0.8	3.81

3.4.4 Comparison with parameters of Gompertzian relation based on experimental data (Burton, 1966)

Gompertzian relation is given by:

$$\frac{v}{v_0} = \exp(k_1(1 - \exp(-k_2t))) \quad (3.7)$$

where, v_0 is the initial volume of the tumor, v is the volume of the tumor at any time, and k_1 and k_2 are the Gompertzian parameters.

According to Burton (1966), the value of k_1 ranges from 6.1 to 16.7 - this is based on the fitting of Gompertzian relation on experimental tumor growth data of around 18 different tumors. In Burton (1966), a Gompertzian relation was fitted to the data (obtained from the model reported therein) and k_1 was determined to be around 8. This model assumed that oxygen is the only nutrient and its consumption rate is constant. As stated earlier, these assumptions are not realistic (Freyer and Sutherland, 1985). Using the proposed model, the values for tumor volume at different times is generated for various combinations of nutrient concentrations considered in. The tumor volume versus time data was used in Equation (3.7) to estimate the parameters k_1 and k_2 . Table 3.3 shows that most of the estimated values of k_1 are in good agreement with the literature values (6.1 - 16.7) indicating the validity of

the proposed avascular tumor growth model. The exceptions occur at the lower value of external oxygen concentration when the external glucose concentration is 5.5 mmol/L or 0.8 mmol/L .

3.5 Conclusions

In this chapter, a new mathematical model for avascular tumor growth was introduced. It is mechanistic and considers all the relevant cellular process (proliferation, apoptosis and necrosis) and their dependency on the diffusion and consumption of the nutrients. The model is simple yet powerful. It was successful in capturing the tumor growth and the maximum volume achieved under different media conditions. On the basis of the results of onset of necrosis, the proposition that necrotic zone is observed when the concentrations of both vital nutrients are below their critical values appears to be true. Moreover, the model is predictive in identifying the size of proliferation zone, quiescent zone and necrotic zone and their effect on the overall tumor growth. Therefore, the proposed model can be a supporting tool for tumor pathologists in determining tumor growth relevant parameters corresponding to the tumor sample extracted from the patients.

Chapter 4

SEQUENTIAL SCHEDULING OF CANCER IMMUNOTHERAPY AND CHEMOTHERAPY USING MULTI-OBJECTIVE OPTIMIZATION

*‘We must develop knowledge optimization initiatives to leverage our key
learnings.’*
- Scott Adams

4.1 Introduction

In the previous chapter, the utility of spatio-temporal models in diagnostic procedures were discussed, while from this chapter onwards, the focus is on using functional models to develop therapeutic strategies. In general, the objectives of any therapy or combination of therapies are to minimize the total number of cancer cells by maintaining it below the lethal level while minimizing the side effects. In this chapter, the main contribution is the therapeutic protocol analysis for a given patient and given time horizon using multi-objective optimization.

Chemotherapy is one of the prominent treatment modalities of cancer and generally, all cancer patients undergo chemotherapy at some stage of their treatment. However, it is not always a comprehensive solution as an adjuvant therapy or as a prime therapy for tumor regression. Therefore, chemotherapy is administered to the patient in synergistic combination with the other treatment modalities such as immunotherapy in order to eliminate the tumor. In the present chapter, chemotherapy using doxorubicin and its combination with adoptive-cell-transfer therapy (ACT) is

considered. ACT is one immunotherapy scheme where the recognized anti-tumor T-cells are cultured externally and administered to the patient (Ho et al., 2003; Dudley and Rosenberg, 2003; Rosenberg et al., 2008). Practically, ACT has proved its worth by causing tumor regression in patients with melanoma or lymphoma (Dudley et al., 2002).

An *in silico* pharmacokinetic/pharmacodynamic model describing the interaction between tumor cells, immune cells and doxorubicin is used to formulate a multi-objective optimization problem by considering clinically relevant objectives and constraints. Then, the multi-objective optimization problem is solved using a Pareto based approach known as non-dominated sorting genetic algorithm (NSGA-II) (Deb et al., 2000) for different cases in order to discover a therapeutically efficacious treatment regimen. Then, a systematic post analysis is performed using L_2 norm method (Kasprzak and Lewis, 2001) in order to choose and recommend an appropriate solution from the Pareto set obtained from NSGA-II. The chosen solution can be considered as the optimal compromise solution, because the optimal solution for one objective may not be the optimal solution for the other objective(s). The details about these methods are provided in the later part of this chapter. In this chapter, the main focus is on the comparison of the efficacy of the chemotherapy alone and its combination with ACT.

4.2 Mathematical model

Tumor-immune interaction models explain interactions between different type of immune cells and tumor cells. There are many tumor-immune interaction models as discussed in chapter 2. The model employed in this chapter is taken from the work of Kuznetsov et al. (1994) because it is the mother model for tumor-immune interactions. It explains different phenomena of tumor-immune interactions like sneak-through and tumor dormancy. “Sneak-through” is the phenomenon in which immune system evades tumor. In tumor dormancy phase, tumor size remains con-

stant with almost no increase in the number of tumor cells. The assumptions of the model are that the tumor is immunogenic and is not metastasized. Here, all immune cells (natural killer cells and cytotoxic T-cells) are considered as effector cells and the tumor growth follows the logistic equation. The interaction between the tumor cells and effector cells is assumed to follow a kinetic scheme in which effector cells interact with the tumor cells and form effector-tumor conjugates which later transform to inactivated effector cells or lethally-hit tumor cells. The parameters of the model were estimated based on the experimental data of B-lymphoma BCL1 in the spleen of the mice (Siu et al., 1986). The activity of the chemotherapeutic drug is included in the model (Martin, 1992). In the following equations, the symbols $E(t)$, $T(t)$, and $M(t)$ represent the number of effector cells, tumor cells and chemotherapeutic drug concentration respectively. It is assumed that the drug reaches the tumor location very quickly after its intervention. Therefore, its transport from the point of injection to the tumor location is negated.

$$\frac{dE}{dt} = s + \frac{pET}{g+T} - mET - d_1E + s_1 - J(M)E \quad (4.1)$$

$$\frac{dT}{dt} = aT(1 - bT) - nET - L(T, M) \quad (4.2)$$

$$\frac{dM}{dt} = u - \gamma M \quad (4.3)$$

$$\left. \begin{aligned} L(T, M) &= k(M - M_{th}) H(M - M_{th}) T \\ J(M) &= K_l(1 - e^{-M}) H_1(M - M_{max}) \end{aligned} \right\} \quad (4.4)$$

where, H is the Heaviside function:

$$\begin{aligned} & \text{if } (M - M_{th}) < 0, \text{ then } H = 0, \\ & \text{if } (M - M_{th}) \geq 0, \text{ then } H = 1, \\ & \text{if } ((M - M_{max}) \geq 0), \text{ then } H_1 = 1, \\ & \text{if } ((M - M_{max}) < 0), \text{ then } H_1 = 0 \end{aligned}$$

Table 4.1
Parameter values (Kuznetsov et al., 1994; Martin, 1992)

Parameter	Value	Unit
a	0.18	day^{-1}
b	2.0×10^{-9}	$cells^{-1}$
n	1.01×10^{-7}	$day^{-1}cells^{-1}$
k	8.4×10^{-3}	$day^{-1}[D]^{-1}$
M_{th}	10	$[D]$
γ	0.27	day^{-1}
s	1.3×10^4	$cellsday^{-1}$
p	0.1245	day^{-1}
g	2.019×10^7	$cells$
m	3.422×10^{-10}	$day^{-1}cells^{-1}$
d_1	0.0412	day^{-1}
M_{max}	50	$[D]$
U_{max}	51	$[D]day^{-1}$
S_{1max}	10^7	$cells$

$[D]$ is the Chemotherapeutic drug (doxorubicin) concentration

Initial conditions

$$E(0) = 3.2 \times 10^5, T(0) = 1 \times 10^{10}, M(0) = 0$$

In Equation (4.1), ‘ s ’ (a fraction of the total lymphocytes in the body) is the natural flow rate of effector cells to the tumor location (non-stimulated by tumor presence). The second term with parameters ‘ p ’ and ‘ g ’ in Equation (4.1) corresponds to the accumulation of effector cells due to stimulation by cytokines (such as interleukin) released from the effector cells that are in contact with tumor cells. Effector cells degrade as a result of their natural life time (d_1E) and their exhaustive interaction with the tumor cells (mET). Biologically, this term denotes the impairment of the effector cells functionality due to their continuous stimulation by the tumor antigens. This could be due to the release of anti-cytokine molecules by tumor cells which reduce the concentration of the cytokines required for the activation of the effector cells. ‘ s_1 ’ is the input rate of externally administered anti-tumor effector cells. $J(M)E$ denotes the elimination of the effector cells when the chemotherapeu-

tic drug concentration exceeds the M_{max} value (Equation (4.4)) where k is the rate of elimination of the effector cells. In Equation (4.2), ‘ a ’ is the maximal growth rate of the tumor cells and it incorporates both their proliferation and death rates whereas ‘ $1/b$ ’ is the carrying capacity of the tumor cells, where $aT(1 - bT)$ signifies tumor growth because of nutrients such as glucose and oxygen without the effect of immune response. The tumor cells are killed by their interaction with effector cells and chemotherapeutic intervention. The pharmacokinetics of the chemotherapeutic drug is illustrated by Equation (4.3) where ‘ u ’ is its input rate and ‘ γ ’ is its decay rate. The pharmacodynamics of the drug is indicated by $L(T, M)$, where it is clarified that the drug can have predominant effect on tumor cells only if its concentration is more than the threshold concentration (M_{th}) (Equation (4.4)). K_l is the rate of elimination of tumor cells due to the chemotherapeutic drug. The parameter values are given in Table 4.1. Another assumption is that parameters of the patient model do not change significantly during the treatment horizon. As a result, the problem of treatment protocol design can be solved as an open loop optimal control problem using the integrated model to explore the efficacious and endurable possibility for tumor regression. The three basic assumptions regarding the delivery of chemotherapeutic drug are:

- (a) Intravenous injection of the drug
- (b) Instantaneous mixing of the drug with the plasma
- (c) the time taken by the drug to reach the tumor site is negligible.

4.3 Multi-objective optimization

Multi-objective optimization (MOO) is the optimization of two or more conflicting objectives of a physical system represented in the form of a mathematical model subjected to some known constraints. MOO is widely used in many fields such as process design, aerospace, medical applications, and automobile design. Unlike

single objective optimization, one gets a set of solutions known as Pareto-optimal set with multi-objective optimization. The decision maker will have the freedom to choose a solution based on his/her experience and acquaintance with the system (Tamaki et al., 1996). The goal of the multi-objective optimization is to find the Pareto set. There are many methods to find the Pareto solutions - e.g. weighted sum method, ε - constraint method (Nemhauser et al., 1989), non-Pareto and Pareto based evolutionary algorithms (Tamaki et al., 1996). In the present work, a Pareto based approach known as non-dominated sorting genetic algorithm (NSGA-II) implemented in MATLAB (R2007a) is used. This algorithm is preferred over other multi-objective algorithms (Pareto-archived evolution strategy (PAES) and strength Pareto evolutionary algorithm (SPEA)) in terms of elitism and computational complexity (Deb et al., 2000).

4.3.1 Non-domination set (Pareto set)

Let us assume that there are ' n ' decision variables and ' p ' objectives. MOO tries to find a point $x = (x_1, \dots, x_n)$ which minimizes (or maximizes) the values of the objective functions $f = (f_1, \dots, f_p)$ within the feasible region F of x .

Definition (Tamaki et al., 1996): Let $x^0, x^1, x^2 \in F$

x^1 is said to be dominated by (or inferior to) x^2 , if $f(x^1)$ is partially greater than $f(x^2)$

$f_i(x^1) \geq f_i(x^2), \forall_{i=1, \dots, p}$ and $f_i(x^1) > f_i(x^2), \exists_{i=1, \dots, p}$.

x^0 is the Pareto-optimal (or non-dominated), if there doesn't exist any $x \in F$ such that x dominates x^0

4.3.2 NSGA-II

The schematic representation of non-dominated sorting genetic algorithm (NSGA) is shown in Figure 4.1. First, the population size and the stopping criteria (e.g. the maximum number of generations) are provided. Then, the population is initialized

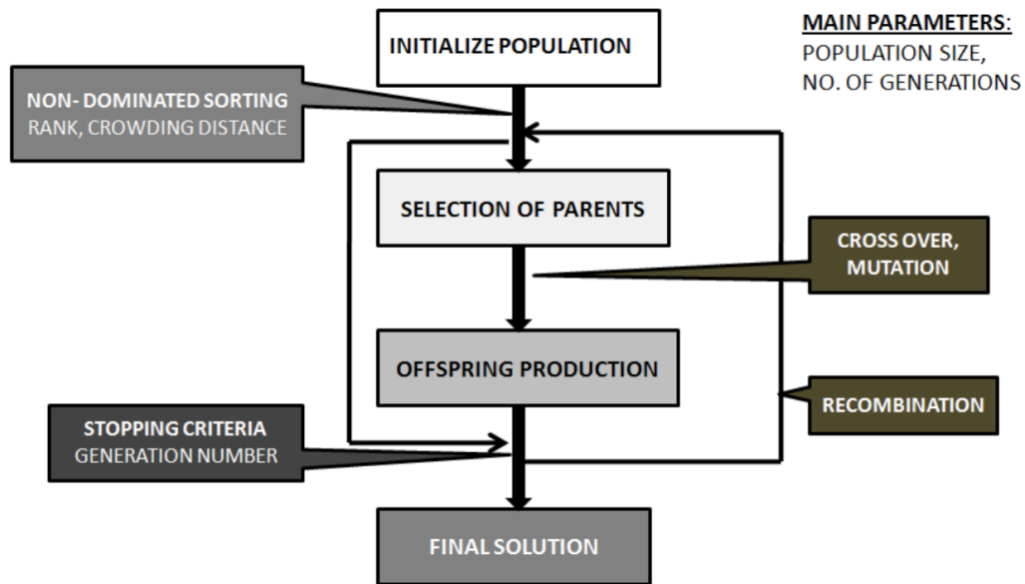


Fig. 4.1. Schematic representation of NSGA-II

randomly within the bounds of the decision variables. The initialized population is sorted out based on the non-domination criteria into different fronts. Parents from this population are selected based on two metrics namely rank and crowding distance. The members of the first front completely belong to the non-dominant set, the second front members are dominated only by the first front and so on. Each individual of the population is assigned a rank (fitness) based on the front in which they are present. Individuals in the first front are assigned rank 1 and in the second front are assigned rank 2 and so on. Crowding distance is a metric that measures the closeness of the individuals to its neighbors. A larger crowding distance is preferred to maintain diversity in the population. Individuals are selected as parents based on the rank value; if two individuals have the same rank, then their crowding distance is considered (a larger crowding distance is preferred). Parent population is sent through the genetic operators such as crossover and mutation to generate the child population. The child population is combined with the current generation population. This is called as recombination. These steps are repeated to produce next generation child population. Elitism of the algorithm is assured, since the previous

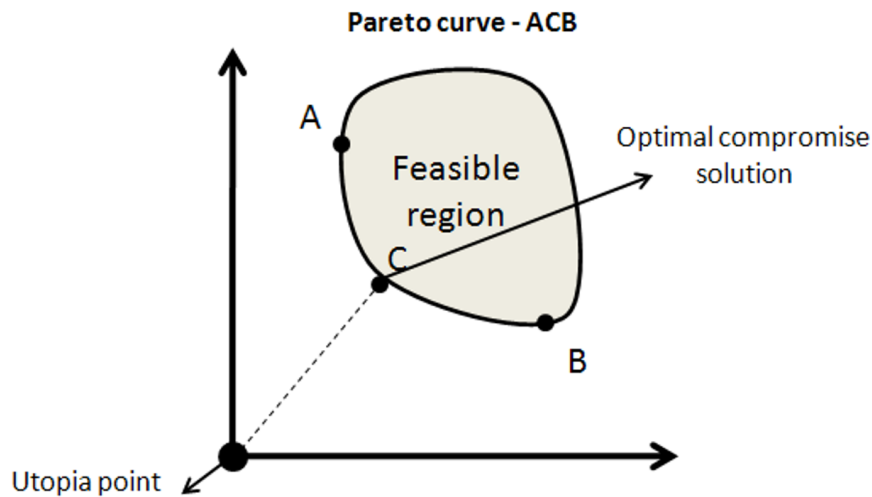


Fig. 4.2. L_2 norm method

and current best individuals are added in the population. The same procedure is continued until the GA evolves to the maximum number of generations. Overall, the prominent tuning parameters in this algorithm are the number of generations, probabilities for crossover and mutation processes. Matlab implementation of NSGA-II can be easily obtained in the internet. The main challenging task in this algorithm is the choice of population size and maximum number of generations. Generally, higher the population size and the number of generations are preferred. However, it is computationally intensive. In this work, the population size and the number of generations are chosen based on the iterative preliminary runs of the optimization problem.

4.3.3 Post-Pareto-optimality analysis

In the literature, there are many methods for post-Pareto-optimality analysis such as clustering techniques, ranking techniques and distance based methods such as L_2 norm. Here, L_2 norm method involving the concept of utopia point is used to find the optimal compromise solution (Kasprzak and Lewis, 2001). Utopia point is the theoretically best performance point; in our case, the origin is assumed as

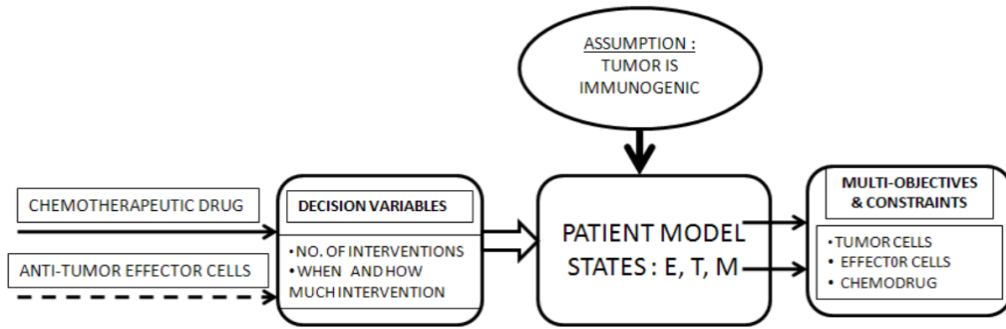


Fig. 4.3. Schematic representation of the problem

the utopia point because the target of giving therapy is to completely eliminate the tumor cells with no drug overload. Hence in accordance with L_2 norm method, the optimal compromise design point is the one which lies on the Pareto frontier and is geometrically nearest to the utopia point (Figure 4.2).

4.4 Problem formulation

The main objective of this work is to determine the optimal time of intervention, type of intervention (chemo or immune) and dosage level of the intervention to achieve a desired and controlled tumor evolution. Figure 4.3 shows the inputs and outputs of this system. The therapeutic agents considered here are doxorubicin and anti-tumor effector cells. In general, oncologists try to attain multiple objectives (e.g. eradication of tumor cells while minimizing the side effects of the drugs) when they treat cancer patients. Oncologists prefer to give treatments in cycles within a stipulated course period. The time period of the cycles are chosen in such a way that the patient would be able to recoup from the effects of the drug administered in the previous cycle. Usually, the side effects are evaluated using the count of blood cells such as neutrophils and platelet cells. Presently, in the standard clinical practice the average cycle time for various chemotherapeutic agents is around three to four weeks and the duration time of the clinical treatment varies from months to a year (Rose, 2005). In this work, the cycle time is assumed to

be four weeks and stipulated course period (t_f) as 1 year. Therefore, the total number of therapeutic interventions (N) is taken as 12. Keeping in view the usual objectives of the oncologists, multiple (three) objectives (McCall et al., 2007) and the constraints to be satisfied for the therapeutic interventions are considered. The objectives considered are listed and discussed next. Mathematically, objective 1 corresponds to minimizing the area under the tumor profile as shown in Figure 4.4. However, with only objective 1, desired results may not be ensured because it may so happen that the number of tumor cells may shoot up to a very high value at any point of time, even while remaining at low values during the rest of the treatment period. Such abrupt increases in the concentration of the tumor cells may lead to further stages of cancer such as vascularization and metastasis. At these stages, the disease is very difficult to treat. In order to handle this issue, the minimization of objectives 2 and 3 are also considered. Objective 2 corresponds to the tumor size on the final day of the stipulated course period which is practically expected to be very low value. Objective 3 controls the maximum possible tumor size throughout the stipulated course time. The incorporation of constraints (ii-iv) in the problem formulation prevents the side effects due to doxorubicin. Constraints (ii) and (iii) are related to input rate and maximum concentration of doxorubicin respectively. High drug concentrations (beyond the safe limits, i.e., greater than M_{max}), could destroy neighboring normal tissues and the patients may experience undesirable side effects. Practically, constraints (ii) and (iii) imply the instantaneous and short-term effects of the drug. Constraint (iv) is a measure of drug clearance in the body. It physically interprets the long-term effect of the drug on the organs such as the heart or liver and the blood cell count. Constraint (vii) conveys that the minimum value of tumor size should be more than or equal to 1 tumor cell. If this is not taken into account, the tumor size will go to a negligibly low value (10^{-20}) which is due to the continuous nature of state variable. Mathematically, the lower value may sound good; however, it has no medical significance.

Objectives

Objective 1: $\min \int_0^{t_f} T(t) dt$

Objective 2: $\min (T(t_f))$

Objective 3: $\min (T_{\max})$

Constraints

(i) : Equations (4.1) through (4.4) i.e. the mathematical model

(ii) : $0 \leq u(t_i) \leq u_{\max}$

(iii): $0 \leq M(t) \leq M_{\max}$

(iv) : $\int_0^{t_f} M(t) dt \leq 4100$

(v) : $t_f = 1$ year

(vi) : N (no. of therapeutic interventions) = 12

(vii): $\min(T(t)) \geq 1$

where, t_i is the intervention time and u_{\max} is the upper bound on the input rate of doxorubicin

In this chapter, the comparison of the efficacies between chemotherapy and its combination with ACT is particularly sought using the above problem formulation. In the case of combination therapy, the number of immunotherapeutic interventions are regarded as a decision variable as well and determined the optimum number of immunotherapeutic interventions required to replace the chemotherapeutic interventions while satisfying all the constraints.

4.4.1 Non-dimensionalization

Model equations (4.1-4.3) are non-dimensionalized in order to simplify the implementation of the optimization method. The reference values of effector cells (E_r), tumor cells (T_r), and chemotherapeutic drugs (M_r) are chosen in such a way that the input rate of externally administered effector cells and chemotherapeutic drug range between 0 and 1. Then, the non-dimensionalized model is crosschecked by comparing the evolutions of tumor and effector cells with the original model for the given initial conditions (as shown in Figure 4.4). The transformed model is as shown below (Equations (4.5 - 4.8)).

$$\frac{dE^\bullet}{dt} = s^\bullet + \frac{pE^\bullet T^\bullet}{g^\bullet + T^\bullet} - m^\bullet E^\bullet T^\bullet - d_1 E^\bullet + s_1^\bullet - J(M^\bullet)E^\bullet \quad (4.5)$$

$$\frac{dT^\bullet}{dt} = aT^\bullet(1 - T^\bullet) - n^\bullet E^\bullet T^\bullet - L(T^\bullet, M^\bullet) \quad (4.6)$$

$$\frac{dM^\bullet}{dt} = u^\bullet - \gamma M^\bullet \quad (4.7)$$

$$\left. \begin{aligned} L(T^\bullet, M^\bullet) &= k(M^\bullet M_r - M_{th}) H(M^\bullet M_r - M_{th}) T^\bullet \\ J(M^\bullet) &= K_l(1 - e^{-M^\bullet M_r}) H_1(M^\bullet M_r - M_{\max}) \end{aligned} \right\} \quad (4.8)$$

$$E^\bullet = \frac{E}{E_r}, T^\bullet = \frac{T}{T_r}, M^\bullet = \frac{M}{M_r}, s^\bullet = \frac{s}{E_r}, g^\bullet = gb, m^\bullet = \frac{m}{b}, s_1^\bullet = \frac{s_1}{E_r}, n^\bullet = nE_r, u^\bullet = \frac{u}{M_r}$$

where, $E_r = 1 \times 10^7$ cells, $T_r = 1/b = 5 \times 10^8$ cells, $M_r = 51 [D]$

4.5 Results and discussion

4.5.1 Case 1: Chemotherapy

In this case external interventions of doxorubicin alone are considered. The problem formulation of multi-objective optimization problem is implemented in MAT-

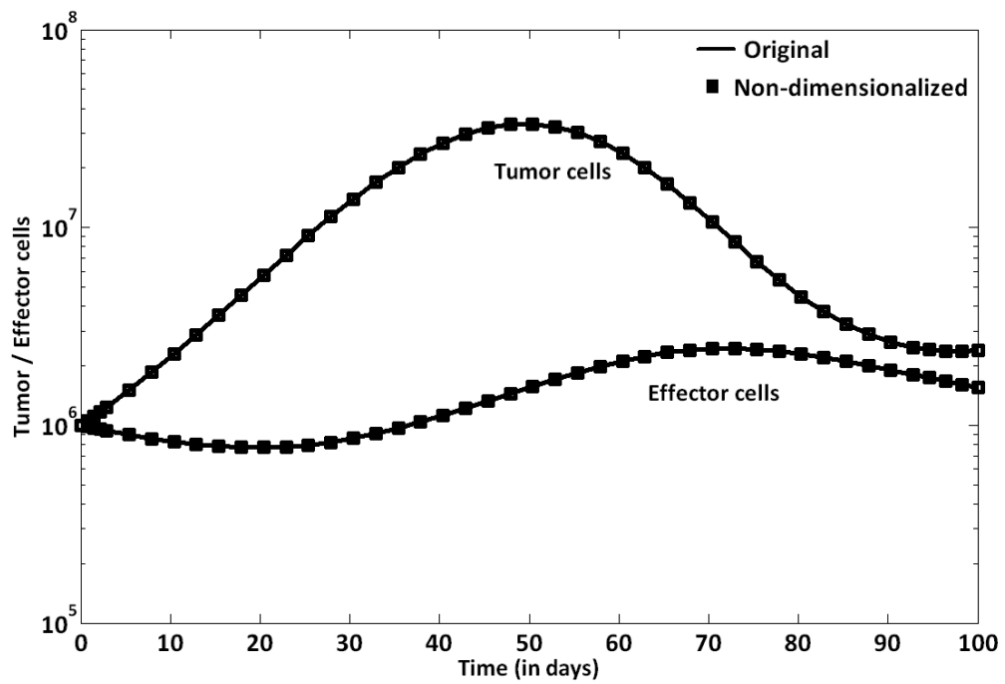


Fig. 4.4. Comparison between original and non-dimensionalized model

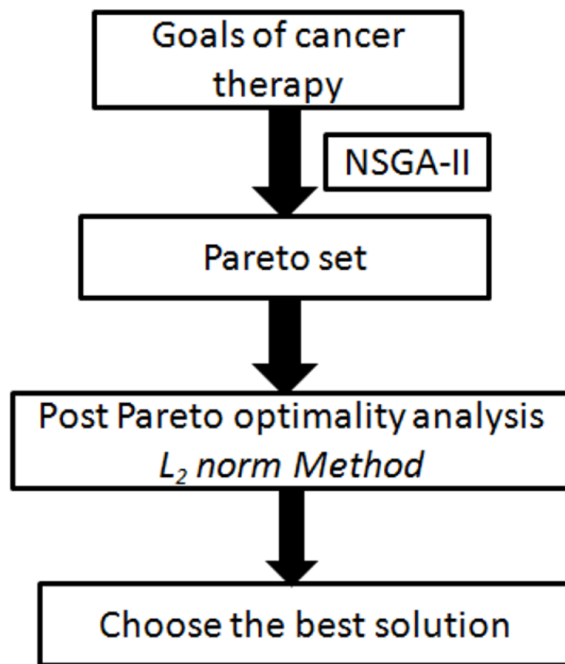


Fig. 4.5. Algorithm to find the optimal compromise solution

LAB (R2007a) and solved to find the timing and dosage of 12 chemotherapeutic interventions within the course time. The population size and number of gener-

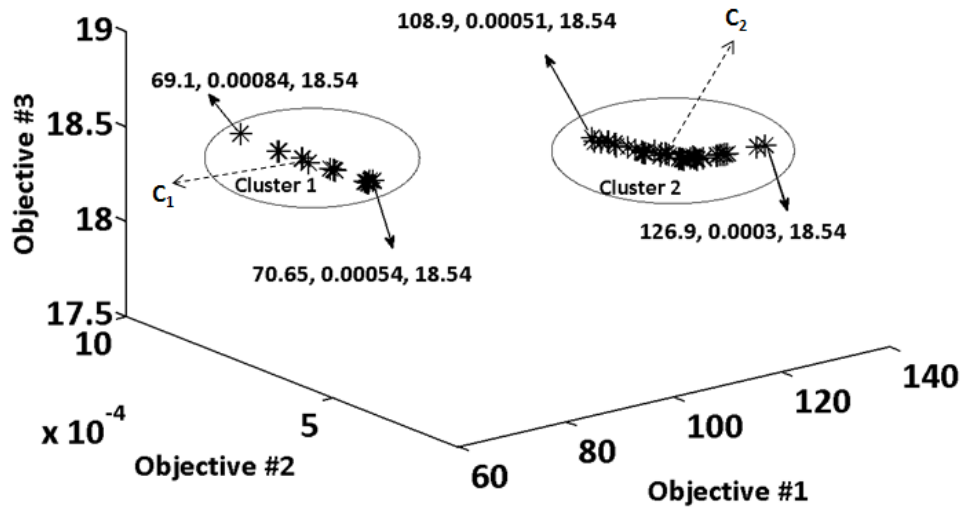


Fig. 4.6. Pareto solutions for the problem formulation for case 1 (i.e. only chemotherapy)

ations in NSGA-II are taken as 100 and 250 respectively. The objectives are as described earlier. The steps to decide the best solution from Pareto solutions are as shown in Figure 4.5. Pareto solution obtained has two clusters as shown in Figure 4.6. Pareto solution highlights that cluster 1 completely favors objective 1 and cluster 2 slightly favors objective 2. Objective 3 is constant and same in both the clusters. The reasons for differences in the clusters are investigated by analyzing the therapeutic design (Intervention timings and profiles of tumor cells, effector cells and doxorubicin) corresponding to the centroids (c_1 and c_2 as shown in Figure 4.6 of cluster 1 and cluster 2. The evolution of tumor cells, effector cells and doxorubicin corresponding to the solutions of the centroid of each cluster is presented in Figure 4.7

In Figure 4.7, the major difference in the tumor profiles is observed between 100th and 150th day and it is due to different intervention timings between 50th and 100th day where the frequency of interventions corresponding to cluster 1 is more than cluster 2. Comparison of the evolution of tumor cells between the two clusters shows that the solutions of cluster 1 will be favorable than cluster 2. Also, the

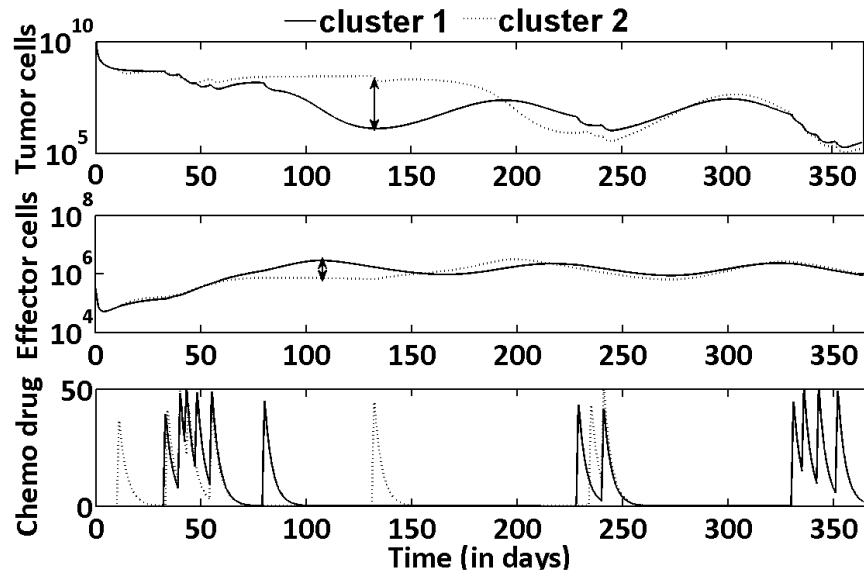


Fig. 4.7. Comparison of evolution of states between cluster 1 and cluster 2

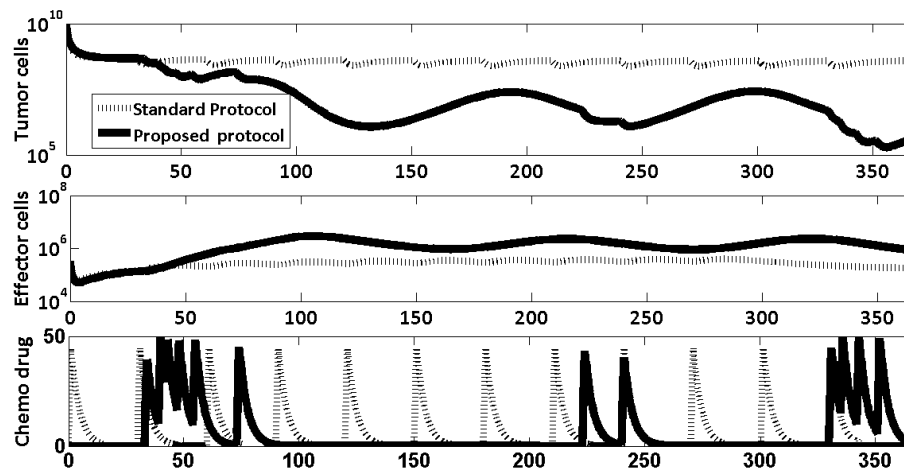


Fig. 4.8. Evolution of states corresponding to the proposed treatment protocol of doxorubicin

optimal compromise solution chosen from the Pareto set using L_2 norm belongs to cluster 1. The evolution of tumor and effector cells corresponding to the finally chosen solution is shown in Figure 4.8 and also it is compared with the standard treatment protocol of doxorubicin where standard dosage (40-50 [D]/day) is given at the beginning of each cycle (Alberts et al., 2002). It is seen in Figure 4.8 that the tumor cells are significantly controlled based on the proposed treatment protocol of doxorubicin than the standard treatment protocol. Also, the evolution of effectors cells corresponding to the proposed solution are maintained at higher level than the standard protocol. In real cases, not all patients are cured with the existing standard protocol. One of the probable reasons could be that it negates the immunogenicity factor (i.e. tumor reduction due to the localization of the effector cells at the tumor site) which is considered in this work. Figure 4.8 shows that even though the tumor cells are eliminated to an extent with the proposed protocol, the effect of chemotherapeutic drug is not sufficient. That is the tumor size at the end of the course time is in the order of 10^5 cells which is more than the cure level ($10^3 - 10^4$ cells) (McCall et al., 2007; Khaloozadeh et al., 2009). Cure level is the level of tumor cells which can be eliminated with the natural ability of the patient without any external intervention. Also, at this size, tumor is not recognizable ($< 10^9$ cells) even with the available imaging techniques and tumor cells relapses very soon. Finally, tumor relapse may lead to critical stages of cancer. In order to avoid this, more chemotherapeutic drug should be given by increasing the frequency or dosage of chemotherapeutic interventions. However, it is not a viable option because of the constraints. Thus, additional intervention of effector cells along with the chemotherapy may result in complete elimination of the tumor. This leads to the following questions: (i) Out of the 12 interventions, how many interventions should be with effector cells? (ii) What is the optimal dosage of the interventions? and (iii) What are the intervention times during the course period? In the following section, optimal chemo-immune combination therapy administration will be developed.

4.5.2 Case 2: Immune-chemo combination therapy

In this case, an additional objective (objective 4, F_2) related to the number of interventions of effector cells (N_e) is included (Equation (4.9)). However, other objectives and constraints in the problem formulation are same as mentioned in Section 4.4. The minimization of objective 4 is important. Biologically, it means, excessive immune cells may lead to the heavy competition among themselves for the cytokine (Ho et al., 2003). Cytokines are proteins that are the limiting and essential constituents for the persistent activation of cytotoxic lymphocytes.

$$F_2 = N_e \quad (4.9)$$

Overall, in the combination therapy optimization problem, there are 4 objectives, 25 decision variables and 3 constraints. Among the 25 decision variables, there are 24 continuous variables and one integer variable. The integer variable corresponds to the number of immunotherapeutic interventions (which could range from 1 to 12), and the 24 continuous variables relate to the timing (12) and amount (12) of the interventions (either chemotherapy or immunotherapy). The multi-objective optimization is now solved again using NSGA-II with population size and number of generations being 100 and 250 respectively. Finally, a Pareto front comprising of multiple solutions is obtained. As it is a 4-dimensional objective function space, the solution cannot be readily visualized. To make visualization easier, the objectives relevant to tumor cells and effector cells are summarized separately. F_1 corresponds to the distance between the tumor related objectives on the Pareto curve and their values in utopia point. Then F_1 is plotted against F_2 (the number of effector cells interventions) as shown in Figure 4.9 .

$$F_1 = \sqrt{(\text{objective } 1)^2 + (\text{objective } 2)^2 + (\text{objective } 3)^2} \quad (4.10)$$

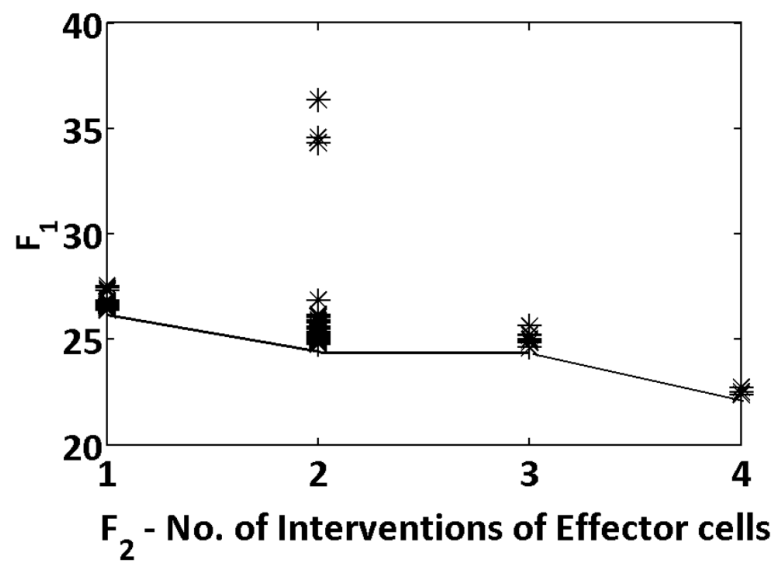


Fig. 4.9. Reduced representation of Pareto solutions for the problem formulation for case 2 (i.e. combination therapy)

The Pareto data set obtained indicates that the maximum value of F_2 is 4 even though the maximum bound for F_2 is specified as 12. This confirms that more than 4 interventions of effector cells may lead to therapeutic burden. In other words, the effect of additional effector cells on tumor regression is negligible. Figure 4.9 shows that the minimum value of F_1 decreases with the increase in number of effector cell interventions and suggests that 4 interventions of effector cells is sufficient for tumor regression within the given course time. Then, the optimal compromise solution is obtained using L_2 norm post-Pareto-optimality analysis method. The treatment protocol corresponding to the optimal compromise solution for the combination therapy is shown in Figure 4.10 and the corresponding progression of tumor cells, effector cells and chemo-drug is presented in Figure 4.11. The tumor cells during and at the end of treatment course are significantly lower in the case of combination therapy than the proposed chemotherapy. The first two consecutive interventions of effector cells are given on first two consecutive days of the course time to immediately check the higher number of initial tumor cells. The maximum dosage of effector cells is given on the first day followed by decreased dosage of the second intervention. This

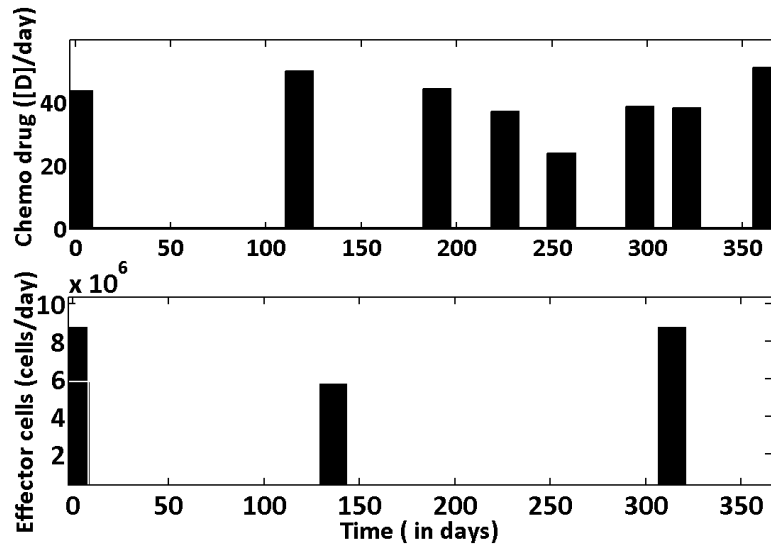


Fig. 4.10. Treatment protocol corresponding to the proposed combination therapy

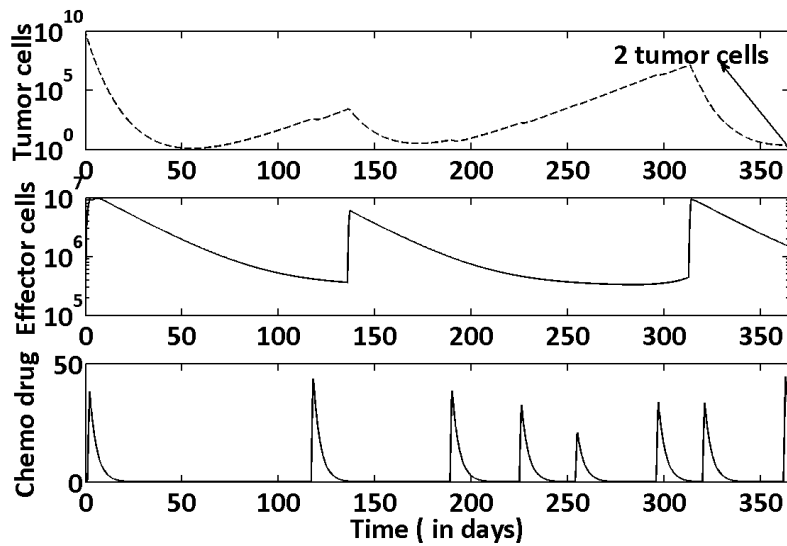


Fig. 4.11. Evolution of states corresponding to the proposed combination therapy

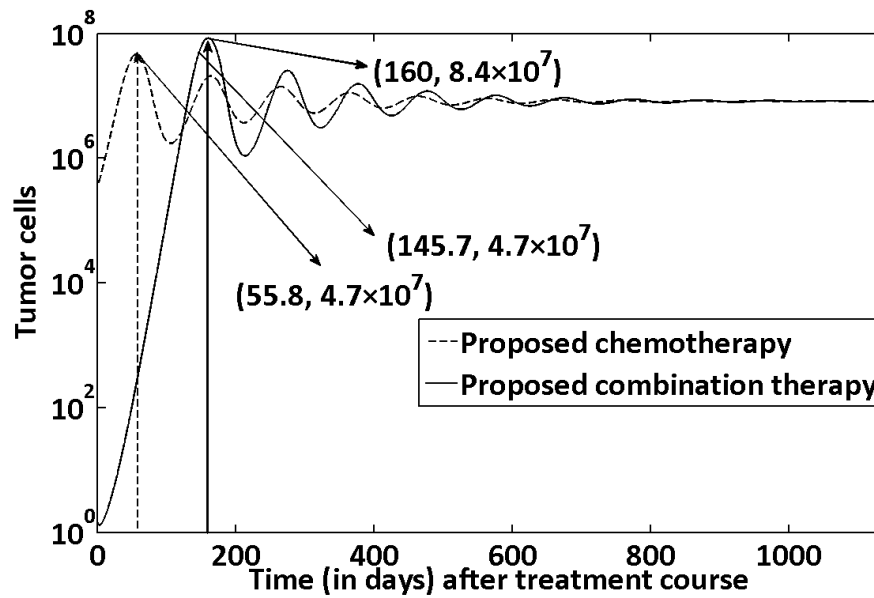


Fig. 4.12. Comparison of tumor relapse time between the proposed chemotherapy and the proposed combination therapy

decrease could be to avoid overdosage and hence therapeutic burden. Instead, the second intervention is accompanied by the maximum dose of doxorubicin to suppress tumor growth. Another interesting observation is the decreasing trend of tumor size until 70 days due to the early interventions and during this period no additional therapeutic interventions are made. The remaining interventions of effector cell and doxorubicin are fairly spread out in time. Moreover, the interventions are made only when the growing phase of tumor cells is detected. Thus, the above features justify the coherency in the proposed combination therapy protocol.

Tumor relapse time (TRT) is considered as another metric to evaluate the effect of the proposed optimal therapeutic strategies in case 1 (chemotherapy only) and case 2 (combination therapy). TRT is defined as the time taken by the tumor to recur and reach peak from its size at the end of the course time. The increase in tumor cells is dangerous and increases the probability of tumor transformation to later stages which limits the efficacy of the therapy (Alberts et al., 2002). A larger value of TRT is better and it indicates patient survival time without interventions.

It is observed in Figure 4.12 that the peak tumor size corresponding to the combination therapy is higher than chemotherapy. This is because of the different ratio of effector cells and tumor cells (E:T) between proposed combination therapy (0.016) and proposed chemotherapy (0.03) at their respective TRTs. Thus, higher ratio (E:T) controls the peak values during tumor progression. Clinically, this suggests that the measurement of the density of effector cells at the tumor location is essential along with blood cell count. Also, the steady state analysis in either case shows no difference in tumor size and time taken to reach steady state after the treatment course. However, TRT for the combination therapy is approximately 3 times more than the chemotherapy (Figure 4.12). Moreover, after combination therapy, it takes an extra 90 days for the tumor to reach the peak value attained with the proposed chemotherapy. Overall, the *in silico* analysis supports that the proposed combination strategy is pragmatic and appears to be effective than chemotherapy alone.

4.6 Conclusions

In this chapter, the main idea was to use multi-objective optimization and post-Pareto-optimality analysis to determine and compare therapeutic strategies for treatment of tumor. Chemotherapy alone and a combination therapy that includes chemotherapy and immunotherapy are considered. The multi-objective functions chosen for achieving the satisfactory tumor reduction and the total number of therapeutic interventions are based on the accepted medical protocols and current clinical practice. The simulation results indicate that the performance of the proposed chemotherapy protocol is better than the standard protocol and suggests taking into account the immunogenicity factor prior to every therapeutic intervention. However, chemotherapy alone is not sufficient for eradicating the tumor in the stipulated course time of one year. Additional intervention of effector cells (i.e. immunotherapy) is required for satisfying all the objectives of the problem. Using

the L_2 norm method to find the optimal compromise solution from the Pareto set, it is seen that four immunotherapeutic interventions out of twelve interventions is a better option for treating tumors. More than four immunotherapeutic interventions lead to unnecessary therapeutic burden with negligible improvement in patient condition. The results suggest that the first two interventions of effector cells should be at the early phase of the course time in order to control the tumor cells. Then, remaining interventions are suggested whenever there is a steep rise in the tumor profile. Thus, the intervention timings seem rational. TRT value is also significantly better for the combination therapy. In broader sense, this chapter highlights that optimization techniques implemented in the treatment planning simulators can support the oncology pharmacists in determining and analyzing the therapeutic schedule of a given therapy. In this chapter, it was assumed that the variation of the patient parameters is negligible. However, in the next chapter, inpatient variability is accounted during the treatment and applied the optimization techniques to guide immunotherapy.

Chapter 5

MODEL-BASED SENSITIVITY ANALYSIS AND REACTIVE SCHEDULING OF DENDRITIC CELL THERAPY

*‘Sensitivity analysis for modellers? Would you go to an orthopaedist
who didn’t use X-ray?’
- Jean-Marie Furbringer*

5.1 Introduction

Inpatient variability is a key challenge in cancer treatment. This makes it necessary to find the factors affecting tumor growth and accordingly schedule therapies over the treatment horizon for a given patient. In this chapter, model-based studies are performed to investigate these issues for optimal immunotherapeutic intervention. Dendritic cell therapy is a targeted immunotherapy where the dendritic cells and its activating agents such as interleukin are engineered, stimulated to recognize and specifically to eradicate tumors. A mathematical model that integrates tumor dynamics and dendritic cell therapy is used to perform the analysis. Unlike the previous chapter, in this chapter different types of immune cells are explicitly considered instead of assuming all of them as effector cells. Global sensitivity analysis of the model is done using high dimensional model reduction (HDMR) technique followed by variance based analysis and the key parameters altering the tumor growth are identified. The variations in these key parameters are deemed to result in inpatient variability during the treatment phase. Then, reactive scheduling is used

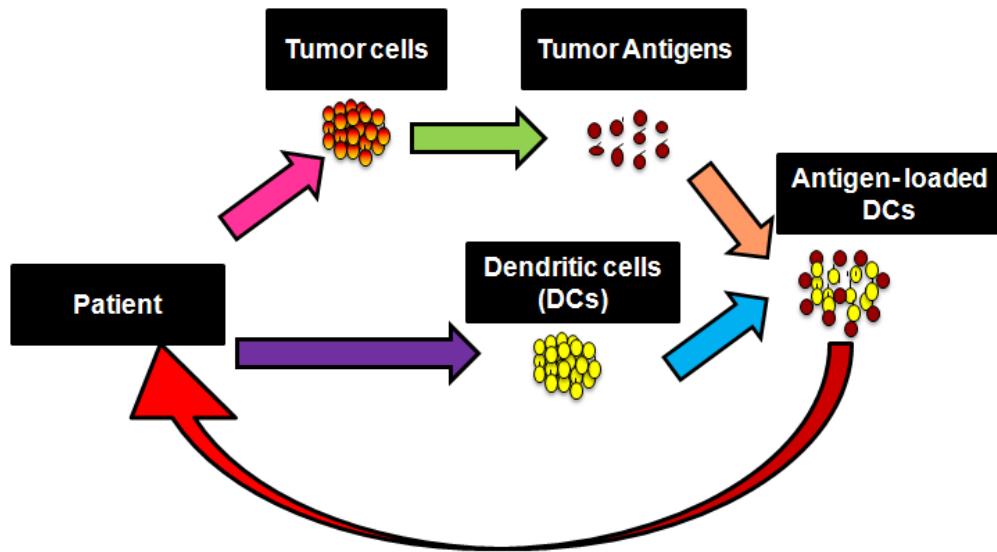


Fig. 5.1. Dendritic cell/Vaccine therapy

to schedule dendritic cell interventions with and without interleukin interventions under the varying conditions of the patient. Moreover, the key parameters obtained from HDMR are verified using the reactive scheduling and nominal scheduling approaches. Besides saving costs, the *in silico* analysis done in this chapter may be useful to the oncology community in designing experiments to clinically measure the influential parameters.

5.1.1 Dendritic cell therapy

Dendritic cells (DC) are the professional antigen presenting cells which are present in small amounts in the blood and almost every tissue. They work at the interface between the peripheral tissues and lymphoid organs and induce the T-cell mediated immune response. In dendritic cancer vaccine (DCV) therapy, dendritic cells are fused with tumor associated antigens to mature and transform to antigen-loaded dendritic cells (Ballestrero et al., 2008; Banchereau et al., 2001; Nencioni et al., 2008). Then, these matured dendritic cells are injected back to the patient (see Figure 5.1). Tumor associated antigens can be of different forms (DNA, RNA,

proteins, peptides, killed tumor cells and cell lysates). Overall, the main parameters of DCV are type of DC subset and its maturation, dosage, frequency and route of injection of DC. Like other therapies, higher frequency of DC dosage might lead to activation-induced death of T-cells. Even the induced cytotoxic T-cells may kill DCs. In either case, efficacy of the vaccine reduces. In order to overcome this, oncologists are proposing combination therapies, presuming their synergistic action on the tumor size. In such cases, adjuvant therapy such as interleukin therapy can be given to maintain the prolonged activity of the T-cells (Banchereau et al., 2001).

5.2 Scheduling under uncertainty

In the domain of mathematical modeling, system uncertainty is a very important issue. Here, one quantifies the uncertainty in the model output that is generated from the uncertainty in the parameters and input factors (Marino et al., 2008; Saltelli et al., 2008). In model-based approaches, uncertainties of model parameters are considered using different methods such as bounded form, probability description, and fuzzy description (Li and Ierapetritou, 2008*a*). Bounded form and probability description methods are used when the historical data related to parameters are available. Else, fuzzy description is used. A probability description is preferred when specific information about the distribution of parameters is known whereas bounded form is considered only when we know the range of the parameters. However, it is not often that parameter of a biological system has a detailed description. Theoretically, in this case, the problem is solved by assuming that parameters follow a simple probabilistic distribution such as uniform distribution. Scheduling under uncertainty is a challenging problem in technological and biomedical systems. It is broadly classified as preventive scheduling (schedule generation) and reactive scheduling (schedule revision) (Li and Ierapetritou, 2008*a,b*). Preventive scheduling is used when the knowledge of the possible uncertain events are available based on the historical experiences. Thus, in this case, rigorous analysis is made before

implementing the schedule. Different techniques for preventive scheduling include stochastic scheduling, robust optimization, fuzzy programming, sensitivity analysis and parametric programming. Contrastingly, in reactive scheduling or rescheduling, the schedule is regularly updated or modified and adapted to the unexpected disturbances of the system (Li and Ierapetritou, 2008b). It is considered that the present problem of DCV therapy falls under the category of reactive scheduling. This is because patients are regularly monitored by oncologists and the treatment plan may be adjusted based on their condition at the time of their regular check up. If there is any change in patient's condition from what was expected, the treatment schedule is suitably rescheduled. However, there are some shortcomings with reactive scheduling. The prime concern is the reaction time available to make updated decisions. The reaction time varies for different unexpected scenarios. Another important point is that the reactive decisions can be taken only after identifying the reasons for the unexpected scenario. In the language of mathematical modeling, this means unraveling the sensitive parameters responsible for uncertainty in the measurable or observable variables. Taking into consideration the positive and shortcomings discussed above, a hybrid approach that involves global sensitivity analysis (Marino et al., 2008) followed by reactive scheduling is proposed in this chapter. This approach involves the application of global sensitivity analysis of the model to find the prominent parameters and considering uncertainty only in these parameters to perform reactive scheduling. The main assumptions in this study are that the parameters follow uniform distribution and the uncertainty in the output of interest (eg., tumor growth) is only because of variations in the parameters.

5.3 Mathematical model

Among all tumor-immune models, the only work which explicitly includes the activity of dendritic cells is that of Piccoli and Castiglione (2006) and this work is focused on the investigation of DCV therapy scheduling. The model explains the

tumor evolution and its interaction with the helper T-cells (CD4+) and cytotoxic T-cells (CD8+) due to the intervention of externally modified and antigen-loaded dendritic cells. The model assumes that all tumor cells are immunogenic. In other words, tumor cells are recognized by injected dendritic cells and are presented to cytotoxic T-cells. The interactions between the cytotoxic T-lymphocytes and the tumor cells are represented by a kinetic scheme and are presented in the form of ordinary differential equations. The states in the model are denoted by

(a) $H(t)$, helper T-cells (CD4+)

(b) $C(t)$, cytotoxic T-cells (CD8+)

(c) $M(t)$, tumor cells

(d) $D(t)$, dendritic cells

(e) $I(t)$, interleukin

$$\frac{dH}{dt} = a_0 - b_0H + c_0Dd_0\gamma(H, f_0) \quad (5.1)$$

$$\frac{dC}{dt} = a_1 - b_1C + c_1I(M + D)d_1\gamma(C, f_1) \quad (5.2)$$

$$\frac{dM}{dt} = d_2\gamma(M, f_2) - e_2MC \quad (5.3)$$

$$\frac{dD}{dt} = -e_3DC + u_1 \quad (5.4)$$

$$\frac{dI}{dt} = a_4HD - c_4CI - e_4I + u_2 \quad (5.5)$$

where

$$\gamma(x, \theta) = x(1 - x/\theta)$$

The first two terms (a_0 , b_0H) in Equation (5.1) depict the natural flow of helper T-cells to the tumor site (non-stimulated by tumor presence) and their natural decay rate respectively. Similarly, the first two terms (a_1 , b_1C) in Equation (5.2) represent the natural flow rate of cytotoxic T-cells to the tumor site (non-stimulated by tumor presence) and their natural decay rate respectively. The model assumes

that tumor growth follows the logistic equation with the constants d_2 and f_2 . d_2 is the maximal growth rate of tumor cells and f_2 is carrying capacity of tumor cells. These parameters signify tumor growth because of nutrients such as glucose and oxygen without the effect of immune response. The term e_2MC in Equation (5.3) represents pharmacodynamics which means the elimination of tumor cells due to CD8+ T-cells. Equation (5.4) explains the pharmacokinetics (e_3DC) and ‘ u_1 ’ is the input rate of the matured and antigen-loaded dendritic cells. Once the dendritic cells are injected, the CD4+ T-cells, CD8+ T-cells, and interleukins are triggered as shown in Equations (5.1, 5.2 & 5.5) respectively by the following terms ($c_0Dd_0\gamma(H, f_0), c_1I(M + D)d_1\gamma(C, f_1), a_4HD$). In the same way, the second and third terms in Equation (5.5) denote the loss of interleukin (IL-2) as a result of its interactions with CD8+ T-cells and its natural decay respectively and ‘ u_2 ’ is the input rate of externally administered interleukin. Another assumption in the model is that externally administered DCV is the only source of dendritic cells. The parameter values of the mathematical model are given in Table 5.1.

5.4 Global sensitivity analysis

Global sensitivity analysis (GSA) is an approach to identify and quantify the factors (parameters) contributing to the variation in the objective of interest (tumor size). Unlike local sensitivity analysis, the factors are varied simultaneously over a wide range in GSA. Saltelli et al. (2008) describe the different methods that are available to perform GSA based on the *a priori* knowledge of the relationship between inputs and outputs. The measures used for linear relationship between the parameters and the output are Pearson correlation coefficient, partial correlation coefficient and regression coefficient. For monotonic nonlinear relationships, rank based transforms such as Spearman rank coefficient, partial rank correlation coefficient and rank regression coefficient could be considered. Variance based methods (VBM) such as Sobol method, extended Fourier amplitude sensitivity tests (EFAST)

Table 5.1
Parameter values (Piccoli and Castiglione, 2006)

Parameter	Description	Value	Units c=cells, h=hours
a_0	birth rate	10^{-4}	$ch^{-1}mm^{-3}$
b_0	death rate	0.005	h^{-1}
c_0	Maximum proliferation rate	10	
d_0	1/2 saturation constant	10^{-2}	$c^{-1}h^{-1}mm^3$
f_0	Carrying capacity	1	cmm^{-3}
a_1	birth rate	10^{-4}	$ch^{-1}mm^{-3}$
b_1	death rate	0.005	h^{-1}
c_1	Maximum proliferation rate	10	
d_1	1/2 saturation constant	10^{-2}	$h^{-1}(mm^{-3}/c)^2$
f_1	Carrying capacity	1	cmm^{-3}
d_2	1/2 saturation constant of tumor	0.02	h^{-1}
e_2	Killing of tumor cells by CD8+ T-cells	0.1	$c^{-1}h^{-1}mm^3$
f_2	Carrying capacity of tumor	1	cmm^{-3}
e_3	CD8+ T cells killing of DC	0.1	$c^{-1}h^{-1}mm^3$
a_4	IL-2 production	10^{-2}	$c^{-1}h^{-1}mm^3$
c_4	IL-2 uptake	10^{-7}	$c^{-1}h^{-1}mm^3$
e_4	IL-2 degradation rate	10^{-2}	h^{-1}

are preferred owing to their wider applicability (Marino et al., 2008; Saltelli et al., 1999). In these approaches variance of the output is decomposed into contributions from different factors. Sensitivity indices are calculated to rank the factors based on their contributions. The main advantages of VBM are: (i) sensitivity measure is model-free (ii) it is able to realize the impact of full range of variations of each input factor and the interactions among the input factors and (iii) reliability. In spite of these advantages, there is one major disadvantage. In most of the cases, direct relationship between input and output factors is unknown. As a result, it is computationally expensive to evaluate output by solving nonlinear differential equations for different set of input factors. In that regard, metamodeling approach is an alternative where the inputs and outputs are directly related and it is a computationally cheaper approximation of the original model. Then, the philosophy of variance based sensitivity analysis can be extended to these metamodels for identify-

ing highly contributing input factors. High dimensional model reduction (HDMR) (Li et al., 2001, 2002) a metamodeling approach is used in this work to find the sensitive dimensionless groups. HDMR requires less number of model executions for computing the sensitivity indices.

5.4.1 Theoretical formulation of HDMR

HDMR not only captures the contributions of individual inputs contribution but also the contributions of their interactions. The mapping between input-output in the domain Ω of X is given by the following expression:

$$f(X) = f_0 + \sum_{i=1}^n f_i(x_i) + \sum_{1 \leq i < j \leq n} f_{ij}(x_i, x_j) + \dots + f_{12\dots n}(x_1, x_2, \dots, x_n) \quad (5.6)$$

In the above equation $f(X)$ is the output variable and x_i 's ($i=1, 2, \dots, n$) are the input variables. f_0 is the mean value (zeroth order) of the function $f(X)$, $f_i(x_i)$ is the individual contribution (first order) of x_i and $f_{ij}(x_i, x_j)$ is the interactive contribution (second order) of x_i and x_j . Similarly, $f_{12\dots n}(x_1, x_2, \dots, x_n)$ is the n^{th} order contribution of all input variables. Component functions $f_i(x_i)$, $f_{ij}(x_i, x_j), \dots, f_{12\dots n}(x_1, x_2, \dots, x_n)$ can also be a nonlinear. Component functions are orthogonal which means that each component function provide unique information. The component functions are optimally tailored for the given output $f(X)$ over the domain Ω of X . Each component function is obtained by minimizing the objective function with orthogonality condition as a constraint

$$\min_{f_{i_1 i_2 \dots i_l}} \int_{\Omega} w_{i_1 i_2 \dots i_l}(\hat{x}, u) Z du$$

$$Z = \left[f(u) - f_0 - \sum_{i=1}^n f_i(u_i) - \sum_{1 \leq i < j \leq n} f_{ij}(u_i, u_j) - \dots - \sum_{1 \leq i_1 < \dots < i_l} f_{i_1 i_2 \dots i_l}(u_{i_1}, u_{i_2}, \dots, u_{i_l}) \right]^2$$

The orthogonality condition confirms that all component functions are determined step-by-step. Here, $\hat{x} = \sigma_f^2$, $du = du_1 du_2 \dots du_n$, and $w_{i_1 i_2 \dots i_l}(\hat{x}, u)$ is a

weight function. There are two different HDMR expansions namely cut- and RS (random sampling)-HDMR. Cut-HDMR is used when the output $f(x)$ is expressed about a known reference point. Conversely, RS-HDMR relies on the average value of $f(X)$ over the whole domain Ω . In this work, RS-HDMR is used to perform global sensitivity assessments.

5.4.2 RS-HDMR

In RS-HDMR, the variables x_i ($i = 1, \dots, n$) are scaled by linear transformations for all i , such that their values lie between 0 and 1. Then, the output function $f(X)$ is defined in the unit hypercube domain $K^n = \{(x_1, x_2, \dots, x_n) | 0 \leq x_i \leq 1, i = 1, 2, \dots, n\}$. The component functions are obtained as indicated in Equations (5.7-5.9) below

$$f_0 = \int_{K^n} f(X) dX \quad (5.7)$$

$$f_i(x_i) = \int_{K^{n-1}} f(x_i, X^i) dX^i - f_0 \quad (5.8)$$

$$f_{ij}(x_i, x_j) = \int_{K^{n-2}} f(x_i, x_j, X^{ij}) dX^{ij} - f_i(x_i) - f_j(x_j) - f_0 \quad (5.9)$$

The model output variance is expressed in terms of the inputs variance (Li et al., 2002) and is shown in Equations (5.10-5.12)

$$\sigma_f^2 = \int_{K^n} [f(X) - f_0]^2 dX \quad (5.10)$$

$$= \sum_{i=1}^n \int_0^1 f_i^2(x_i) dx_i + \sum_{1 \leq i < j \leq n} \int_0^1 \int_0^1 f_{ij}^2(x_i, x_j) dx_i dx_j + \dots \quad (5.11)$$

$$= \sum_{i=1}^n \sigma_i^2 + \sum_{1 \leq i < j \leq n} \sigma_{ij}^2 + \dots \quad (5.12)$$

Let

$$V_f = \sigma_f^2, V_i = \sum_{i=1}^n \sigma_i^2, V_{ij} = \sum_{1 \leq i < j \leq n} \sigma_{ij}^2$$

$$S_i = \frac{V_i}{V_f}, S_{ij} = \frac{V_{ij}}{V_f}, \dots$$

where, V_f is the variance of the model output and V_i, V_{ij} are the partial variances of the inputs. S_i, S_{ij} are the sensitivity indices. The sum of all sensitivity indices is equal to 1.

$$\sum_{i=1}^n S_i + \sum_{1 \leq i < j < n} S_{ij} + \dots + S_{1,2,\dots,n} = 1 \quad (5.13)$$

The integrals in Equations (5.7-5.11) can be evaluated using Monte Carlo techniques, but would be highly computational intensive. In order to overcome the computational effort and simplify the problem, the component functions are approximated by the orthonormal basis functions as seen in Equations (5.14-5.15).

$$f_i(x_i) \approx \sum_{r=1}^k \alpha_r^i \varphi_r(x_i) \quad (5.14)$$

$$f_{ij}(x_i, x_j) \approx \sum_{p=1}^l \left(\sum_{q=1}^{l'} \beta_{pq}^{ij} \varphi_p(x_i) \varphi_q(x_j) \right) \quad (5.15)$$

In the above equations, k, l, l' denote the order of the polynomial expansion, α_r^i and β_{pq}^{ij} are constant coefficients that need to be determined, and $\varphi_r(x_i), \varphi_p(x_i), \varphi_q(x_j)$ are the orthonormal basis functions. The orthogonal conditions for the basis functions are given in Equations (5.16-5.17)

$$\int_a^b \varphi_k(x) dx = 0 \quad (5.16)$$

$$\int_a^b \varphi_k(x) \varphi_l(x) dx = 0 \quad (5.17)$$

Table 5.2
Parameter bounds

Parameter	Lower bound	Upper bound
a_0	0.5×10^{-4}	2×10^{-4}
b_0	2.5×10^{-3}	1×10^{-2}
c_0	5	20
d_0	5×10^{-3}	2×10^{-2}
a_1	5×10^{-5}	2×10^{-4}
b_1	2.5×10^{-3}	1×10^{-2}
c_1	5	20
d_1	5×10^{-3}	2×10^{-2}
d_2	1×10^{-2}	4×10^{-2}
e_2	1×10^{-1}	4×10^{-1}
e_3	5×10^{-2}	2×10^{-1}
a_4	5×10^{-3}	2×10^{-2}
c_4	5×10^{-8}	2×10^{-7}
e_4	5×10^{-3}	2×10^{-2}
H_0	1×10^{-2}	4×10^{-2}
C_0	1×10^{-2}	4×10^{-2}
M_0	5×10^{-2}	2×10^{-1}

Thus, in HDMR, the main objective is to find the constant coefficients in the basis functions approximate the component functions. According to Li et al. (2002), for most of the practical applications, the second order HDMR expansion suffices.

5.5 Results and discussion

5.5.1 Uncertainty and sensitivity analysis using HDMR

The parameters of the mathematical model given in Table 5.1 are perturbed over a range as indicated by the lower and upper bounds in Table 5.2. A uniform distribution is used for the parameters within those ranges. The lower bound and upper bound of parameter distribution are as shown in Table 5.2. Monte Carlo simulations are used to comprehend the variance of model output (uncertainty analysis). Monte Carlo simulations involve choosing of parameters from the distribution based on different sampling techniques to evaluate the model output. In the present work,

Latin hypercube sampling is used, because, it requires lesser samples (compared to other sampling strategies) to provide an unbiased estimate of the model output and ensures the coverage of the entire domain of the parameter space. The model output of interest, in this case, is related to the tumor cells and the expression is given by Equation (5.18).

$$G = \int_0^{t_f} M(t, P) dt \quad (5.18)$$

where, G is model output, P is the parameter set (inputs) and t_f is the final time. It is assumed that measurement error associated with G is negligible. It implies that the variations in G is only because of variations in the parameters. Uncertainty analysis of G is done for different sample sizes (N) and the HDMR model in combination with variance based method is then applied to uncover the key parameters. The HDMR model is justified based on the accuracy value for first and second order component functions and the average G values (f_0). It is known that a good meta-model (HDMR model) is possible if it is built using larger number of samples. Table 5.3 shows that with the increase in sample size from 1000 to 7000, Δf_0 is observed to decrease drastically to a very low value. So, HDMR analysis is concluded with 7000 samples. Relative percentage error is the allowable percentage of error in predicting the validation data set by the HDMR model. Accuracy value denotes the prognostic ability of the HDMR model. If the accuracy value is 100%, it means that the model is able to reproduce the results of the data used for validation. It is obvious that accuracy value of a model always increases with the increase in relative percentage error and for a given sample size, similar trend is observed for both first order and second order component function HDMR models. Also, for a given sample size and relative percentage error, the accuracy value increase appreciably from first order to the second order component function. The accuracy values for 20% relative error are more than 97% for all sample sizes and for both 1st and 2nd order component functions. Overall, Table 5.3 conveys that a reasonable and simple metamodel can represent the data generated by the parameter perturbations. Table 5.4 presents

Table 5.3
Variation of accuracy with sample size and relative error

Sample Size (N)	f_0 (average G value)	Δf_0 $= (f_0)_{j+1} - (f_0)_j $	Accuracy					
			1 st order Relative error (%)			2 nd order Relative error (%)		
			5%	10%	20%	5%	10%	20%
1000	0.821	0.031	63.5	93.5	97.5	84	97	98.5
3000	0.852	0.01	72.5	93.7	98	82.7	97.5	99.2
5000	0.862	0.001	78.6	95.8	98.3	98.2	99.2	99.7
7000	0.863		80.4	95.3	97.5	93.7	97.8	98.9

Table 5.4
Parameter ranking (R)

Sample Size (N)	1 st order (S_i)				$\sum S_i$	2 nd order (S_{ij})					$\sum S_{ij}$
	R_1	R_2	R_3	R_4		R_1	R_2	R_3	R_4	R_5	
1000	9	6	10	5	0.812	(9,10)	(6,9)	(5,10)	(5,9)	(5,6)	0.102
3000	9	6	10	5	0.798	(6,9)	(5,6)	(9,10)	(5,9)	(6,10)	0.1477
5000	9	6	10	5	0.834	(6,9)	(9,10)	(6,10)	(5,9)	(5,6)	0.1375
7000	9	6	10	5	0.842	(6,9)	(9,10)	(5,9)	(5,6)	(5,10)	0.1096

ranking order of the individual and interactive contributions of the parameters to the output G . The parameter numbers provided in Table 5.4 follows to the serial number order mentioned in Table 5.2. Consistency in the ranking of the individual contributions of the parameters is seen for all the sample sizes. The summation of the sensitivity indices of individual contributions and interactive contributions account for approximately 80% and 12% respectively for the total variance of G . Although, there is disparity in the sequence of the interactive contributions, the interactive parameter sets are almost the same for all sample sizes. Thus, the sensitive parameters responsible for the tumor evolution are d_2 , b_1 , e_2 and a_1 . The overall contributions of the parameters are (evaluated using Equations (5.10-5.13)): d_2 (31%), e_2 (21%), b_1 (16%), a_1 (15%), other first order interactions (12%) and higher order interactions (5%).

5.5.2 Validation of HDMR results using reactive scheduling

The sensitive parameters obtained via HDMR analysis are verified by the application of reactive scheduling approach on the dendritic cell therapy planning problem. The physiological model described in section 5.3 will serve as the “patient”. In this regard, three cases are considered. The first case is nominal scheduling, where the schedule for the total time horizon is based on the initially observed parameter values and does not consider their variation. In the second and third cases, reactive scheduling is considered by varying the sensitive parameters and insensitive parameters (as found from the HDMR analysis) respectively. Then, the results of all the cases are compared. In this optimization problem, the objective is to minimize the number of tumor cells by the end of time horizon using appropriate interventions of dendritic cells. The interventions are assumed to be spaced evenly at two weeks. The duration of each intervention is fixed to be 1 hour. Practically, this implies that the patient’s condition is checked once every two weeks and appropriate dendritic cell intervention is provided (Banchereau et al., 2001). Here, the time horizon to eliminate the tumor is taken to be around 6 months (or 4500 hours). Thus, the patient undergoes 14 interventions over the treatment horizon. The nominal schedule resembles the situation where the physician designs the treatment schedule based on initial observation of the patient and proceeds to give corresponding dosage of dendritic cells until the end of the time horizon. However, in reactive scheduling, the treatment schedule is updated based on the patient’s condition at the time of each intervention. As a result, the number of interventions for which the dosage of dendritic cells to be planned will decrease everytime by 1 at each intervention point. The dosage of dendritic cells is constrained between 0 and 2 units (Banchereau et al., 2001). This optimization problem is solved using simulated annealing (Kirkpatrick et al., 1983) algorithm implemented in MATLAB.

Problem formulation

Objectives

- $\min_{u(t_k)} M(t_f)$
 where, k is the intervention number and $k = 1, 2, \dots, 14$

Constraints

- Mathematical model
 - $t_f = 6$ months
 - Intervention timings are fixed, $t_k = (k - 1) \times 14 \times 24$
- $$\left. \begin{array}{l} \text{if } (t_k < t < t_k + 1) \\ 0 \leq u_1 \leq 2 \\ \text{else} \\ u_1 = 0 \end{array} \right\}$$

Decision Variables

- Dosage of dendritic cells at each intervention

5.5.3 Comparison between nominal and reactive schedule for cases 1-3

In cases 1 and 3, the dosages of dendritic cells are expected to be the same with either nominal schedule or reactive schedule. This is because case 1 considers no variation in parameters and case 3 considers variation only in the non-key parameters. From Figure 5.2, it is seen that the dosage rates for case 1 in either schedules are almost same. In case 2, the key parameters (d_2 , b_1 , e_2 and a_1) found from HDMR analysis are varied randomly and Figure 5.3 shows that there is a significant difference between dosage values of dendritic cells to achieve approximately the same final tumor size. In Figure 5.4 which corresponds to case 3, the dosage rates are observed to be practically the same except at the interventions 2 and 4.

Defining a metric α (= sum of absolute dosage differences of dendritic cells between nominal scheduling and reactive scheduling) helps us to compare cases 1, 2 and 3. Recall that, in every case for both nominal scheduling and reactive scheduling, the intervention timings and number of interventions are fixed and only the dosage values are different. From Figure 5.5, it is seen that α is significantly more

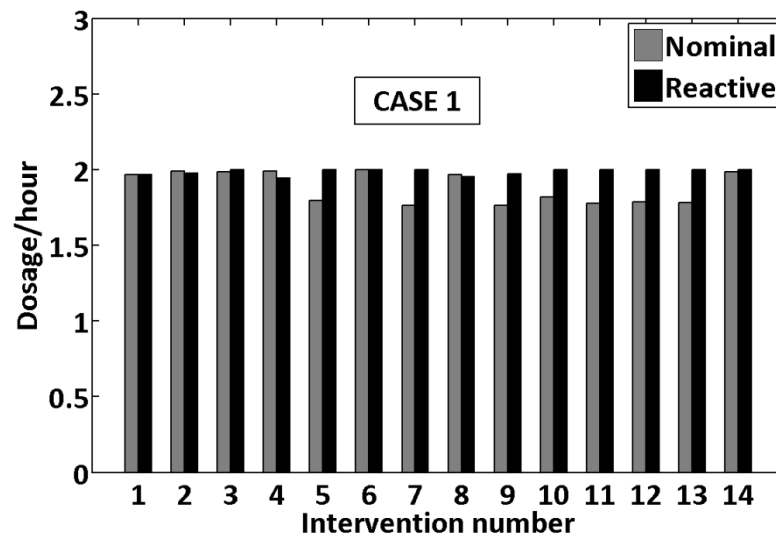


Fig. 5.2. Comparison between nominal and reactive schedule when parameters are not varied

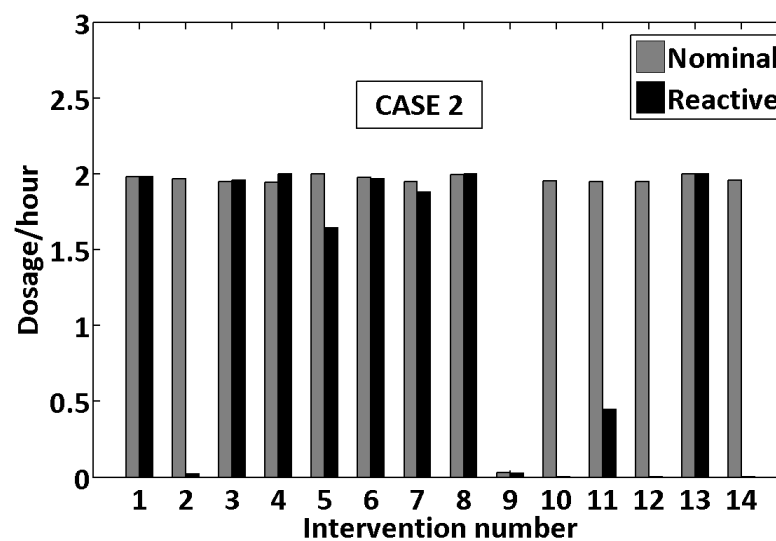


Fig. 5.3. Comparison between nominal and reactive schedule when key parameters are varied

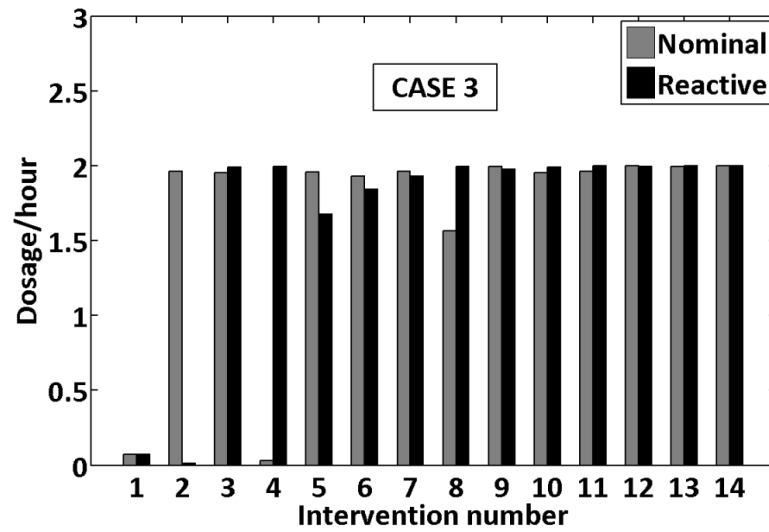


Fig. 5.4. Comparison between nominal and reactive schedule when non-key parameters are varied

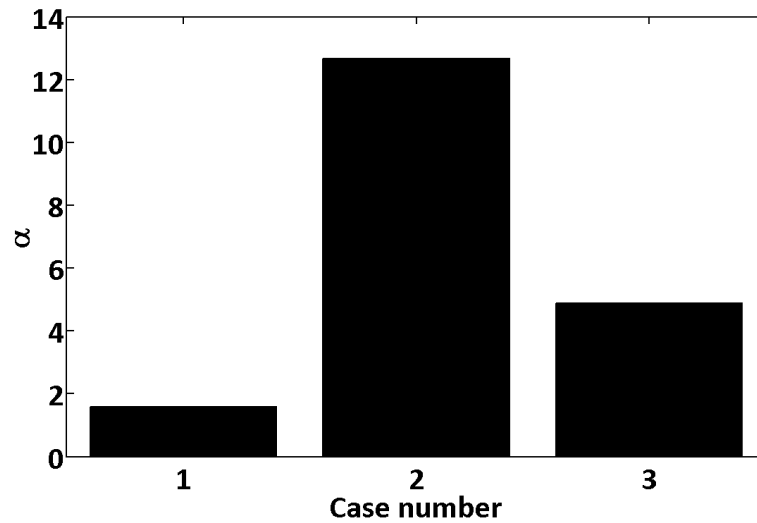


Fig. 5.5. Comparison of α value for the three cases

for case 2 than cases 1 and 3. The slight difference observed between cases 1 and 3 is probably due to neglecting of the minor contribution of non-key parameters on the tumor size. Thus, validation with reactive scheduling is able to support and consolidate the findings of HDMR analysis about the key parameters contributing to the tumor growth. These results emphasize the need for clinicians to perform suitable experiments and measurements in order to find out the values of key effects and

use them to plan the further course of treatment. In the following section, reactive scheduling is extended to the combination of dendritic cell therapy and interleukin therapy, while taking into account the variation of the key parameters during the treatment course.

5.5.4 Reactive scheduling of combination therapy and dendritic cell therapy

Here, reactive scheduling is used to determine the schedule of combination therapy (dendritic cell and interleukin) and compared with dendritic cell therapy, while considering the inpatient variability. Inpatient variability is accounted by varying the key parameters (d_2 , e_2 , b_1 , a_1) randomly between the consecutive interventions and these variations are shown in Table 5.5. The arrow marks in Table 5.5 indicate the increase or decrease of a parameter with respect to its previous value. The problem formulation for the combination therapy is same as before except that an integer variable is included to represent whether the intervention is with dendritic cell or interleukin. The decision variables are the dosage values of dendritic cell or interleukin at each intervention. As seen earlier, for reactive scheduling, the number of decision variables decrease after every intervention of either dendritic cells or interleukin. The additional constraint is that tumor size at any point of time should be greater than $1 \times 10^{-10} \text{ cells/mm}^3$ (≈ 0 tumor cells). According to the literature, the number of tumor cells per mm^3 is in the range of 10^6 (Laszlo Kopper, 2001). If this constraint is not included then the dosage values will be such that the number of tumor cells goes to the order of 10^{-20} by the end of the course. This implies that more dosage of dendritic cells is given even when the number of tumor cells is significantly small. A branch and bound algorithm implemented in MATLAB is used to solve this mixed integer nonlinear problem (MINLP) ¹.

¹<http://tomopt.com/tomlab/optimization/minlp.php>

Problem formulation

Objectives

- $\min_{u(t_k)} M(t_f)$
where k is the intervention number and $k = 1, 2, \dots, 14$

Constraints

- Mathematical model
- $t_f = 6$ months
- Intervention timings are fixed, $t_k = (k - 1) \times 14 \times 24$
- i is an integer variable which decides if the intervention is with dendritic cells ($i = 1$) or interleukin ($i = 2$)

Table 5.5
Variation of key parameters

Parameter variation Time (hours) (adjacent Intervention timings)	$a_1 \times 10^3$	b_1	d_2	e_2
Initial	0.1	0.005	0.02	0.1
135.8(0-336)	0.0562 (↓)	0.0039(↓)	0.0333(↑)	0.1096(↑)
572.1(336-672)	0.0540(↓)	0.0049(↑)	0.0488(↑)	0.1555(↑)
722.7(672-1008)	0.0474(↓)	0.0032(↓)	0.0419(↓)	0.0895(↓)
1210.5(1008-1344)	0.0692(↑)	0.0026(↓)	0.0255(↓)	0.1256(↑)
1550.6(1344-1680)	0.0892(↑)	0.0022(↓)	0.0263(↑)	0.0688(↓)
1788.4(1680-2016)	0.0710(↓)	0.0028(↑)	0.0397(↑)	0.1203(↑)
2195.8(2016-2352)	0.0813(↑)	0.0032(↑)	0.0504(↑)	0.0759(↓)
2360.5(2352-2688)	0.0945(↑)	0.0016(↓)	0.0338(↓)	0.0462(↓)
2859.9(2688-3024)	0.0981(↑)	0.0023(↑)	0.0253(↓)	0.0501(↑)
3342.9(3024-3360)	0.0772(↓)	0.0016(↓)	0.0192(↓)	0.0937(↑)
3448.2(3360-3696)	0.0932(↑)	0.0014(↓)	0.0272(↑)	0.1269(↑)
3718.7(3696-4032)	0.1088(↑)	0.0017(↓)	0.0490(↑)	0.2448(↑)
4359.6(4032-4368)	0.0781(↓)	0.0016(↓)	0.0536(↑)	0.3359(↑)

- $$\left. \begin{array}{l} \text{if } (t_k < t < t_k + 1) \\ 0 \leq u_i \leq u_{i \max} \\ \text{else} \\ u_i = 0 \end{array} \right\}$$
- $\min(M(t)) \geq 1 \times 10^{-10} (\approx 0)$

Decision Variables

- Dosage of dendritic cells or interleukin at each intervention

The effect of inpatient variability on the tumor growth can be better understood from the tumor profile in no therapy case (Figure 5.6). The tumor progresses steeply until 720 hours (approximately) due to the increase in the rate of nutrients (glucose and oxygen) supply to tumor cells ($d_2 \uparrow$). Then, at 1210 hours a drop in tumor size is observed. This can be related to the following effects - a net increase in natural infiltration of CD8+ T-cells ($a_1 \uparrow, b_1 \downarrow$), an increased activity of CD8+ T-cells on tumor cells ($e_2 \uparrow$) and increased resistivity of nutrient supply ($d_2 \downarrow$). Similarly, the tumor progression can be correlated with the biological changes for the decreasing trend after 3000 hours.

The controlled tumor growth due to the dendritic cell therapy and combination therapy is also highlighted in Figure 5.6. Tumor is almost eliminated by the end of time horizon in either therapy. The plot suggests that for this given patient variability (Table 5.5), dendritic cell therapy is sufficient rather than the combination therapy and the corresponding treatment protocol of the dendritic cell therapy is projected in Figure 5.7. The fluctuation in the dosage levels is noticed in Figure 5.7 and medical reasons are analyzed next. Interventions such as 2, 6, and 12 are reduced from their previous interventions because the tumor size is very small at that time point. However, there are interventions (3, 9, and 10) where the dosage values are less even though the tumor size is at a higher value and similarly, the

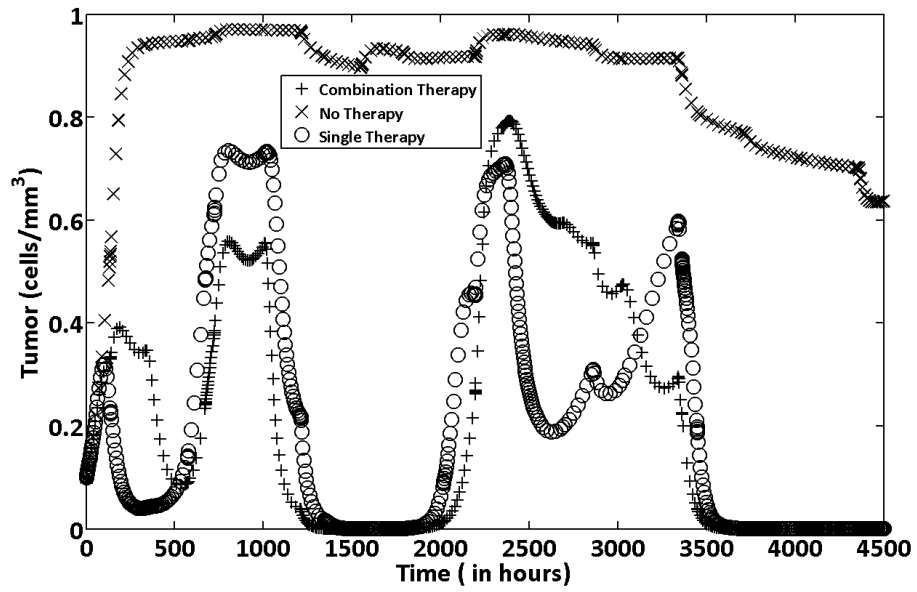


Fig. 5.6. Evolution of tumor for different therapy cases

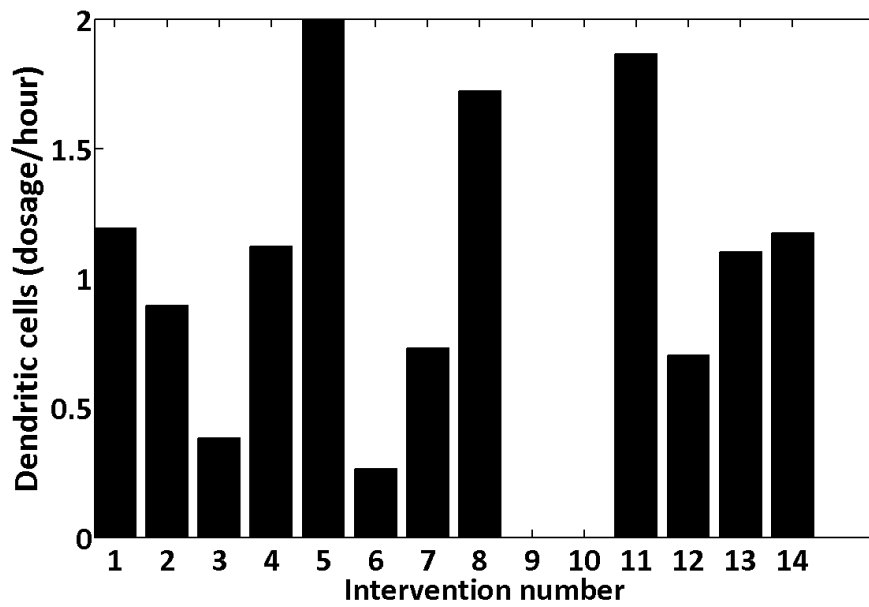


Fig. 5.7. Reactive schedule of dendritic cell therapy

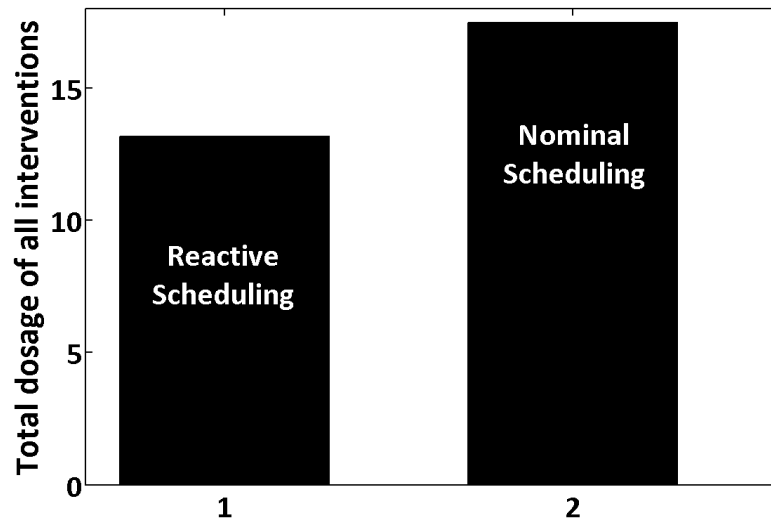


Fig. 5.8. Comparison of total dosage between reactive scheduling and nominal scheduling

interventions (13, 14) after 3000 hours are of higher value when the tumor size is low. This shows that in the latter case, the interventions are purely based on the parameter values at that time (Table 5.5). For example at intervention 3, e_2 is at a higher value which means the natural ability of elimination tumor by CD8+ T-cells is more, so there is a reduction in dosage. Thus, reactive scheduling checks the tumor size and patient parameters at every intervention and makes the decision accordingly to avoid overdosage. It is observed that the total dosage with reactive schedule is approximately 25% less than the nominal schedule (Figure 5.8).

5.6 Conclusions

The main challenge addressed in this chapter was inpatient variability during treatment course. Inpatient variability can be understood by investigating the key mechanisms responsible for tumor growth. In this chapter, a mathematical model representing the immune action of dendritic cells on the tumor was analyzed using a global sensitivity analysis technique and the key parameters of the model contributing to the tumor growth were elucidated. The key mechanisms were found

to be proliferation of tumor cells, its interaction with CD8+ T-cells and the source and decay mechanisms of CD8+ T-cells. From a broader perspective, the biological implication from the global sensitivity analysis is that development of drugs that can activate and perpetuate CD8+ T-cells is important to eliminate tumors. The results of HDMR were validated by formulating an optimization problem and by comparing the outcomes of nominal and reactive scheduling. This work points to the importance of using tumor size data to determine the key model parameters and using the latest parameter estimates to schedule future therapeutic interventions on the patient. Reactive scheduling was also applied to compare combination therapy and dendritic cell therapy. In the case study, it was seen that dendritic cell therapy is enough to eliminate tumor. Overall, reactive scheduling is very useful in the medical field to plan therapies considering the inpatient variability and avoid side effects.

Chapter 6

APPLICATION OF SCALING AND SENSITIVITY ANALYSIS FOR TUMOR-IMMUNE MODEL REDUCTION

*‘Although our intellect always longs for clarity and certainty, our
nature often finds uncertainty fascinating.’*

- Karl Von Clausewitz

6.1 Introduction

In the previous chapters, it is seen that mathematical modeling plays a facilitating role in comprehending tumor growth and its interaction with the immune system. However, there are some hindrances in modeling these phenomena. Firstly, the complexity of the tumor-immune model increases with the inclusion of dynamics of different types of immune cells. In this chapter, complexity is considered in terms of number of parameters and differences in the order of magnitude of their values. This may result in non-identifiability, imprecise measurement/ estimation of the parameters. Secondly, very few parameters in the model will significantly influence the evolution of state variables and it is important for us to know these sensitive parameters.

In this chapter, a recent and elaborate tumor-immune model is considered and its reduced parametric representation is obtained through a systematic approach without any loss in its predictive ability. The schematic representation of the sequential methodology (scaling analysis followed by sensitivity analysis) adopted in

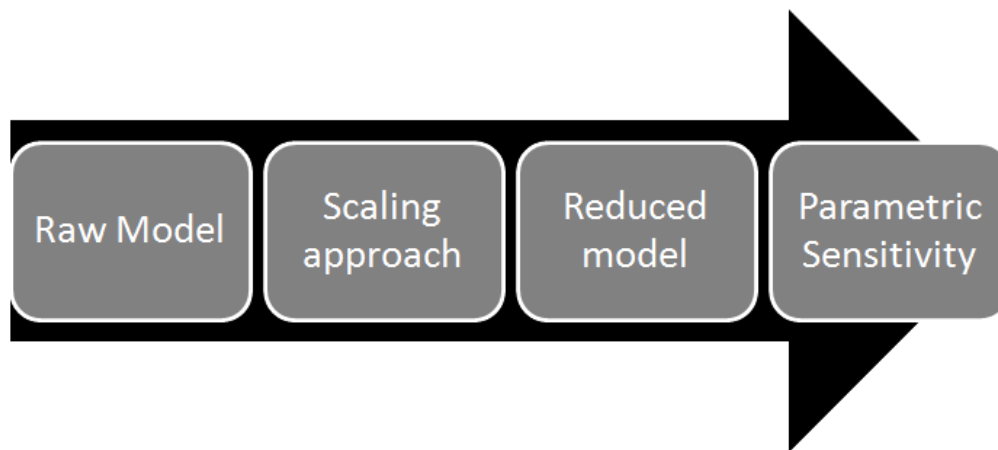


Fig. 6.1. Sequential methodology

this chapter is shown in Figure 6.1. Scaling analysis is a systematic technique which involves grouping of parameters in a model and representing it in a reduced parametric form. Scaling approach also ensures that the coefficients in the model (parametric groups) are approximately in the order-of-one. The advantage of scaling approach is quantified using theoretical identifiability analysis and by evaluating the condition number of the Fisher information matrix. With reduced models, the computational time taken for model evaluation may be significantly reduced. Subsequently, global sensitivity analysis of the reduced model is performed to unearth the key parametric groups of the model. Such model reduction and parameter analysis may be necessary in order to increase the possibility of bringing model-based approaches to standard medical practice and patient care.

6.2 Mathematical model

Tumor-immune model considered in this chapter is adapted from the work by de Pillis et al. (2009). In the model, it is considered that, symbols, T , N , L , C , I represent tumor cells, natural killer (NK) cells, cytotoxic (CD8+) T-cells, circulating lymphocytes, and interleukin respectively. The units of immune cells (N , L , C) and cytokines (I) are given in number of cells per litre of blood and international unit

(IU) per litre of blood respectively, while the tumor (T) is represented as total number of cells. In Equation (6.1), the first term corresponds to the nutrients based on tumor growth. The second and third terms explain the elimination of tumor cells due to NK cells, CD8+ T-cells. The expression for D is given in Equation (6.2) where d and l signify the immune strength (recognizing and attacking capacity) known as immunogenicity against the tumor cells. In Equation (6.3), eC denotes the localization of natural killer cells at the tumor site based on the number of circulating lymphocytes. fN denotes the natural decay of NK cells. The loss of natural killer cells due to its interaction with tumor cells is given by pNT . The activation of NK cells by interleukin is given by $p_NNI/(g_N + I)$. In Equation (6.4), $jTL/(k+T)$ elucidates the stimulation of the CD8+ T-cells as a result of the presence of lysed tumor cells debris. Similarly, r_1NT represent the stimulation of cytotoxic cells due to the presence of the NK-lysed tumor cells. The localization of activated CD8+ T-cells at the tumor location is captured by r_2CT term. The activation of cytotoxic cells by interleukin is described by $p_ILI/(g_I + I)$. However, excessive number of cytotoxic cells in the presence of interleukin leads to its deactivation and is shown by the term $uL^2CI/(\kappa + I)$. In previous work (de Pillis et al., 2006), the natural decay of cytotoxic T-cells was expressed as $-mL$. Later, in de Pillis et al. (2009), it was modified to $\theta mL/(\theta + I)$ owing to the realization that the cytotoxic T-cells decrease only due to the increased concentration of interleukin above a threshold limit. In Equation (6.5), $-\mu_I I$, φC and $\omega LI/(\zeta + I)$ quantify the natural decay of interleukin, production of interleukin by the helper T-cells and CD8+ T-cells respectively. In Equation (6.6), α is the natural ability of the bone marrow to generate lymphocytes in any individual and β is the overall decay rate of the circulating lymphocytes. The parameter values are given in Table 6.1.

$$\frac{dT}{dt} = aT(1 - bT) - cNT - DT \quad (6.1)$$

$$D = d \frac{(L/T)^l}{s + (L/T)^l} \quad (6.2)$$

$$\frac{dN}{dt} = eC - fN - pNT + \frac{p_N NI}{g_N + I} \quad (6.3)$$

$$\frac{dL}{dt} = \frac{\theta mL}{\theta + I} + \frac{jTL}{k + T} - qLT + (r_1 N + r_2 C)T - \frac{uL^2 CI}{\kappa + I} + \frac{p_I LI}{g_I + I} \quad (6.4)$$

$$\frac{dI}{dt} = -\mu_I I + \varphi C + \frac{\omega LI}{\zeta + I} \quad (6.5)$$

$$\frac{dC}{dt} = \alpha - \beta C \quad (6.6)$$

Model reduction analysis is applied on the model and Equations (6.1-6.6) are considered while applying scaling and sensitivity analysis. The above model has 29 parameters and this can pose significant challenges for parameter estimation in the face of limited patient data. We might therefore benefit by obtaining a minimal parametric model and determining the key parameter combinations with high accuracy for enabling clinical applications.

6.3 Scaling analysis

Scaling analysis is a systematic procedure for non-dimensionalization of dependent and independent variables as well as their derivatives in a mathematical model representing a physical process. Non-dimensionalization is done such that the variables and their derivatives are bounded by order-of-one scale which is a unique aspect of the scaling analysis proposed by Krantz (2007*b,a*). The order-of-one scaling ensures that the values of the dimensionless variables, their derivatives and coefficients in the model lie between zero and more-or-less one. Order-of-one scaling not only facilitates minimum parametric representation but also supports model simplification based on the magnitude of the dimensionless parameter groups. One key advantage of the scaled model is that if the coefficient value of any term is very low, it can be ignored. Similar conclusions cannot be made based on coefficient values in the case of the original model.

Table 6.1
Parameter values

Parameter	Value	Units
a	4.31×10^{-1}	Day^{-1}
b	1.02×10^{-9}	$Cells$
c	2.9077×10^{-13}	$l/Cells^{-1}perday^{-1}$
e	1.3875×10^{-3}	Day^{-1}
f	1.25×10^{-2}	Day^{-1}
p	2.794×10^{-13}	$Cells^{-1}perday^{-1}$
p_N	6.68×10^{-2}	Day^{-1}
g_N	2.5036×10^5	IU/l
m	9×10^{-3}	Day^{-1}
θ	2.5036×10^{-3}	IU/l
q	3.422×10^{-10}	$Cells^{-1}perday^{-1}$
r_1	2.9077×10^{-11}	$Cells^{-1}perday^{-1}$
r_2	5.8467×10^{-13}	$Cells^{-1}perday^{-1}$
p_I	2.971	Day^{-1}
g_I	2.5036×10^3	IU/l
u	4.417×10^{-14}	$l^2/Cells^{-2}perday^{-1}$
κ	2.5036×10^3	IU/l
j	1.245×10^{-2}	Day^{-1}
k	2.019×10^7	$cells$
α	1.4175×10^7	$Cells/lday^{-1}$
β	6.3×10^{-3}	Day^{-1}
v	5.199×10^{-1}	Day^{-1}
μ_I	11.7427	Day^{-1}
ω	7.874×10^{-2}	$IU/Cells^{-1}perday^{-1}$
φ	2.38405×10^{-7}	$IU/Cells^{-1}perday^{-1}$
ζ	2.5035×10^3	IU/l
d	2.34	Day^{-1}
l	2.09	
s	3.8×10^{-3}	

6.3.1 Algorithm

1. Mathematical model representing the physical process (tumor-immune interactions): model equations, initial, boundary and auxiliary conditions are assumed to be available.
2. Introduce scale factors and reference factors for all dependent, independent variables and their derivatives.

3. Form dimensionless variables in the model equations.
4. Use the coefficient of the dominating phenomenon and divide both sides of the equations with it.
5. Determine the scale factors and reference factors.
6. Check if the magnitude of all the dimensionless coefficients in the model is of the order-of-one. If not, the algorithm is repeated from step 4.
7. After successful implementation of steps 1 to 6, the minimum parametric representation of the model is obtained.

In the equations below, subscripts ‘ f ’ and ‘ s ’ refers to reference factors and scale factors respectively. The reference values T_f , N_f , L_f , I_f , C_f are considered to be zero because their minimum possible value is zero. $1/\alpha_1$, $1/\alpha_2$, $1/\alpha_3$, $1/\alpha_4$, $1/\alpha_5$ refer to scaling factors for time derivatives of T , N , L , I and C respectively. The transformed variables are as given below.

$$T^* = \frac{T-T_f}{T_s}, N^* = \frac{N-N_f}{N_s}, L^* = \frac{L-L_f}{L_s}, I^* = \frac{I-I_f}{I_s}, C^* = \frac{C-C_f}{C_s}, \left(\frac{dT}{dt}\right)^* = \alpha_1 \left(\frac{dT}{dt}\right),$$

$$\left(\frac{dN}{dt}\right)^* = \alpha_2 \left(\frac{dN}{dt}\right), \left(\frac{dL}{dt}\right)^* = \alpha_3 \left(\frac{dL}{dt}\right), \left(\frac{dI}{dt}\right)^* = \alpha_4 \left(\frac{dI}{dt}\right), \left(\frac{dC}{dt}\right)^* = \alpha_5 \left(\frac{dC}{dt}\right)$$

6.3.2 Reduced model

The minimum parametric model is shown in Equations (6.7-6.11) and the scale factors are given below.

$$T_s = \frac{1}{b}, N_s = \frac{eC_s}{f}, C_s = \frac{\alpha}{\beta}, L_s = 5.268 \times 10^5, I_s = 1073, \alpha_1 = \frac{1}{abT_s^2}, \alpha_2 = \frac{1}{eC_s},$$

$$\alpha_3 = \frac{1}{r_1N_sT_s}, \alpha_4 = \frac{1}{\mu I_s}, \alpha_5 = \frac{1}{\alpha}$$

$$\left(\frac{dT}{dt}\right)^* = \alpha_1 \left(\frac{dT}{dt}\right) = T^* - T^{*2} - \Pi_1 N^* T^* - \Pi_2 T^* \left(\frac{L^*}{T^*}\right)^{\Pi_3} \quad (6.7)$$

$$\left(\frac{dN}{dt}\right)^* = \alpha_2 \left(\frac{dN}{dt}\right) = C^* - \Pi_4 N^* - \Pi_5 N^* T^* + \frac{\Pi_6 N^*}{\left(\frac{\Pi_7}{I^*} + 1\right)} \quad (6.8)$$

Table 6.2
Parametric groups

Groups	Expression	Value
Π_1	$(cN_s)/a$	1.6849×10^{-4}
Π_2	$(d/as)(L_s/T_s)^l$	2.0949×10^{-4}
Π_3	l	2.0900
Π_4	$(fN_s)/(eC_s)$	1
Π_5	$(pN_sT_s)/(eC_s)$	0.0219
Π_6	$(p_NN_s)/(eC_s)$	5.344
Π_7	$(g_N)/(I_s)$	233.3
Π_8	$(\theta mL_s)/(r_1N_sT_sI_s)$	1.5538×10^{-9}
Π_9	$(jL_s)/(r_1N_sT_s)$	9.2121×10^{-4}
Π_{10}	K/T_s	0.0206
Π_{11}	$(qL_s)/(r_1N_s)$	0.0248
Π_{12}	$(r_2C_s)/(r_1N_s)$	0.1811
Π_{13}	$(uL_s^2C_s)/(r_1N_sT_s)$	3.8739
Π_{14}	κ/I_s	2.333
Π_{15}	$(p_IL_s)/(r_1N_sT_s)$	0.2198
Π_{16}	$(g_I)/(I_s)$	2.333
Π_{17}	$(\varphi C_s)/(\mu I_s)$	0.0426
Π_{18}	$(\omega L_s)/(\mu I_s)$	3.2921
Π_{19}	ζ/I_s	2.333

$$\left(\frac{dL}{dt}\right)^* = \alpha_3 \left(\frac{dL}{dt}\right) = \Pi_8 \left(\frac{L^*}{I^*}\right) + \frac{\Pi_9 L^*}{\left(\frac{\Pi_{10}}{T^*} + 1\right)} - \Pi_{11} L^* T^* + N^* T^* + \Pi_{12} C^* T^* - \frac{\Pi_{13} L^{*2} C^*}{\left(\frac{\Pi_{14}}{I^*} + 1\right)} + \frac{\Pi_{15} L^*}{\left(\frac{\Pi_{16}}{I^*} + 1\right)} \quad (6.9)$$

$$\left(\frac{dI}{dt}\right)^* = \alpha_4 \left(\frac{dI}{dt}\right) = -I^* - \Pi_{17} C^* + \frac{\Pi_{18} L^*}{\left(\frac{\Pi_{19}}{I^*} + 1\right)} \quad (6.10)$$

$$\left(\frac{dC}{dt}\right)^* = \alpha_5 \left(\frac{dC}{dt}\right) = 1 - C^* \quad (6.11)$$

The number of parameters in the model has been reduced significantly from 29 to 19 as a result of the scaling procedure. This reduction implies that the number of measurements required for model parameter estimation can be reduced. The dimensionless groups are shown in Table 6.2. The reduced model is verified by com-

paring the evolution of its states with that of original model for a set of given initial conditions and parameter values (Figure 6.2). The approximation error between the original model and the reduced model depends on the terms that are neglected; in the present study, the approximation error is about 3%. The coefficients of various terms in the reduced model are approximately in the same range and are within order-of-one scale (Table 6.3). From Table 6.4, the magnitude of scale factors for the rate of change of the states is found to be in the order given below:

$$L^* > I^* > T^* > N^* > C^*$$

The rate of change for N and C are significantly less than the others and it implies that N and C remain almost constant. This is in accordance with evidence presented in the literature that the number of N and C cells present in the body is

Table 6.3
Values of dimensionless coefficients

Coefficients reduced model	Value	Coefficients reduced model	Value
Π_1	2×10^{-4}	Π_{11}	2.48×10^{-2}
Π_2	2×10^{-4}	Π_{12}	0.1811
Π_4	1	$(\Pi_{13})/(\Pi_{14} + I^*)$	≈ 1.6
Π_5	2.19×10^{-2}	$(\Pi_{15})/(\Pi_{16} + I^*)$	$\approx 10^{-2}$
$(\Pi_6)/(\Pi_7 + I^*)$	≈ 0.0228	Π_{17}	4.26×10^{-2}
Π_8	1.533×10^{-9}	$(\Pi_{18})/(\Pi_{19} + I^*)$	≈ 1.4109
$(\Pi_9)/(\Pi_{10} + T^*)$	$\approx 10^{-4} - 10^{-2}$		

Table 6.4
Scale factors of rate of change of the scaled states

State	Expression	Value
T^*	$1/(\alpha_1 T_s)$	0.43
N^*	$1/(\alpha_2 N_s)$	0.012
L^*	$1/(\alpha_3 L_s)$	13.51
I^*	$1/(\alpha_4 I_s)$	11.74
C^*	$1/(\alpha_5 C_s)$	0.0063

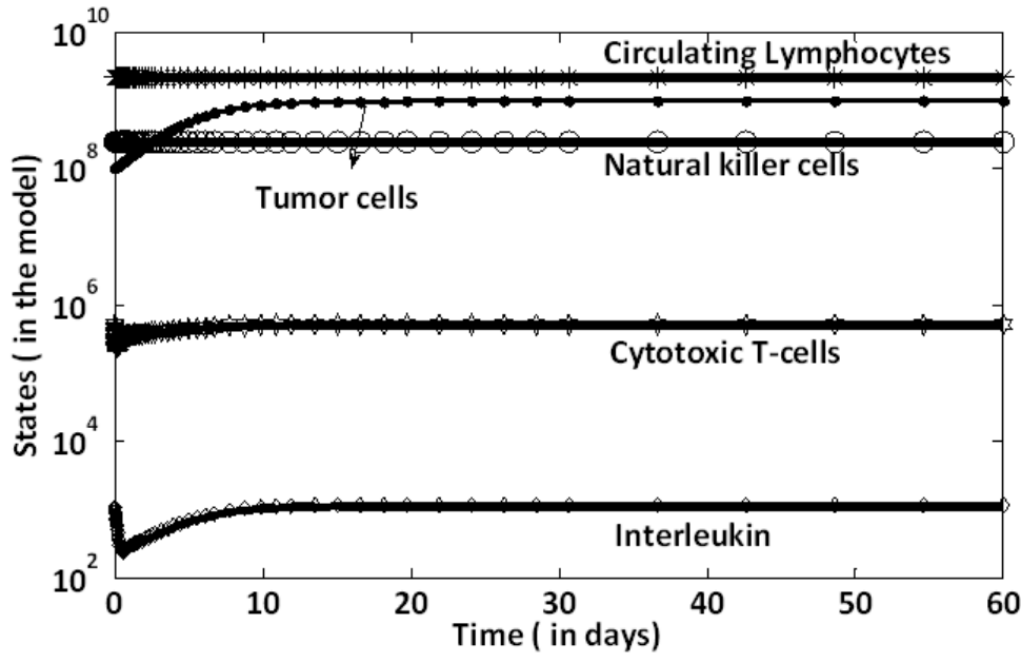


Fig. 6.2. Comparison of evolution of states between original model and reduced model

very high and only a small fraction of it interacts with the tumor (de Pillis et al., 2009).

The parametric groups presented in Table 6.2 reveals that some dimensionless groups are related. Also, not all dimensionless groups will have significant effect on tumor growth. The implication is that it is no need to estimate all the dimensionless groups for obtaining the complete model to predict the tumor growth. Next, global sensitivity analysis is applied to find out the key mechanisms for tumor growth.

6.4 Global sensitivity analysis for correlated inputs

Let us assume that there are n inputs $(x_{i=1,2,\dots,n})$ and $f(X)$ is the model output. In HDMR, the model output is expressed in terms of the orthogonal contributions of the input factors. This is also known as ANOVA representation.

$$f(X) = f_0 + \sum_{i=1}^n f(x_i) + \sum_{i \neq j}^n f(x_i, x_j) + \dots + f(x_1, x_2, \dots, x_n) \quad (6.12)$$

$$f(X) = f_0 + \sum_{j=1}^{2^n-1} f_{p_j}(X_{p_j}) \quad (6.13)$$

f_0 is the average value of the output and $f(x_i)$ is the individual contributions. Then, $f(x_i, x_j), \dots, f(x_1, x_2, \dots, x_n)$ represent the interactive contributions. The total number of terms including individual and interactive contributions is $2^n - 1$. And $f_{p_j}(X_{p_j})$ is the generalized representation of contribution of all terms. If Z is taken as the overall variance of the model output, one can define partial variance as follows: $Z_{i=1,2,\dots,n}$ is the partial variance of the individual input i , $Z_{ij(i \neq j)}$ is the partial variance of the input factors i and j , $Z_{ijk(i \neq j \neq k)}$ is the partial variance of the input factors i , j and k and so on.

$$Z = V(f(X)) = \int_{K^n} f^2(X) dX - f_0^2 \quad (6.14)$$

$$f_0 = \int_{K^n} f(X) dX \quad (6.15)$$

$$Z_i = V_i = \int_0^1 f_i^2(x_i) dx_i, \quad Z_{ij} = V_{ij} = \int_0^1 \int_0^1 f_{ij}^2(x_i, x_j) dx_i dx_j, \dots \quad (6.16)$$

The sensitivity indices are defined as:

$$S_i = \frac{Z_i}{Z}, \quad S_{ij} = \frac{Z_{ij}}{Z}, \quad S_{ijk} = \frac{Z_{ijk}}{Z}, \dots \quad (6.17)$$

The sum of all the sensitivity indices add up to 1

$$\sum_{i=1}^n S_i + \sum_{1 \leq i < j \leq n} S_{ij} + \dots + S_{123\dots n} = 1 \quad (6.18)$$

$$\sum_{j=1}^{2^n-1} S_{p_j} = 1 \quad (6.19)$$

The definitions for sensitivity indices given in Equations (6.18 -6.19) are under the assumption that the input factors are independent. The usage of these equations to find sensitivity indices for the correlated input factors may lead to ambiguous results (Xu and Gertner, 2008; Li et al., 2010). To handle this situation, a novel technique known as structural and correlative sensitive analysis (SCSA) is introduced (Li et al., 2010). According to Li et al. (2010), metamodeling using HDMR is same for both correlated and uncorrelated input factors. The main difference lies in the evaluation of sensitivity indices. In the former case, the contribution of an input or subset of inputs (X_{p_j}) is the combination of structural and correlated contribution (Equation 6.20). While in the latter case, the contribution of an input or subset of inputs is same as the structural contribution. Superscripts 'a' and 'b' correspond to structural and correlated sensitivity indices respectively and the estimation of their sensitivity indices are given by Equations (6.21-6.22).

$$S_{p_j} = S_{P_j}^a + S_{P_j}^b \quad (6.20)$$

$$S_{p_j} = \frac{Cov(f_{P_j}, f(X))}{V(f(X))} \approx \frac{\sum_{s=1}^{N_1} f_{P_j}(x_{P_j}^{(s)})(f(X)^{(s)} - f_m)}{\sum_{s=1}^{N_1} (f(X)^{(s)} - f_m)^2} \quad (6.21)$$

$$S_{P_j}^a = \frac{Var(f_{P_j})}{V(f(X))} \approx \frac{\sum_{s=1}^{N_1} (f_{P_j}(x_{P_j}^{(s)}))^2}{\sum_{s=1}^{N_1} (f(X)^{(s)} - f_m)^2} \quad (6.22)$$

where 's' correspond to number of samples generated by varying the input factors within a chosen sample space and f^m is the average value of all samples ($f(X)^{(s)}$).

6.5 Results and discussion

6.5.1 Comparison between original model and reduced model via theoretical identifiability analysis

The main idea in this section is to quantify the advantage of scaling analysis via theoretical identifiability analysis. Identifiability analysis is one of the key steps before parameter estimation in the model building process (Rodriguez-Fernandez and Banga, 2010). It questions the existence of a unique solution of model parameters for a given set of observations. Broadly, there are two main classes of identifiability analysis, *a priori* and *a posteriori* identifiability analysis. In *a priori* identifiability analysis, the uniqueness is tested with the assumption that the real system and model have identical structure; there are no experimental constraints for collecting the output data. In addition, it is assumed that the measured output data is perfect data, i.e., noise free data. Hence, it is also called as the theoretical identifiability analysis. To the contrary, in *a posteriori* identifiability analysis (practical identifiability analysis), measured output data is noisy and it considers the practical constraints such as variations of manipulated variables, cost involved in conducting the experiments.

In the present work, the focus is on theoretical identifiability analysis using the sensitivity matrix i.e., the Jacobian matrix of the model output at different times for a parameter set of the considered model structure. Therefore, it is also called as sensitivity identifiability (Cintron-Arias et al., 2009).

Let us assume a nonlinear dynamic system of the form

$$\begin{aligned}\frac{dY}{dt} &= g(Y(t), U(t), t, P) \\ M(t) &= h(Y(t), P) \\ Y(0) &= Y_0(P)\end{aligned}\tag{6.23}$$

where Y , U , P , t represent the states, inputs, parameters and time variable respectively. Y_0 is the initial condition of the state vector Y . $g(\cdot)$ and $h(\cdot)$ includes the state equations and output equations respectively. In the tumor-immune model, Y corresponds to tumor cells, natural killer (NK) cells, cytotoxic (CD8+) T-cells, circulating lymphocytes, and interleukin respectively. M corresponds to the daily measurement of tumor cells over the 1 month period. Tumor data is generated by simulating the original model and subsequently used for performing the identifiability analysis on original and reduced model. The information about the system captured in the measurements is quantified by Fisher information matrix (FIM) as given in Equation (6.24). The sufficient condition for theoretically identifiable is the non-singularity (i.e. low condition number) of FIM.

$$FIM = \sum_{i=1}^{\nu} G_i^T G_i \quad (6.24)$$

where

$$G_i = \begin{bmatrix} \frac{\partial y_1}{\partial p_1} & \frac{\partial y_1}{\partial p_2} & \cdots & \frac{\partial y_1}{\partial p_j} \\ \frac{\partial y_2}{\partial p_1} & \frac{\partial y_2}{\partial p_2} & \cdots & \frac{\partial y_2}{\partial p_j} \\ \cdots & \cdots & \cdots & \cdots \\ \frac{\partial y_m}{\partial p_1} & \frac{\partial y_m}{\partial p_2} & \cdots & \frac{\partial y_m}{\partial p_j} \end{bmatrix}_i \quad (6.25)$$

is the sensitivity matrix and ν is the number of measurements (equal to 31 in this case). The number of parameters is indicated by the variable j ($j = 29$ for the original tumor-immune model and $j = 19$ for the reduced model). Let $FIM_1(29 \times 29)$ and $FIM_2(19 \times 19)$ represent the Fisher information matrix for the assumed measurement data for the original and reduced model respectively. Let C_{N1} and C_{N2} refer to the condition numbers of FIM_1 and FIM_2 respectively. R_c is the index which quantifies the effect of scaling analysis on the conditioning of FIM.

$$R_c = \frac{\log(C_{N2})}{\log(C_{N1})} \quad (6.26)$$

The values of C_{N1} and C_{N2} are estimated to be 6.7×10^{51} and 5.7×10^{24} respectively and therefore R_c is 0.4774. This value of R_c indicates that the conditioning of FIM is improved significantly after scaling analysis (which helped to reduce the parameter set from 29 to 19). Indirectly, scaling analysis favors the re-parameterization of the model such that parameters are better identifiable. However, the value of C_{N2} is still high implying that scaling analysis alone may not ensure the complete identifiability of the parameters. Hence, it is necessary to find the sensitive parameters to the measured output.

The sensitivity matrix corresponding to the reduced model is further analyzed to identify the sensitive parameters. As discussed before, it is assumed that only tumor size is measured daily for a period of one month. At any given i^{th} measurement, the sensitivity matrix is as given below

$$G_i = \left[\frac{\partial T}{\partial \Pi_1} \quad \frac{\partial T}{\partial \Pi_2} \quad \cdots \quad \frac{\partial T}{\partial \Pi_j} \right]_i \quad (6.27)$$

where $i = 0, 1, 2, \dots, 30$ and $j = 19$.

$$G^* = \begin{bmatrix} G_0 \\ G_1 \\ * \\ * \\ G_{30} \end{bmatrix}_i = \begin{bmatrix} \left[\frac{\partial T}{\partial \Pi_1} \quad \frac{\partial T}{\partial \Pi_2} \quad \cdots \quad \frac{\partial T}{\partial \Pi_{19}} \right]_0 \\ \left[\frac{\partial T}{\partial \Pi_1} \quad \frac{\partial T}{\partial \Pi_2} \quad \cdots \quad \frac{\partial T}{\partial \Pi_{19}} \right]_1 \\ * \\ * \\ \left[\frac{\partial T}{\partial \Pi_1} \quad \frac{\partial T}{\partial \Pi_2} \quad \cdots \quad \frac{\partial T}{\partial \Pi_{19}} \right]_{30} \end{bmatrix} \quad (6.28)$$

The total sensitivity matrix for 31 measurements is given by G^* and it is scaled as shown below

$$G^S = G^* \times \text{diag}[\Pi_1 \quad \Pi_2 \quad * \quad * \quad \Pi_{19}] \quad (6.29)$$

$$G^S = [\text{col}_1 \quad \text{col}_2 \quad \dots \quad \text{col}_{19}] \quad (6.30)$$

$$SI_1 = \text{sum}(\text{col}_1), \quad SI_2 = \text{sum}(\text{col}_2), \quad \dots, \quad SI_{19} = \text{sum}(\text{col}_{19})$$

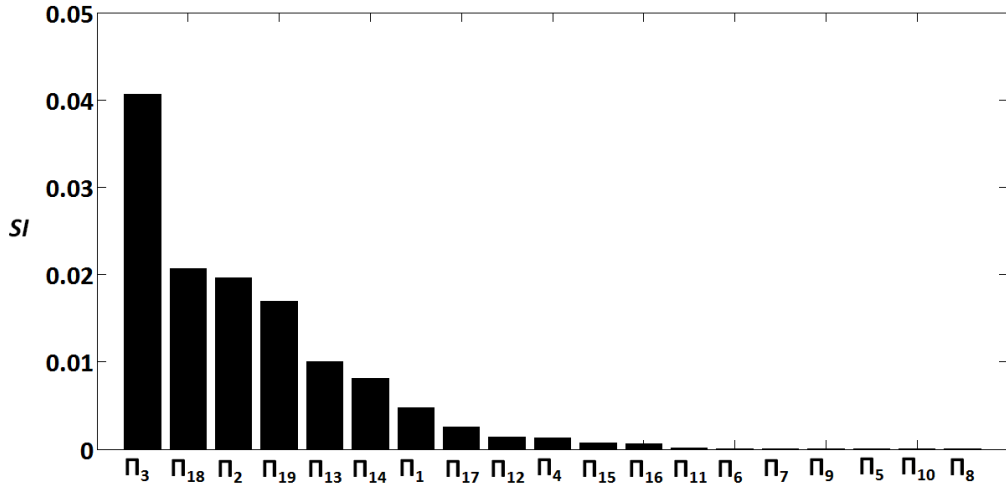


Fig. 6.3. Sensitivity indices of the parametric groups

“ col_i ” stands for columnwise elements of G^s sensitivity index and “ SI ” is an index which implies the variation of tumor cells with respect to the parametric groups (Π_i). In Figure 6.3 the values of SI for all the parameters are projected in the decreasing order of their contribution. It is observed that the parameters Π_3 , Π_{18} , Π_2 , Π_{19} , and Π_{13} are the most sensitive parametric groups. The determination of these sensitive parameters guides parameter estimation in deciding the parameters to be estimated and the parameters to be fixed at their nominal values for a given dataset of measured variables (discussed in Section 6.5.3). In the following section, the sensitive parametric groups are further verified using global sensitivity analysis.

6.5.2 Sensitive parametric groups based on global sensitivity analysis

The parameters (i.e., dimensionless groups (Π_i)) of the reduced model are directly varied by 25% of their nominal values. The nominal values of the dimensionless groups are obtained by substituting the nominal values of the parameters of original model (Table 6.1). The dimensionless groups (Π_i) are assumed to follow a uniform distribution within their sample space (Marino et al., 2008). The samples are chosen from the sample space using experimental designs such as Latin hypercube sampling

for HDMR. The main advantage of this experimental designs is the “better” coverage of the entire sample space for the given sample size (McKay et al., 1979). Then, the chosen parameter samples (inputs) are used to evaluate the output uncertainty by using Monte Carlo strategy. This can also be defined as *in silico* population based studies. Then, GSA techniques are applied on the HDMR model generated from the data set of inputs and output to find the sensitive input factors responsible for the output variability. The output of interest (O) is given in Equation (6.31) and it is clinically measured to study therapeutic effects.

$$O = \int_0^{t_f} T(t) dt \quad (6.31)$$

The results of relative importance of the parameters are based on both structural and correlated contributions are presented in Table 6.5. In Table 6.5, N_1 is the number of samples used for building the HDMR model and R_i is the i^{th} rank of an input or subset of inputs. According to Li et al. (2002), for many systems HDMR expansion upto second order contribution is a good approximation of the output. The first and second order contributions are calculated for different sample sizes. A very high degree of consistency in the parameter rankings is seen for different sample sizes. The average first order and the second order contributions of the key parameters are found to be approximately 77% and 19% of the total variance of O respectively. The important point is that most of the parameters and parameter combinations are common in both first and second order contributions for the different sample sizes. The key parameters affecting the tumor evolution are Π_3 , Π_{18} , Π_2 , Π_{19} , and Π_{13} . Moreover, the values of the structural sensitivity indices for the key parameters (Table 6.6) indicate that the structural contribution is dominating.

Table 6.5
Relative importance of parameter groups (Π_i) based on S_{p_j} using HDMR model

Sample Size (N_1)	Ranking of 1 st order contribution					$\sum S_i$
	R_1	R_2	R_3	R_4	R_5	
7000	Π_3 (0.401)	Π_{18} (0.166)	Π_2 (0.106)	Π_{19} (0.075)	Π_{13} (0.038)	0.786
9000	Π_3 (0.405)	Π_{18} (0.176)	Π_2 (0.107)	Π_{19} (0.073)	Π_{13} (0.043)	0.804
10000	Π_3 (0.375)	Π_{18} (0.162)	Π_2 (0.097)	Π_{19} (0.07)	Π_{13} (0.036)	0.740
Sample Size (N_1)	Ranking of 2 nd order contribution					$\sum S_{ij}$
	R_1	R_2	R_3	R_4	R_5	
7000	(Π_3, Π_{18}) 0.084	(Π_3, Π_{19}) 0.047	(Π_2, Π_3) 0.032	(Π_3, Π_{13}) 0.021	(Π_{18}, Π_{19}) 0.018	0.202
9000	(Π_3, Π_{18}) 0.089	(Π_2, Π_3) 0.031	(Π_{18}, Π_{19}) 0.018	(Π_2, Π_{18}) 0.015	(Π_2, Π_{13}) 0.004	0.157
10000	(Π_3, Π_{18}) (0.084)	(Π_3, Π_{13}) (0.047)	(Π_2, Π_3) (0.030)	(Π_2, Π_{18}) (0.02)	(Π_{13}, Π_{18}) (0.019)	0.20

Table 6.6
Structural sensitivity indices ($S_{p_j}^a$) for the key parameters

Sample Size (N_1)	Ranking of 1 st order contribution				
7000	Π_3 (0.396)	Π_{18} (0.164)	Π_2 (0.107)	Π_{19} (0.0751)	Π_{13} (0.0375)
9000	Π_3 (0.41)	Π_{18} (0.177)	Π_2 (0.107)	Π_{19} (0.078)	Π_{13} (0.045)
10000	Π_3 (0.373)	Π_{18} (0.156)	Π_2 (0.098)	Π_{19} (0.069)	Π_{13} (0.037)
Sample Size (N_1)	Ranking of 2 nd order contribution				
7000	(Π_3, Π_{18}) 0.082	(Π_3, Π_{19}) 0.048	(Π_2, Π_3) 0.033	(Π_3, Π_{13}) 0.022	(Π_{18}, Π_{19}) 0.0178
9000	(Π_3, Π_{18}) 0.092	(Π_2, Π_3) 0.0325	(Π_{18}, Π_{19}) 0.0195	(Π_2, Π_{18}) 0.017	(Π_2, Π_{13}) 0.004
10000	(Π_3, Π_{18}) (0.0817)	(Π_3, Π_{13}) (0.0456)	(Π_2, Π_3) (0.0294)	(Π_2, Π_{18}) (0.0212)	(Π_{13}, Π_{18}) (0.0198)

It is seen from Figure 6.4 that the component functions change monotonically with variations in most of the parameters ($\Pi_3, \Pi_2, \Pi_{19}, \Pi_{13}$). O decreases with the increase of Π_2, Π_3 , and Π_{19} and O increases with the increase of Π_{13} . The

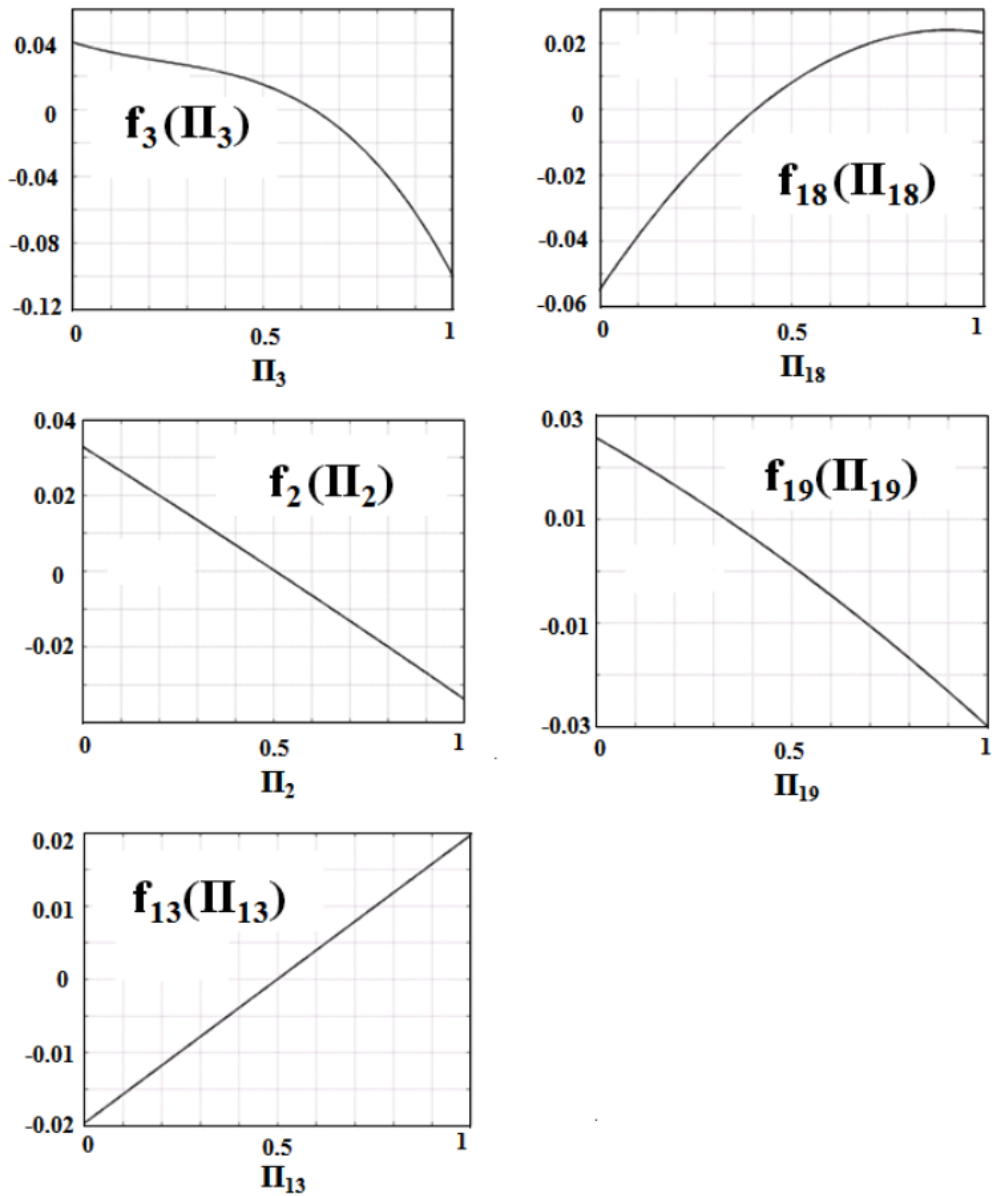


Fig. 6.4. Patterns of HDMR component functions with the variations in key parameters. X-axis: Scaled key parameter values, Y-axis: Scaled values of the component functions

component function corresponding to the parameter Π_{18} increases at a decreasing rate and reaches a maximum value very close to $\Pi_{18} = 1$. In addition, the sensitive parameters obtained via global sensitivity analysis are the same sensitive parameters obtained in the identifiability analysis step. Thus, the model analysis indicates that the major mechanisms controlling tumor growth are the immunogenicity and cytotoxicity of CD8+ T-cells over tumor cells; effect of tumor microenvironment

such as nutrients (Π_2, Π_3, Π_{13}) and the activation of cytokines (interleukin) in the presence of CD8+ T-cells (Π_{18}, Π_{19}). This macroscale analysis suggests to tumor pathologists that they could look at the gene networks related to these mechanisms and locate the responsible genes.

Here, the analysis is done after the parameters are known. However, in reality, all these 19 parameters of the reduced model are not known. In that case, patient specific tumor growth and immunological data could be used to estimate them. Then, sensitivity analysis within a range of these parameter estimates might help tumor pathologists in designing experiments for finding the key mechanism (Kontoravdi et al., 2005). Appropriate therapies can then be developed to target the respective genes and control the tumor growth. This emphasizes that experiments should be designed in a way that the identified key parameters are precisely estimated.

6.5.3 Comparison between original model and reduced model - Parameter estimation

Parameter estimation is one of the prime steps in the model building process. It is an optimization problem where the objective is to minimize the nonlinear least squares measure i.e., the closeness of fit between the measurements (data) (y_i) and the model output (y_i^M) (as shown in Equation (6.32)). The values of y_i^M is based on the decision variables (model parameters (P_r)) guided by the optimizer (Englezos and Kalogerakis, 2001). In this section, the confidence intervals of the parameter estimates of the original and reduced models are compared. There are two types of confidence intervals for parameters: individual confidence intervals and joint confidence intervals. Former type assumes that the parameters are independent from each other; as a result it may be misleading. The joint parameter regions can be obtained from different methods such as linear approximation and F-test or log-likelihood. In the present work, F-test method is used because it avoids the error

arising from the approximations of derivatives or Hessian matrices. The joint confidence interval of the parameters (J_c) is computed using Equation (6.33). K_n is the number of parameters, N_b is the number of observations, ψ_1 is the significance level and $S(P_r^*)$ is the objective value corresponding to the parameter estimates. In this respect, *in silico* data is generated using the nominal parameter values given in Table 6.1. The data (y_i) consists of tumor size for 30 days with the initial number of 10^8 cells. Different datasets are generated by adding different levels of noise in order to imitate real world clinical data. These datasets are then used for parameter estimation using both models. In the case of reduced model, only the sensitive parameters found in the previous section are estimated, while fixing other parameters at their nominal values. Because sensitive parameters are better identifiable than the insensitive parameters (Sobol, 2001). This optimization problem is solved using gradient-based methods ('fmincon') implemented in MATLAB (R2007a).

$$S(P_r) = \sum_{i=1}^N [y_i^M - y_i]^T [y_i^M - y_i] \quad (6.32)$$

$$J_c = S(P_r^*) \left[1 + \frac{K_n}{N_b - K_n} F_{K_n, N_b - K_n}^{\psi_1} \right] \quad (6.33)$$

The results presented in Table 6.7 shows that the objective values for both models are approximately of the same order, but the confidence region increases with the increase in the magnitude of the noise level. The confidence region is smaller for the parameter estimates of the reduced model than for the original model. This could be attributed to fewer parameters in the reduced model. In Table 6.7, the computational effort is indicated in terms of function counts and iterations. The results clearly indicate that the computational effort for any given dataset for reduced model is significantly lower for the reduced model than for the original model. Moreover, the closeness between parameter estimates and the "true" values is lesser for reduced model than original model (Table 6.8). The definition for closeness is as given below:

Table 6.7
Comparison of confidence regions between original and reduced models

% Noise added	Original model		
	Objective function value $S(p_r^*)$	J_c	Function count (iterations)
0	4.75×10^{-6}	0.0066	2828(51)
1	3.9×10^{-4}	0.5434	2422(55)
5	1.3×10^{-2}	18.02	2812(37)
-1	5.2×10^{-4}	0.725	2182(48)
-5	6.4×10^{-3}	8.863	2511(50)
% Noise added	Reduced model		
	Objective function value $S(p_r^*)$	J_c	Function count (iterations)
0	2.13×10^{-5}	3.78×10^{-5}	27(2)
1	5.35×10^{-4}	9.47×10^{-4}	18(2)
5	2.33×10^{-2}	4.12×10^{-2}	363(21)
-1	1.1×10^{-3}	1.9×10^{-3}	28(2)
-5	7.1×10^{-3}	1.26×10^{-2}	80(10)

Table 6.8
Closeness between parameter estimates and “true” values

% noise added	Original model	Reduced model
0	15.01	1.33×10^{-2}
1	15.65	8.7×10^{-5}
5	16.85	2.7×10^{-2}
-1	14.06	0.76
-5	6.08	2.04

Let us assume that “ D_F ” represents the difference between parameter estimates and “true values (T_V)” and $R_F = D_F/(T_V)$. Closeness measure (C_M) is the logarithm of sum of absolute values of “ R_F ”.

$$C_M = \log_{10}(\text{sum}(\text{abs}(R_F))) \quad (6.34)$$

Overall, the reduced model performs better and can thus be used for practical applications such as designing model-based diagnostic and therapeutic protocols. In spite of these advantages, scaling analysis can become very difficult for large and complex systems, particularly if done manually. We are aware that some research groups (apart from ours) are trying to develop computer codes to automate the scaling analysis procedure. When these codes are available, scaling large scale models in an error free manner can be easily accomplished.

6.6 Conclusions

This chapter exemplifies the significance of model reduction techniques in comprehending tumor-immune interactions. However, complexity of physiological models may hinder their clinical applications. Tumor-immune model elucidating the immunogenic tumor growth was considered in this work. Scaling approach was used to obtain a minimal tumor-immune model with significantly smaller number of parameters and without any loss in the predictive ability. The magnitude of coefficients in the minimal model is in the order-of-one value unlike the original model. The time derivative scale factors showed that rate of change of CD8+ T cells is very high in comparison with natural killer cells and circulating lymphocytes. The advantage of scaling analysis is quantified and found the identifiable parameters using theoretical identifiability analysis. It was observed that the scaling analysis helps in conditioning the Fisher Information matrix. Further, global sensitivity analysis was performed to identify the key parameters affecting the tumor growth. The re-

sults obtained from global sensitivity analysis were in agreement with the results of theoretical identifiability analysis. The mechanisms controlling the immunogenic tumor growth were tumor microenvironment, immunogenicity and amplification of cytokine production due to CD8+ T-cells. This suggests that the pathologists may look into these relevant gene networks for discovering the genetic factors and facilitate personalized therapy. The results presented in this work computed that the uncertainty of the parameter estimates of reduced model is smaller than that of the original model. Also, the computational effort of reduced model for parameter estimation is significantly less compared to the computational effort required for the original model. In the next chapter, this reduced tumor-immune model is used to conduct model-based population studies wherein the population is generated *in silico* by varying the key parameters affecting the tumor growth. This may help us to understand and address the effect of interpatient variability on protocol design.

Chapter 7

POPULATION BASED OPTIMAL EXPERIMENTAL DESIGN IN CANCER DIAGNOSIS AND CHEMOTHERAPY - *IN SILICO* ANALYSIS

'In my opinion, no single design is apt to be optimal for everyone.'

- Donald Norman

7.1 Introduction

Interpatient variability is one of the critical issues in the clinical implementation of cancer diagnostic and therapeutic protocols. Presently, cancer diagnostic and therapeutic protocols are suggested based on clinical trials conducted on a particular cohort of patients. However, these developed protocols are used on other patient groups as well (Kleinsmith, 2005). Also, for a given treatment protocol, only few patients may be fully cured and others may not be. In fact, it is necessary to know the reasons behind the observed variability in the effect of diagnostic and treatment protocols on patients - this will help to tailor and improve the protocols to meet the treatment objectives. These experiments will cost significant time and money. According to recent studies, the cost involved in the research and development of a new drug for Food and Drug Administration (FDA) approval is between US \$ 500 million and US \$ 800 million and the development time is around 10-12 years. It is reported that 1 out of 1000 potential drugs reaches the clinical stage and around 90% of the drugs fail during clinical trials (Holford et al., 2010).¹ This means, failure of a

¹<http://www.news-medical.net/news/2004/12/07/6730.aspx>

drug can be quite frustrating in terms of wasted effort and expenditure. Currently, big pharmaceutical companies are trying to minimize this loss by embracing the option of modeling and simulation (*in silico* experiments) based clinical trials (Holford et al., 2010). In fact, FDA is recognizing and encouraging clinical trial simulations using pharmacokinetic and pharmacodynamic models to ease the approval of new drugs with lesser number of experiments (Hooker and Vicini, 2005).² At the same time, these *in silico* experiments might help in customizing optimal dosing regimens of existing therapies for a specific population.

According to recent reviews on modeling of cancer growth (Lowengrub et al., 2010) and optimization of anticancer therapies (Swierniak et al., 2009), little or no work has been done on population based studies for designing diagnostic protocol and the post-therapy analysis of therapeutic protocols. Consequently, the main questions addressed in this chapter are: (i) how does one design diagnostic protocols such that the patient specific parameters are better estimated and (ii) how to capitalize on previous records of patient treatment to find patient specific parameters that decide the outcome of the therapy. In order to address these issues, reduced tumor-immune model from the previous chapter is used for performing population-scale studies. In this chapter, a diagnostic protocol is proposed for the population using the concept of optimal design of experiments. Figure 7.1 projects the idea of choosing a diagnostic protocol based on information index for a given *in silico* patient cohort. To do this, a multi-objective optimization problem is formulated with the objectives: (i) maximization of information index and (ii) minimization of measurement effort during the medical examinations.

Even though treatment protocol for a given drug or therapy is suggested based on human trials, the application of the same treatment protocols might fail with some patients (as shown in Figure 7.2). This is to be expected because the human trials

²<http://www.fda.gov/downloads/Drugs/GuidanceComplianceRegulatoryInformation/Guidances/UCM072137.pdf>

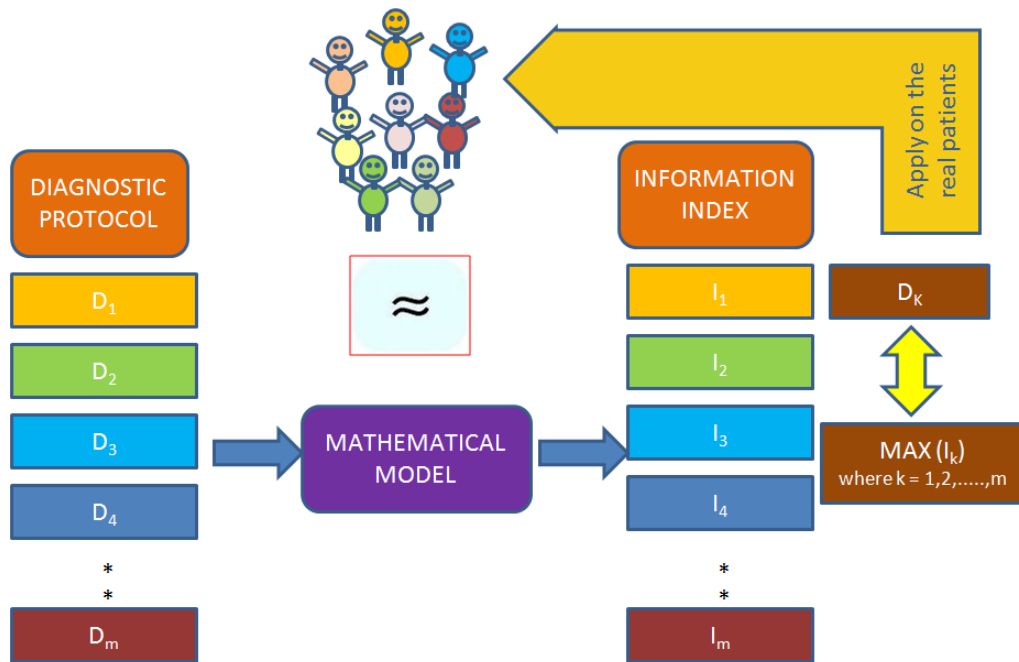


Fig. 7.1. Determination of diagnostic protocol (D_i) for a patient population based on information index (I_i) evaluated using the mathematical model

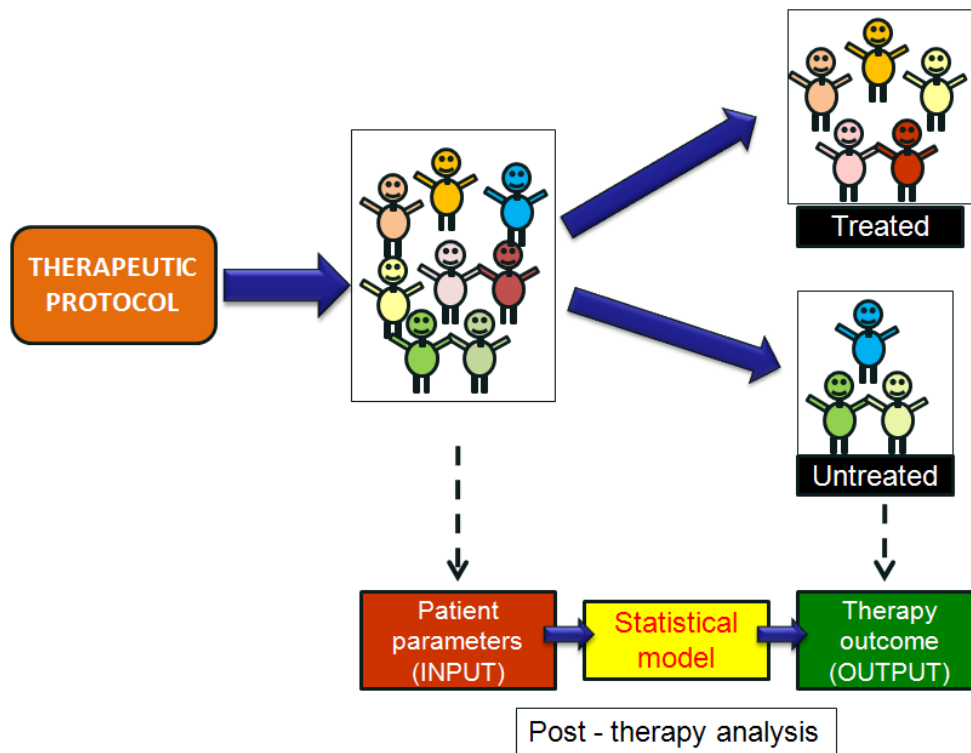


Fig. 7.2. Post - therapy analysis using statistical modeling to find the rules determining the therapeutic effect on a patient

do not cover the entire range of population. In this regard, post-therapy analysis of historical treatment database of any therapy can be helpful in determining therapeutic success. Consequently, the outcome of the analysis can guide in suggesting a therapeutic protocol to new patients. To facilitate this, another multi-objective optimization problem based on optimal control theory is formulated and a treatment protocol is chosen from Pareto solutions for the given patient cohort. Then, the chosen protocol is applied on the same patient cohort and the patients are classified based on the tumor response at the end of treatment course. Patient parameters (treated as input data) and the treatment outcome (treated as output data) are used to build a classification model and rules are determined based on the parameters to estimate the therapy outcome.

7.2 Mathematical model

The only difference in the model presented below from the previous chapter is that the pharmacokinetics and pharmacodynamics of doxorubicin are also included. Symbols T , N , L , C , I , M in the model stand for tumor cells, natural killer (NK) cells, cytotoxic (CD8+) T-cells, circulating lymphocytes, interleukin and chemotherapeutic drug (doxorubicin) respectively. Equation (7.6) describes the pharmacokinetics of doxorubicin and its pharmacodynamic effects are given by last terms in Equations (7.1, 7.3 & 7.5). Π_{24} is the pharmacokinetic parameter and Π_{20} , Π_{21} , Π_{22} , Π_{23} are the pharmacodynamic parameters and U is the input rate of doxorubicin. α_1 , α_2 , α_3 , α_4 , α_5 are the time derivative scale factors and T_s , N_s , L_s , I_s , C_s are the scale factors for tumor cells, NK cells, CD8+ T-cells, interleukin and circulating lymphocytes respectively. The reduced tumor-immune model is as given below.

$$\alpha_1 T_s \left(\frac{dT^*}{dt} \right) = T^* - T^{*2} - \Pi_1 N^* T^* - \Pi_2 T^* \left(\frac{L^*}{T^*} \right)^{\Pi_3} - \Pi_{20} (1 - \exp(-M^* M_s)) T^* T_s \quad (7.1)$$

$$\alpha_2 N_s \left(\frac{dN^*}{dt} \right) = C^* - \Pi_4 N^* - \Pi_5 N^* T^* + \frac{\Pi_6 N^*}{\left(\frac{\Pi_7}{I^*} + 1 \right)} - \Pi_{21} (1 - \exp(-M^* M_s)) N^* N_s \quad (7.2)$$

$$\alpha_3 L_s \left(\frac{dL^*}{dt} \right) = \Pi_8 \left(\frac{L^*}{I^*} \right) + \frac{\Pi_9 L^*}{\left(\frac{\Pi_{10}}{T^*} + 1 \right)} - \Pi_{11} L^* T^* + N^* T^* + \Pi_{12} C^* T^* - \frac{\Pi_{13} L^{*2} C^*}{\left(\frac{\Pi_{14}}{T^*} + 1 \right)} + \frac{\Pi_{15} L^*}{\left(\frac{\Pi_{16}}{I^*} + 1 \right)} - \Pi_{22} (1 - \exp(-M^* M_s)) L^* L_s \quad (7.3)$$

$$\alpha_4 I_s \left(\frac{dI^*}{dt} \right) = -I^* - \Pi_{17} C^* + \frac{\Pi_{18} L^*}{\left(\frac{\Pi_{19}}{I^*} + 1 \right)} \quad (7.4)$$

$$\alpha_5 C_s \left(\frac{dC^*}{dt} \right) = 1 - C^* - \Pi_{23} (1 - \exp(-M^* M_s)) C^* C_s \quad (7.5)$$

$$M_s \left(\frac{dM^*}{dt} \right) = -\Pi_{24} M^* M_s + U \quad (7.6)$$

7.3 Population-based studies

7.3.1 Optimal design of experiments for cancer diagnosis

After tumor detection, different diagnostic tests are carried out to analyze the tumor characteristics. The components of immune system are monitored to investigate the immune action on the tumors before the treatment process is initiated. It is not practical to continuously monitor the tumor and immune system behavior. The time gap between the tumor detection and initiation of treatment depends on several factors such as type of cancer, stage of cancer, physician-patient interaction.³ Here, the time gap is taken as 1 month. During this period, sampling times of tumor and immune cells can be very important and the measurement should yield accurate information on the patient's health status i.e. measurements should be such that the patient parameters can be accurately estimated.

An optimization problem is formulated to determine which states (tumor, CD8+ T-cells and interleukin) are to be measured and at what time points they should be measured. The objective is to minimize the covariance matrix of the estimated

³<http://www.cancerhelp.org.uk/about-cancer/cancer-questions/waiting-times-for-tests-and-treatment-after-cancer-diagnosis>

parameters which is equivalent to maximization of Fisher information matrix (FIM) (Englezos and Kalogerakis, 2001). The elements of FIM are the sensitivity indices of the parameters. Generally, the maximization of FIM is done by reducing the matrix to a scalar quantity. In this regard, there are different scalar criteria to maximize FIM - these include D-optimality, A-optimality and E-optimality. D-optimality is the most common approach (which uses the determinant value of FIM as the scalar metric for optimization) and it gives equal weightage to all the parameters (k). There are many biomedical applications based on D-optimality criterion, one such example is the work by Hulting et al. (2006).

$$FIM = \sum_{i=1}^{\nu} G_i^T G_i \quad (7.7)$$

where

$$G_i = \begin{bmatrix} \frac{\partial z_1}{\partial k_1} & \frac{\partial z_1}{\partial k_2} & \cdots & \frac{\partial z_1}{\partial k_p} \\ \frac{\partial z_2}{\partial k_1} & \frac{\partial z_2}{\partial k_2} & \cdots & \frac{\partial z_2}{\partial k_p} \\ \cdots & \cdots & \cdots & \cdots \\ \frac{\partial z_m}{\partial k_1} & \frac{\partial z_m}{\partial k_2} & \cdots & \frac{\partial z_m}{\partial k_p} \end{bmatrix}_i \quad (7.8)$$

$$Cov(\hat{k}) \geq FIM^{-1} \quad (7.9)$$

In Equations (7.7) and (7.8), z represents states, k represents parameters, m is the number of states, p is the number of parameters and ν is the number of observations. According to Cramer-Rao inequality, the covariance matrix of the parameters is greater than or equal to inverse of FIM (Equation 7.9).

One key focus of the present work is on optimal design of experiments for a given population where the objective is to maximize population Fisher information matrix (PFIM) (Aarons and Ogungbenro, 2010; Hooker and Vicini, 2005; Silber et al., 2009). This is essential in order to take care of interpatient variability. In this work, a patient is assumed to be represented by the reduced form of tumor-immune model which was explained in Section 7.2. In the previous chapter, using the same model, the key parameteric groups ($\Pi_3, \Pi_{18}, \Pi_2, \Pi_{19}, \Pi_{13}$) affecting the tumor growth (no

treatment case) were determined using global sensitivity analysis techniques. In the present study, interpatient variability is simulated by varying the key parametric groups influencing the tumor growth while fixing the remaining insensitive parametric groups at their nominal values. The parametric groups are assumed to follow uniform distribution. And another assumption is that the measurement error associated with state variables (tumor, immune cells and interleukin) is negligible. It means the variation in the state variables is only because of the variations in the parametric groups. Then, the key parametric groups are varied by $\pm 25\%$ of their nominal values and the patient population is chosen from the parameter space using Latin hypercube sampling. The above population selection is quite similar to later phases of clinical trial where different individuals are randomly selected to test the new protocols (Airley, 2009; Kleinsmith, 2005). Here, the population size (n_{P1}) is chosen as 300 which is equivalent to considering 300 patients for analyzing the features of their tumors. In formulation A of the problem, objective 1a corresponds to the determinant of the Fisher information matrix and objective 2a is the numbers of states to be measured (y_1). The practical implication of second objective is to reduce the measurement effort. The decision variables included are the sampling timings (x_i) and two integer variables y_1 and y_2 . y_1 represents the number of states (CD8+ T-cells, interleukin) to be measured in addition to the measurement of tumor. If y_1 turns out to be 1, then it means only tumor measurement is enough. If y_1 turns out to be 3, then it means all states need to be measured at the sampling times. For $y_1 = 2$ there are two possibilities (tumor and CD8+ T-cells ($y_2 = 1$) or tumor and interleukin ($y_2 = 2$)). The choice of the possibility is based on the integer variable y_2 .

Problem formulation A

Objectives

$$\text{Objective 1a: } \min_{x_i, y_1, y_2} -\log_{10} \left(\text{mean} \left(\sum_{j=1}^{n_{P1}} |\det(FIM_j)| \right) \right)$$

Objective 2a: $\min(y_1)$

Decision variables

x_i ($i = 1, 2, \dots, 5$) are the sampling times

y_1 - number of states to be measured in addition to state 1

y_2 - combination of states to be measured if $y_1 = 2$

Constraints

Constraint 1a: $0 \leq x_i \leq 30$ days (Continuous variable)

Constraint 2a: $1 \leq y_1 \leq 3$ (Integer variable)

Constraint 3a: $1 \leq y_2 \leq 2$ (Integer variable)

This mixed integer dynamic optimization problem is solved using non-dominated sorted genetic algorithm (NSGA II) implemented in MATLAB (R2007a) (Deb et al., 2000). The main advantages of NSGA II are that it is very easy to implement and requires less computational effort than other genetic algorithms. The Pareto set obtained is projected in Figure 7.3. Lesser value of objective 1a implies that more information is captured. Figure 7.3 shows that the information content increases by 133% when another state (CD8+ T-cells) is measured in addition to tumor size. Adding the extra measurement of interleukin (to CD8+ T-cells & tumor size measurement) increases the information content by an extra 20%. This makes sense because most of the information about interleukin dynamics can be captured from the dynamics of CD8+ T-cells. Overall, maximum information is captured by measuring all the states. The best times for sampling the states are presented in Figure 7.4. Clearly, three groups of sampling times is observed from Figure 7.4. The frequency of sampling is higher in the initial days after detection. The first two samples must be collected on 2^{nd} day and then the next two samples must be taken on the

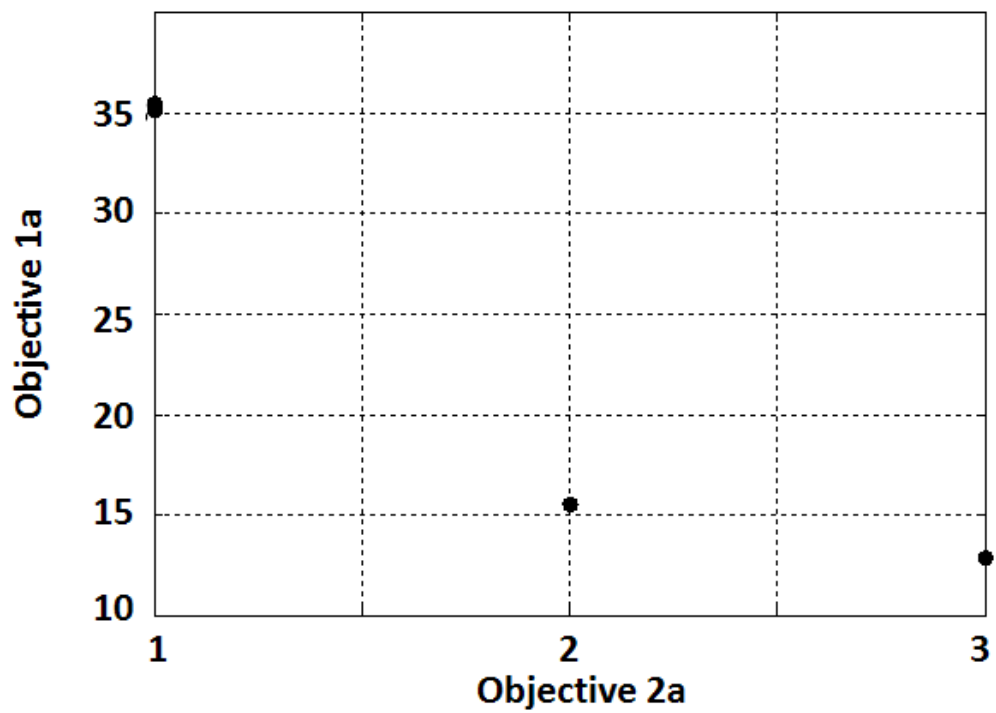


Fig. 7.3. Pareto solution (problem formulation A) corresponding to population based design of diagnostic protocol

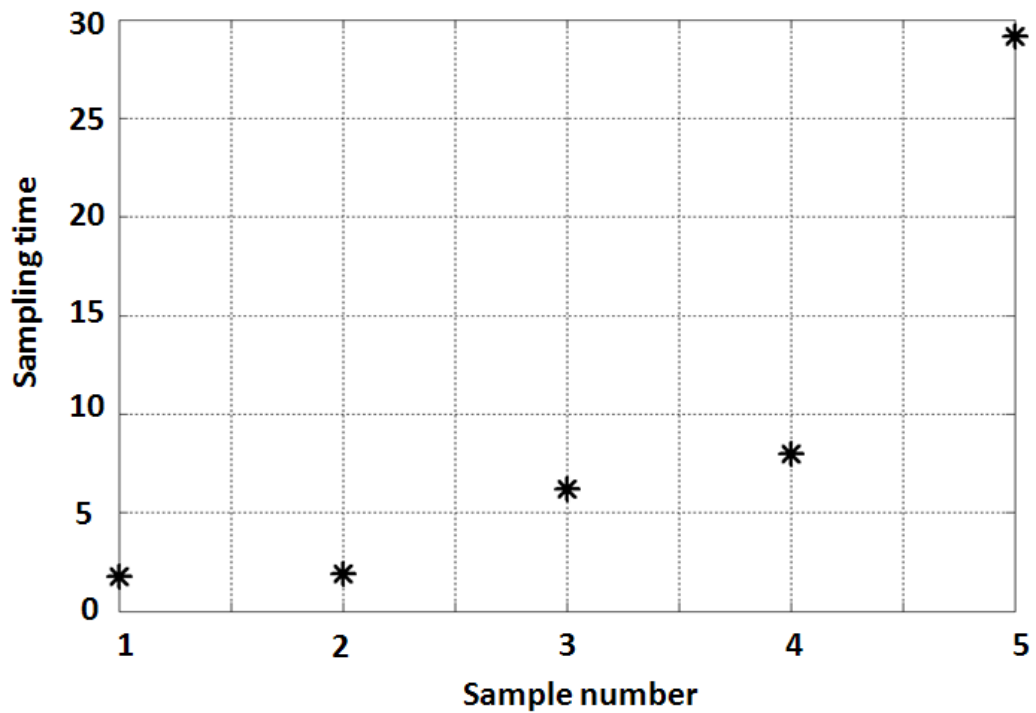


Fig. 7.4. Proposed sampling times of tumor, CD8+ T-cells and interleukin during diagnosis

7th and 8th days. The final sample must be taken close to the end of diagnostic time. This is an acceptable and logical result because the system dynamics is significant during the first 10 days after the tumor detection and, after that; the system has almost reached a steady state.

7.3.2 Optimal design of chemotherapeutic protocol and post-therapy analysis

Tumor diagnosis is followed by selection of the treatment modalities and dosage planning. Usually, chemotherapy (being a systemic therapy) is preferred (Stuschke and Pottgen, 2010; Kleinsmith, 2005) and is administered periodically over the treatment course. For example, doxorubicin ($60 - 75 \text{ mg}/\text{m}^2$) is given once every 3 – 4 weeks (Airley, 2009). In this work, for simplicity, the intervention is assumed to be given once every 3 weeks and the treatment horizon is considered as one year. The approximate number of interventions (n_I) per year is equal to 18. However, sometimes, the side effects of chemotherapy such as neutropenia (Rivera et al., 2003) and cardiotoxicity (Swain et al., 2003) are more critical than the tumor growth itself. Therefore, it is necessary to include relevant constraints on doxorubicin while designing the treatment protocol. To understand the effect of doxorubicin, a patient cohort is generated by changing the values for parametric groups in the model. The parameters in this part of the study include not only those found to be important from global sensitivity analysis but also the pharmacokinetic (Π_{24}) and pharmacodynamic (Π_{20} , Π_{21} , Π_{22} , Π_{23}) parameters. From Equation (7.6), lower value of Π_{24} indicates the decrease in the decay of doxorubicin. As a result, the drug concentration in the body might increase. Similarly, lower value of pharmacodynamic parameters signifies the phenomenon of drug resistance. Another important question posed is whether the key parameters affecting the tumor remain the same or change due to the inclusion of pharmacokinetics and pharmacodynamics of doxorubicin. This question is answered in the later sections based on post-therapy analysis.

A multi-objective optimization problem is formulated to find a compromise solution balancing the objectives: tumor elimination and reduction of side effects. In the formulation below, objectives 1b-3b are related to tumor cells and they correspond to overall tumor growth control, minimization of final tumor size at the end of treatment course and the minimization of maximum possible tumor size respectively. The remaining objectives 4b and 5b emphasize on the reduction of doxorubicin dosages and controlled regulation of circulating lymphocytes respectively. Therefore, these objectives serve to prevent infections due to the imbalance in immune cells (Rivera et al., 2003). Constraint 1b is the time duration to achieve the targets of the treatment. Constraint 2b relates to the total number of interventions (n_I). C_3 and C_4 represents the constraint on the maximum drug concentration and drug concentration in the body during the treatment course respectively (Hon and Evans, 1998; Laginha et al., 2005). Constraints 3b and 4b help to prevent immediate and long term side effect on the patients respectively.

Problem formulation B

Objectives

$$\text{Objective 1b: } \min \left(\frac{\sum_{j=1}^{n_{P2}} \left(\int_0^{t_f} T dt \right)_j}{n_{P2}} \right)$$

$$\text{Objective 2b: } \min \left(\frac{\sum_{j=1}^{n_{P2}} (T_f)_j}{n_{P2}} \right)$$

$$\text{Objective 3b: } \min \left(\frac{\sum_{j=1}^{n_{P2}} (\max(T))_j}{n_{P2}} \right)$$

$$\text{Objective 4b: } \sum_{i=1}^{18} q_i$$

$$\text{Objective 5b: } \max \left(\frac{\sum_{j=1}^{n_{P2}} (\min(C))_j}{n_{P2}} \right)$$

Decision variables: q_i where n_{P2} is the population size (300), q_i is the dosage of each intervention

Constraints

Constraint 1b: $t_f = 365$ days

Constraint 2b: $n_I = 18$

Constraint 3b: $C_3 = \left((M_{\max})_{i=1,2,\dots,n} \right)_{\max} \leq 50$

Constraint 4b: $C_4 = \left((AUC)_{i=1,2,\dots,n} \right)_{\max} \leq 4100$

The above multi-objective optimization problem is solved using NSGA-II algorithm implemented in MATLAB (R2007a). The obtained Pareto solution space is as shown in Figure 7.5. From the problem formulation, it is clearly seen that the

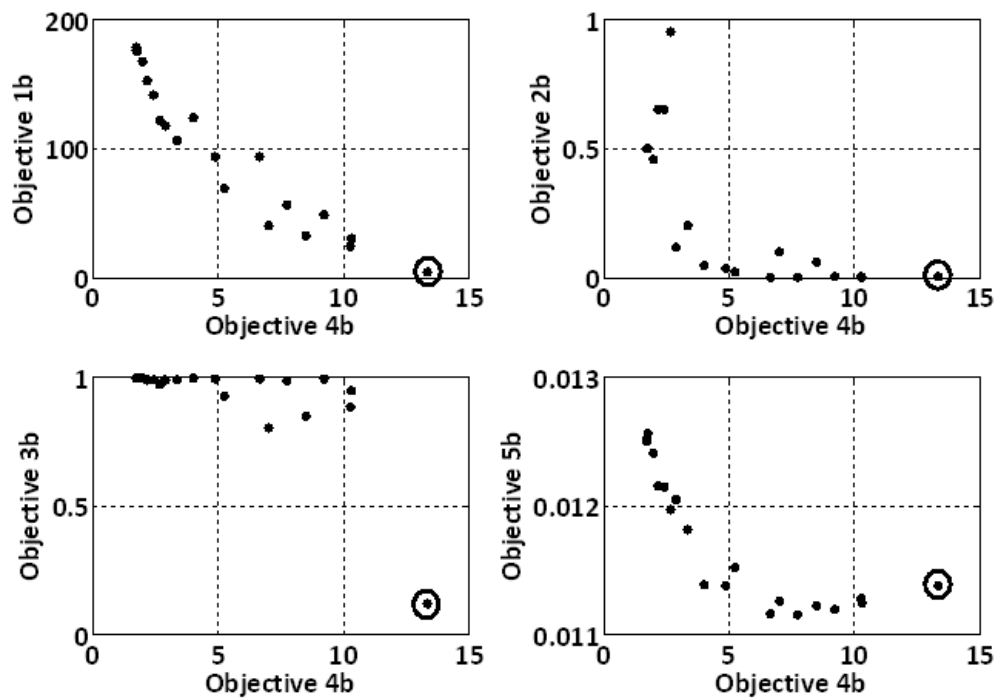


Fig. 7.5. Pareto solution (problem formulation B) corresponding to population based design of treatment protocol

main concern is to understand the effect of chemotherapy on tumor cells and circulating lymphocytes. Thus, in Figure 7.5, the objectives related to tumor cells (objectives 1b, 2b, and 3b) and circulating lymphocytes (objectives 5b) are plotted against the objective 4b (total dosage of doxorubicin (given in scaled units))⁴. It is observed that objectives 1b, 2b decreases with the increase in doxorubicin dosage. Initially, the decrease of objective 2b is steep with the increase in objective 4b and after that, it stays almost constant. It implies that the effect of doxorubicin dosage becomes insignificant in decreasing the final tumor size when the total doxorubicin dosage exceed 5 units. However, it is noticed that the decrease of objective 3b (maximum possible tumor size) is significant only when the value of the total drug dosage is greater than 10 units. Also, from the values of objective 5b in Figure 7.5, it can be said that the variation of objective 5b with objective 4b is practically negligible. Overall, Pareto solution suggests that the total doxorubicin dosage should be in between 10 units and 15 units in order to satisfy all the objectives related to tumor growth. Thus, the therapeutic protocol corresponding to the encircled point in Figure 7.5 is chosen and is presented in Figure 7.6.

The selected treatment protocol is then implemented on the patient cohort used in the optimization problem and their corresponding tumor evolution is computed (Figure 7.7). It is noticed that tumor regression is observed in 43% of the patients while there is no effect of the therapy on the others. According to Khaloozadeh et al. (2009), a patient is said to be in “safer zone” if the number of tumor cells is less than 10^4 . Thus, the treatment protocol applied on the patient cohort indicates that only some patients are brought to a safe level. This resembles the real scenario wherein due to interpatient variability only a portion of patients with same tumor size are cured with the standard treatment protocols.

It is important to derive the “rules” which determine the success of the proposed treatment protocol. In this regard, the patient cohort is divided into two groups viz. *cured* and *uncured* at the end of the treatment period. A dataset which includes the

⁴One scaled unit is equivalent to 60 mg/m^2

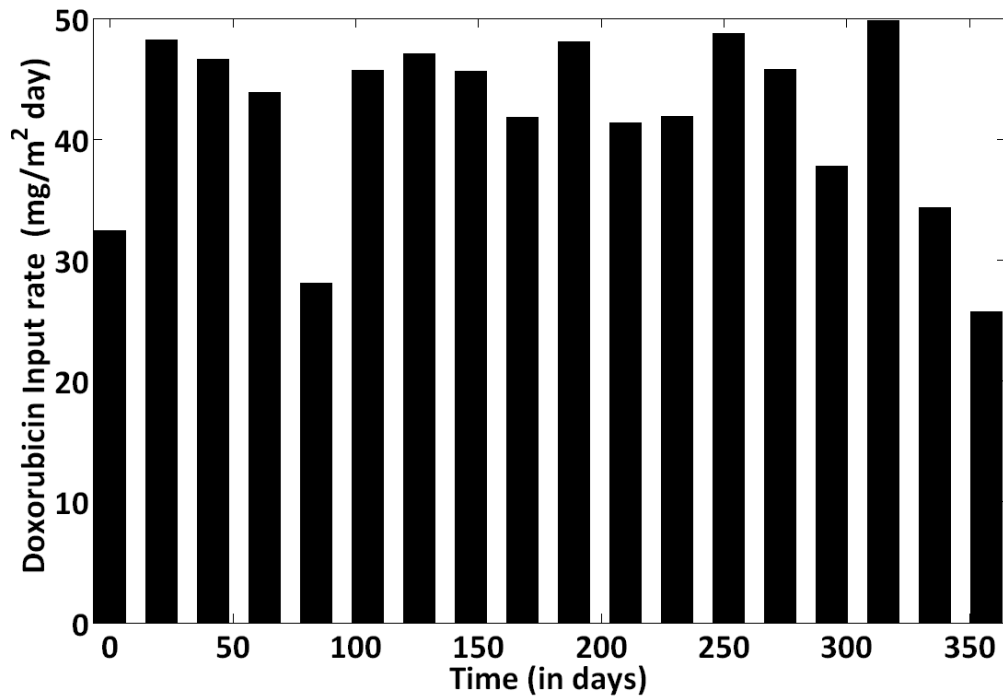


Fig. 7.6. Proposed treatment protocol for the considered patient cohort

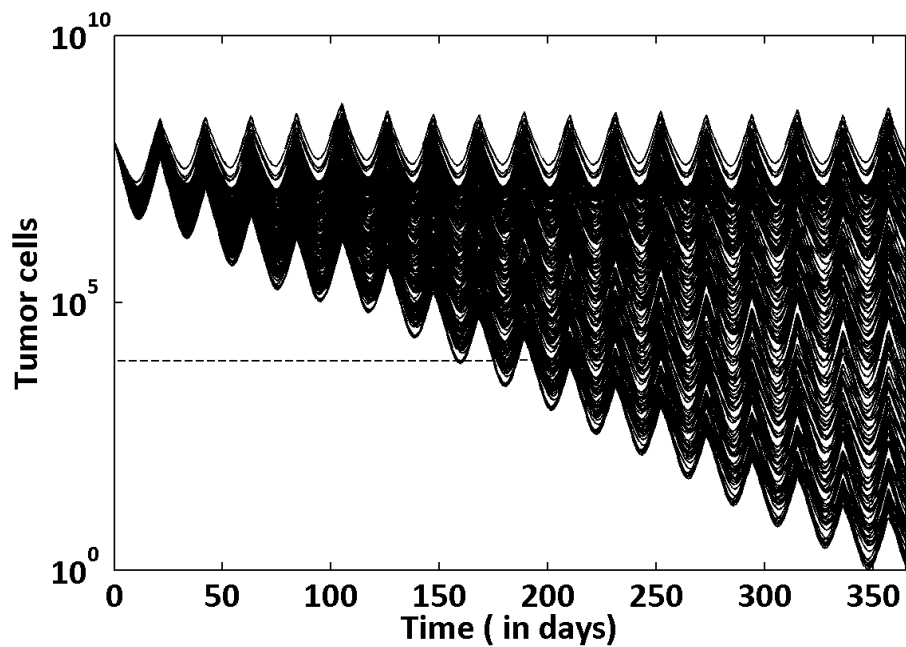


Fig. 7.7. Tumor evolution in different patients

patient parameters and their therapy outcome (after the execution of the proposed treatment protocol) is created for this purpose. This dataset is used to develop a

statistical model in the form of classification tree using the classification algorithm “*classregtree*” command implemented in MATLAB (R2007a). This command generates a classification tree for the response variable as a function of the predictors (patient parameters).

Initially, 100 model building runs are carried out on the dataset. In each run, the dataset is randomly divided into training (70%) and testing (30%) sets and a classification model is generated using training set. Each generated model is tested with their respective testing set. Models with more than 90% correct classification of test samples are selected from these 100 models and in our case, 2 such models were found. In order to choose a model among these two selected models, further testing is performed.

Each selected model is checked for its consistency in terms of correct classification by carrying out 1000 runs where, in each run, the training and testing samples are selected randomly. Finally, the best model is chosen and its decision tree is

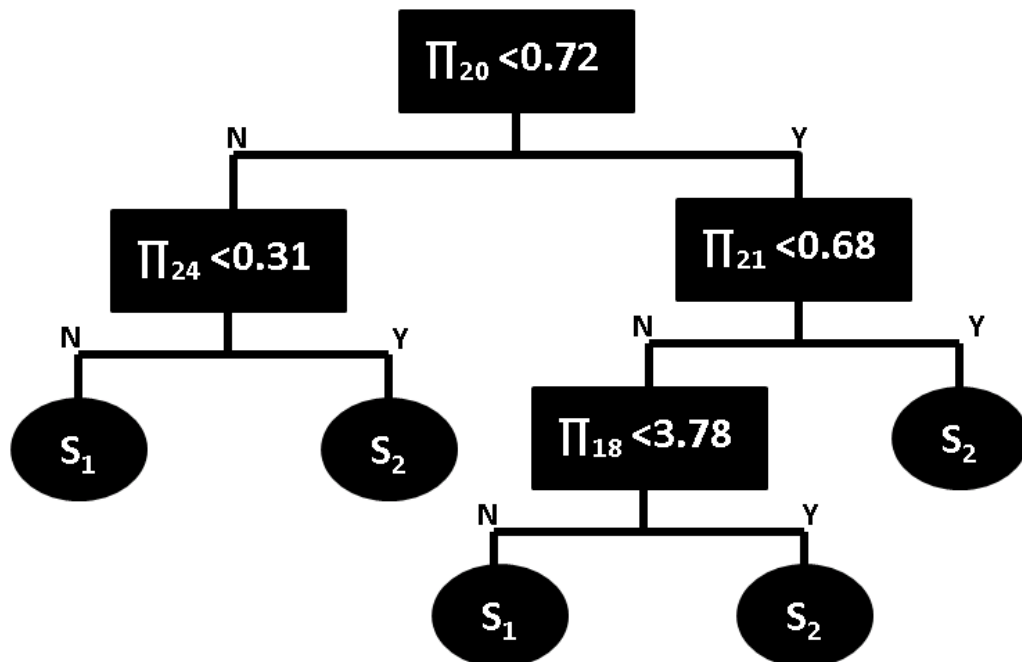


Fig. 7.8. Rules to determine the success of proposed treatment protocol on the population

presented in Figure 7.8. It is observed that the average correct classification by the decision tree is 90%. In Figure 7.8, ‘N’ and ‘Y’ means no and yes respectively, S_1 and S_2 corresponds to the safe level and unsafe level of tumor size by final time respectively. The prominent parameters influencing the treatment protocol and grouping of patient cohort are found to be pharmacodynamic parameters (Π_{20} , Π_{21}), pharmacokinetic parameter (Π_{24}) and the parameter related to the activation of interleukin due to presence of CD8+ T-cells (Π_{18}). Furthermore, the decision tree (given in Figure 7.8) is cross validated with the decision tree obtained from the commercial data mining software, CART⁵. The decision tree obtained from CART confirms that pharmacokinetic (Π_{24}) and pharmacodynamic parameters (Π_{20} , Π_{21}) determine the treatment outcome which is also in agreement with the literature (Canal et al., 1998). If the pharmacokinetic and pharmacodynamic parameters are low, then the drug concentration in the patient remains at a high level leading to acute side effects. This highlights that it is very important and informative to monitor the drug activity in the patient to estimate the pharmacokinetic and pharmacodynamic parameters during the initial interventions. Such early quantification of drug activity can help to decide whether to increase the drug dosage (within the safer limits) or opt for alternative drugs in the future interventions on this patients. Analysis of historical record of the outcomes obtained by applying different therapies on different patient cohorts may help to pave way for understanding the epidemiological differences and personalizing therapy for the patients by making effective use of existing treatment modalities.

7.4 Conclusions

This work exemplifies the significance of modeling and optimization techniques in designing diagnostic and therapeutic protocols for cancer. Tumor-immune model elucidating the immunogenic tumor growth was considered in this work. The sim-

⁵<http://salford-systems.com/cart.php>

plified model is used to imitate cohort based clinical trials to find optimal sampling times of measurement of tumor, CD8+ T-cells and interleukin during diagnosis and determine optimal doxorubicin dosage for the standard protocol. Multi-objective optimization problems were formulated to study optimal design of diagnosis and therapy. The results of diagnosis protocols reveal that more information can be captured by measuring interleukin concentration and CD8+ T-cells along with the tumor measurement. It was found that the frequency of sampling needs to be high within first 10 days after tumor is detected which is in coherent with the dynamics of the states. Similarly, “cohort based” studies were performed to determine a better treatment protocol of doxorubicin. Then, statistical classification techniques helped to identify that pharmacokinetic, pharmacodynamic and CD8+ T-cells activation parameters determine the success of the proposed treatment protocol. Such *in silico* analysis can be helpful in the eventual development of personalized therapy.

Chapter 8

CONCLUSIONS AND RECOMMENDATIONS FOR FUTURE WORK

‘One ounce of practice is worth a thousand pounds of theory.’

- Swami Vivekananda

8.1 Conclusions

Cancer is a global issue and an important multidisciplinary field of research with a lot of open ended and challenging problems. The main thrust of this thesis is to highlight that application of process systems engineering techniques can play an important role in addressing the problems related to cancer dynamics and its treatment. The main focus of this thesis is to study the initial stages of cancer progression - avascular tumor growth and its interaction with the therapeutic agents. In the first two chapters, the role of modeling in cancer, broader review of works which were done hitherto, challenges and contributions of this thesis were introduced.

The first objective of this work was to develop a mechanistic mathematical model to describe the avascular tumor growth. The proposed model accounts for all the pertinent cellular processes (proliferation, apoptosis and necrosis) and their dependency on the diffusion and consumption of the nutrients. The model was able to synchronize with the experimental results in terms of predicting tumor growth and maximum volume achieved under different microenvironment conditions. The results of onset of necrosis clarifies the proposition that necrotic zone is the consequence

of the critical concentrations of both vital nutrients. The time at which necrotic zone starts might indicate tumor vascularization (connection with the nearby blood vessels). Additionally, the model is prognostic in distinguishing the size of proliferation zone, quiescent zone and necrotic zone and their effect on the overall tumor growth. Practically, it is formidable to measure the diffusive and consumption rate parameters of the nutrients. Therefore, the proposed model can be useful for tumor pathologists in determining those parameters from the multicellular tumor spheroid experimental data using the sample extracted from the patient.

The second objective was to propose a therapeutic protocol for a given patient while considering practical multiple objectives associated with cancer therapies. Chemotherapy is the common adjuvant therapy given to the patient at stage or another during the course of cancer treatment and, nowadays, they are combined with the targeted therapies to reduce the side effects. Thus, the multiple objectives can be broadly related to tumor reduction and reduction of side effects. This scenario is dealt in chapter 4 by formulating a multi-objective optimization problem using a tumor-immuno-chemo model (patient representation) adapted from the literature. NSGA -II was used to find the solution set known as Pareto set and the decision variables represented the timing and dosage of the interventions. Then, post-Pareto-optimality analysis was done to choose a solution from Pareto set. The results for the considered patient have shown that the performance of the proposed chemotherapy protocol was better than the standard protocol employed in medical practice. However, at the end of the treatment course the number of tumor cells were in the range of 10^5 cells. Alternatively, the combination of chemotherapy and immunotherapy resulted in almost complete elimination of tumor cells. Also, post-treatment analysis based on tumor relapse time has indicated that combination therapy is better than chemotherapy. As a whole, this work suggests that the immunogenicity factor (intensity of tumor-immune interactions) must be taken into account prior to every therapeutic intervention. The real outcome of this work

emphasizes on the utility of computer based pre-treatment analysis or treatment planning decision-support system for oncologists in deciding a treatment protocol for a patient.

Inpatient variability is one of the major challenges in cancer therapy because variability in patient dynamics (response to drugs) might result in overdose or underdose of therapeutic agents. Thus, it is necessary to monitor the patient regularly and look for tumor growth variations which can be attributed to different factors. The questions addressed were related to the parameters which are to be monitored when a patient visits the clinic and how to reschedule the interventions based on those parameter values. In chapter 5, this challenge was investigated using a mathematical model elucidating the interaction between tumor cell and different types of immune cells. The key parameters affecting the tumor growth were found out using global sensitivity analysis techniques. The key mechanisms were found to be the proliferation of tumor cells due to nutritional effect, its interaction with CD8+ T-cells and the availability of CD8+ T-cells. These key parameters are further crosschecked by formulating an optimization problem and comparing the nominal and reactive schedules of the dendritic cell interventions. The nominal and reactive schedules for variation in non-key parameters were approximately the same, while in the case of key parameter variations they were different. Similar results were observed in these simulation studies. Further, for a given parametric variation, reactive scheduling was applied to propose the dosage interventions of single therapy of dendritic cells and the combination therapy of dendritic cells and interleukin. The case study has shown that dendritic cells interventions alone were enough to control and bring down the tumor size. Moreover, the cumulative dosage of dendritic cells for the reactive scheduling was lesser than the nominal scheduling. The practical implication is that combination therapy is not an absolute solution when the patient variability is significant. So, it is important to re-estimate the patient parameters

regularly and this kind of treatment planning simulators/decision-support systems will be useful in rescheduling the therapeutic interventions.

Another issue addressed in this thesis relates to the importance of simplification of complex physiological models in order to facilitate its clinical applications. The complexity of physiological models increases with the inclusion of updated knowledge about them. In this regard, scaling and sensitivity analysis approaches were utilized to obtain a reduced parametric model. As a case study, a comprehensive and highly parameterized tumor-immune model was taken from literature. Scaling analysis helped in obtaining a minimal model with lesser number of parameters than the original model without any loss of information. That is, no reduction in the predictive ability of the model. At the same time, the values of the coefficients in the model equation were in the order-of-one. This implies that corresponding terms in the equation with lowest coefficient values can be nullified. Also, the advantage of scaling analysis is quantified using theoretical identifiability analysis. Further, the application of global sensitivity analysis helped in finding the key parameters affecting tumor growth. The key mechanisms were found to be the effect of nutrients, intensity of interaction between tumor cells and CD8+ T-cells and they are in agreement with the previous case study done in chapter 5. Another comparison between reduced and original model was done on the basis of parameter estimation. The results have shown that the uncertainty of the parameter estimates of the reduced model is smaller than that of the original model (as expected). Also, the computational effort is significantly less for the parameter estimation of reduced model when compared to the original model.

The simplified model was used to imitate cohort-based clinical trials and accounted for interpatient variability. Then, for a given patient cohort (generated by varying key parameters), optimal sampling times for collecting tumor cells and immune cells from patient during diagnosis (before treatment is commenced) and

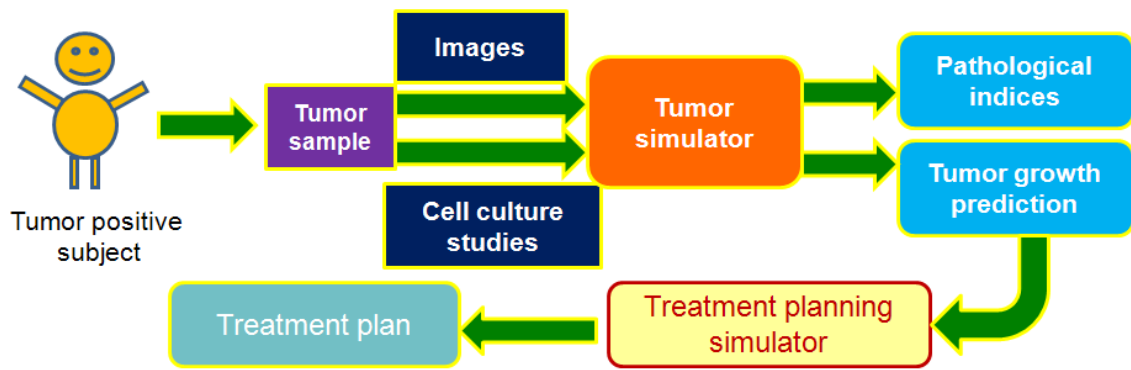


Fig. 8.1. Application of this thesis work in the clinical practice

optimal doxorubicin dosage for the existing standard protocol were suggested. In this regard, multi-objective optimization problems were formulated for studying optimal design of diagnosis and therapy. The results for optimal design of diagnostic protocol indicates that more information can be captured by measuring interleukin concentration and CD8+ T-cells along with the tumor measurement. Similarly, cohort based studies were performed to determine a better treatment protocol for the generated patient cohort. However, only some patients were cured and some weren't after the application of the chosen treatment protocol. Then using this patient cohort data (parameters and therapeutic outcomes), a statistical analysis was performed to outline rules based on parameter values that would ensure the success of the proposed treatment protocol. In summary, the above contributions stress that *in silico* analysis can be helpful in studying the failure analysis of a given treatment protocol and helps in suggesting an appropriate treatment plan for a patient.

Overall, algorithms and tools developed in this research work can be used as tumor and treatment planning simulators by tumor pathologists, oncologists and oncology pharmacists. The ideas generated in this thesis are supported theoretically and are envisioned with a mission (Figure 8.1) to implement tumor and treatment planning simulators in the clinics to achieve the goals of cancer therapy in a more efficient way.

8.2 Recommendations for future work

8.2.1 Validation of the tumor growth models

The main limitation of mathematical modeling is that there is no perfect model which can exactly replicate all the scenarios observed in a real system. Also, model accuracy is dependent on the dataset used to build the model and numerical techniques used to solve the model. Hence, a model should be thoroughly validated and understand its range of predictive capability before using it for real time applications.

The mechanistic model developed in this work (Chapter 3) was validated with some of the *in vitro* and *in vivo* tumor growth data. However, it needs to be validated further with some more cell studies encompassing different types of cancer in order to test its robustness. Moreover, the mechanistic avascular tumor growth model developed in this work focused only on the diffusion of nutrients, but not on the dynamics of the growth factors. It was assumed that the presence of growth factors allows the tumor cells to uptake the nutrients and nurture. It is necessary to understand the mechanism that underlies how the presence of growth factors regulates the tumor growth. Another issue is the availability of wide range of models to explain a given phenomenon, for example, tumor-immune interactions. The question is which model is to be chosen for tumor growth predictions and therapeutic analysis. One of the ways could be the approaches of model discrimination. Eventually, a model chosen from model discrimination procedure can be used to analyze the clinical data on tumor growth which is available in the form of images. The probable challenge is in using the image data to estimate model parameters.

8.2.2 Model-based therapeutic design

In the present thesis work, therapeutic analysis were done using doxorubicin, immune cells and interleukin interventions by formulating optimization problems.

Similar analysis can be extended to other types of cancer drugs for improving their protocol design and for proposing innovative combinatorial strategies. In addition, even though the present work has focused on model simplification which helps in reducing model simulation time, it did not address the issue of computational time for optimization which is one of the important factors in order to promote *in silico* analysis in the clinical applications. In this regard, a comparative study of different optimization algorithms can be done for solving a therapeutic design based optimization problem and also novel algorithms can be proposed.

8.2.3 Multiscale modeling

Cancer diagnosis is a very crucial phase to reap the benefits of available treatment modalities. Presently, tumor pathological studies based on multicellular tumor spheroid (MCTS) experiments have made a great impact in grading the tumor cells (Rodríguez-Enríquez et al., 2008; Mueller-Klieser, 1997). These experiments closely resemble *in vivo* tumor growth experiments. The effect of microenvironment, therapeutics and cell-cell interactions on tumor growth is better understood and treatment regimens can be planned accordingly. Many mathematical modeling approaches have been suggested to extract the physiological reasons and to test different hypotheses on MCTS growth. However, most of the mechanistic models (replicating MCTS experiments) discussed so far capture the macroscopic level observations and ignore the microscopic level issues. Cancer cells are formed due to genetic changes which eventually result in the distortion of the cell division process. The prime objective of the work proposed here is to pinpoint the distortion. In general, a cell divides by passing through different phases of the cell cycle. The phases of the cell cycle are G1, S, G2 and M. G1 and G2 are the preparatory phases for the DNA-duplication (S) and mitosis (M) respectively. In different phases different activated proteins are needed to carry on the cell cycle events. These proteins are activated via phosphorylation by phase-wise phosphorylated cyclin dependent

kinases (cdk) complexes (Qu et al., 2003). Formation and phosphorylation of cdk complexes initiate as soon as a cell is divided into two daughter cells. The source for the activation of cdk complexes are phase dependent cyclins and adenosine triphosphate (ATP) produced from the glucose metabolism. Transfer from one phase of the cell cycle to other phase indirectly depends on the concentration of ATP which is the product of glycolysis and oxidative phosphorylation. According to the controversial theory of Warburg effect, enhanced glycolysis is a feature of a cancer cell. It means that the oxidative phosphorylation process is avoided in the cell and the total ATP is produced only by the glycolytic pathway (Moreno-Snchez et al., 2007; DeBerardinis et al., 2008). In addition to this, there are cell cycle checkpoints based on the threshold concentration of the growth factors and proteins. Usually, if any abnormality is observed, p53 pathway triggers the cell to commit suicide known as apoptosis (Danilo and Jose, 2009). But, these controlling mechanisms are believed to be inactive in the cancer cells. Most of the previous works were focused on particular individual pathways. So, the future work could focus to integrate the aforementioned biochemical pathways of cell cycle progression and cell division with the glucose metabolism and analyze the cancerous features by calculating the time taken to complete a cell cycle.

The main steps include:

1. Acquisition and preprocessing of metabolome, proteome and genome data from the available databases.
2. Application of data mining techniques to develop the network models elucidating the causality and relationship among the metabolites, proteins, and genes.
3. Parametric sensitivity analysis of the network models will be performed to investigate the key parameters affecting the cell cycle progression and its division.

4. Application of multiscale modeling to predict the tumor growth and the variation in the tumor morphology over time.

The above four steps will be explained in detail below.

Building of network models

The goal of the proposed work is to develop a network model among the metabolites, proteins and genes which quantify biochemical pathways from the omics data. With the advent of whole genome sequence and other high-throughput experimental technologies, biological research has transformed from data poor to a data rich discipline (Mosca et al., 2010; Joyce and Palsson, 2006). The large data sets being interpreted to find the relationships and causalities. Relationship analysis is a subset of causality, as causality not only checks the relationship between the components but also highlights the direction of the relationship. The network model obtained should be validated prior to its usage for further research and applications. In this regard, the complete dataset should be preprocessed and can be divided into training and validation datasets. Preprocessing is necessary in order to reduce the effect of noise in the data on the network model construction. Then network models can be built using training sets and verified using validation sets. The topology of the network models can be further consolidated by comparing with available pathways from the literature. Particularly, available information on feedback loops (positive or negative) can be checked. Alternatively, the developed network model can be split into smaller networks and some networks with strong theoretical backup can be selected for comparison.

Identification and ranking of the key mechanism of the network

Network models facilitate the comprehension of the integrated biochemical pathways driving the cell cycle. However, these models are complex with numerous variables and parameters. Model complexity is one of the issues of multiscale net-

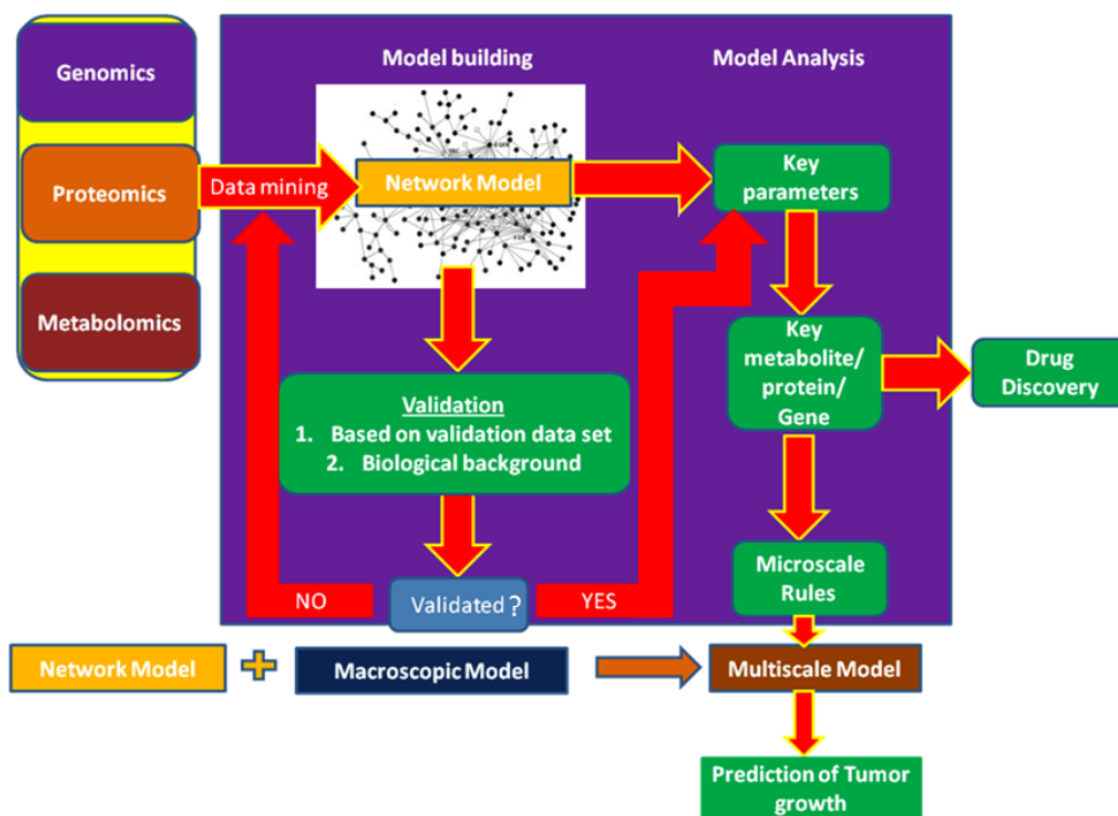


Fig. 8.2. A multiscale framework for comprehending cancer using OMICS data

work models. Unlike the systematic but heuristic scaling approach used in this work, alternative scaling approaches for large scale systems need to be developed to simplify the models and enable their applications. Moreover, often, very few parameters significantly influence the evolution of components in the network. Perturbation analysis of the models can be performed to find the dominant parameters and hence, enable us to identify the significant mechanisms. Sensitivity analysis is the approach to identify the factors contributing to the uncertainty of an objective of interest. The output variance can be decomposed into contributions from different factors. Sensitivity indices can be calculated to rank the factors based on their contributions to the overall uncertainty. The rules based on the key factors affecting the intracellular processes can be combined with the macroscopic models to understand the multiscale phenomena. The expected outcome might be the

development of a topology of complex and large datasets of different scales. The analysis of the topology may help in understanding the key differences of intracellular processes between normal and cancer cells. Practically, this kind of studies may enable the identification of specific biomarkers for specific types of cancer. This may ultimately lead to the discovery and design of targeted therapies. In this perspective, the application of data mining techniques and multiscale modeling supports the investigation of cancer biomarkers, development of novel drugs and prediction of tumor progression. The gist of the proposition is presented in Figure 8.2.

8.2.4 Statistical analysis using clinical data of cancer

In general, cancer related clinical data includes patient details (e.g. age, sex, race), background information (e.g. symptoms, family history/predisposing conditions, tobacco use), cancer type/location/stage (findings based on physical examination, laboratory tests and image analysis), treatment plan/summary (height, pretreatment weight, therapy regimen, route of administration, schedule, side effects). Hitherto, around 100 types of cancer have been discovered and huge clinical data have been generated. However, very few works have focused on transforming

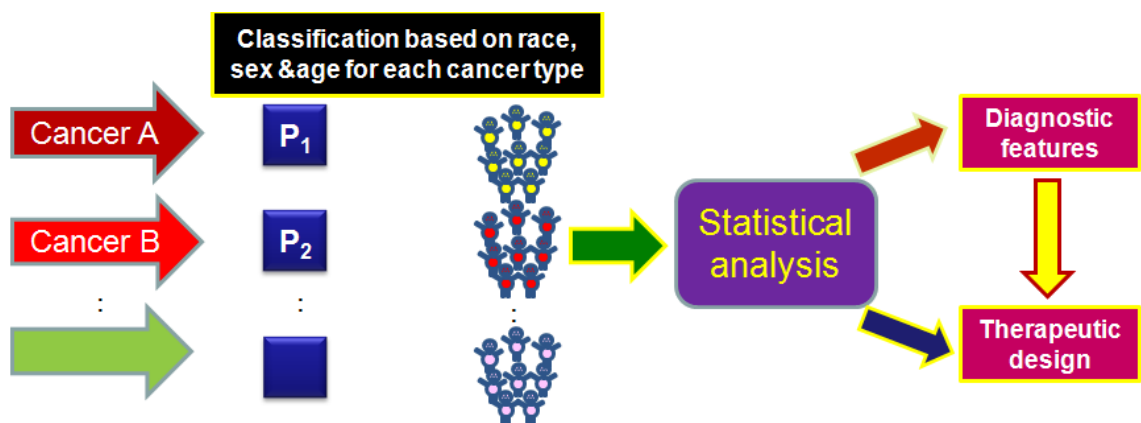


Fig. 8.3. Identification of diagnostic features and the prediction of therapeutic design using clinical data

the available data to knowledge. In this regard, statistical analysis of clinical data can be helpful. The first step could be to construct a database using data from cancer clinics in a given geographical region. Then, the patients could be classified according to sex, age, race, location for a given cancer type (Figure 8.3). After classification, the data sets could be analyzed using statistical tools to find out cancer prone diagnostic features and relate them to the therapeutic design. Overall, the above-mentioned approach might help in bringing the personalized therapy in practice.

REFERENCES

- Aarntzen, E., Figdor, C., Adema, G., Punt, C. and de Vries, I. (2008), ‘Dendritic cell vaccination and immune monitoring’, *Cancer Immunology, Immunotherapy* **57**(10), 1559–1568.
- Aarons, L. and Ogungbenro, K. (2010), ‘Optimal design of pharmacokinetic studies’, *Basic Clinical Pharmacology and Toxicology* **106**(3), 250–255.
- Abbott, R. G., Forrest, S. and Pienta, K. J. (2006), ‘Simulating the hallmarks of cancer’, *Artificial Life* **12**(4), 617–634.
- Adam, J. A. (1986), ‘A simplified mathematical model of tumor growth’, *Mathematical Biosciences* **81**(2), 229–244.
- Adam, J. A. (1987*a*), ‘A mathematical model of tumor growth. ii. effects of geometry and spatial nonuniformity on stability’, *Mathematical Biosciences* **86**(2), 183–211.
- Adam, J. A. (1987*b*), ‘A mathematical model of tumor growth. iii. comparison with experiment’, *Mathematical Biosciences* **86**(2), 213 – 227.
- Adam, J. A. (1988), ‘A mathematical model of tumor growth by diffusion’, *Mathematical and Computer Modelling* **11**, 455–456.
- Adam, J. A. (1989), ‘A mathematical model of tumor growth by diffusion’, *Mathematical Biosciences* **94**(1), 155–155.
- Adam, J. A. and Maggelakis, S. A. (1989), ‘Mathematical models of tumor growth. iv. effects of a necrotic core’, *Mathematical Biosciences* **97**(1), 121–136.
- Adam, J. K., Odhav, B. and Bhoola, K. (2003), ‘Immune responses in cancer’, *Pharmacology and Therapeutics* **99**, 113–132.
- Agur, Z., Arnon, R. and Schechter, B. (1988), ‘Reduction of cytotoxicity to normal tissues by new regimens of cell-cycle phase-specific drugs’, *Mathematical Biosciences* **92**(1), 1–15.
- Airley, R. (2009), *Cancer chemotherapy*, Wiley-Blackwell, Hoboken, NJ.
- Alberts, B., Johnson, A., Lewis, J., Raff, M., Roberts, K. and Walter, P. (2002), *Molecular biology of the cell*, 4th edn, Garland Science., New York.
- Ambrosi, D. and Preziosi, L. (2002), ‘On the closure of mass balance models for tumor growth’, *Mathematical Models and Methods in Applied Sciences* **12**(5), 737–754.
- Anderson, A. R. A. and Quaranta, V. (2008), ‘Integrative mathematical oncology’, *Nat Rev Cancer* **8**(3), 227–234.

- Araujo, R. P. and McElwain, D. L. S. (2004), ‘A history of the study of solid tumour growth: the contribution of mathematical modelling’, *Bulletin of Mathematical Biology* **66**(5), 1039–1091.
- Ballestrero, A., Boy, D., Moran, E., Cirmena, G., Brossart, P. and Nencioni, A. (2008), ‘Immunotherapy with dendritic cells for cancer’, *Advanced Drug Delivery Reviews* **60**(2), 173–183.
- Banchereau, J., Schuler-Thurner, B., Palucka, A. K. and Schuler, G. (2001), ‘Dendritic cells as vectors for therapy’, *Cell* **106**(3), 271–274.
- Barbolosi, D. and Iliadis, A. (2001), ‘Optimizing drug regimens in cancer chemotherapy: a simulation study using a pk-pd model’, *Computers in Biology and Medicine* **31**(3), 157–172.
- Bell, H. S., Whittle, I. R., Walker, M., Leaver, H. A. and Wharton, S. B. (2001), ‘The development of necrosis and apoptosis in glioma: experimental findings using spheroid culture systems’, *Neuropathology 38; Applied Neurobiology* **27**, 291–304.
- Bellomo, N., Angelis, E. D. and Preziosi, L. (2003), ‘Review article: Multiscale modeling and mathematical problems related to tumor evolution and medical therapy’, *Journal of Theoretical Medicine* **5**(2), 111–136.
- Bellomo, N., Bellouquid, A. and De Angelis, E. (2003), ‘The modelling of the immune competition by generalized kinetic (boltzmann) models: Review and research perspectives’, *Mathematical and Computer Modelling* **37**(1-2), 65–86.
- Bellomo, N. and Preziosi, L. (2000), ‘Modelling and mathematical problems related to tumor evolution and its interaction with the immune system’, *Mathematical and Computer Modelling* **32**(3-4), 413–452.
- Bertuzzi, A., Fasano, A., Gandolfi, A. and Sinisgalli, C. (2007), ‘Atp production and necrosis formation in a tumour spheroid model’, *Math. Model. Nat. Phenom.* **2**(3), 30–46.
- Beward, C., Byrne, H. and Lewis, C. (2003), ‘A multiphase model describing vascular tumour growth’, *Bulletin of Mathematical Biology* **65**(4), 609–640.
- Beward, C. J. W., Byrne, H. M. and Lewis, C. E. (2002), ‘The role of cell-cell interactions in a two-phase model for avascular tumour growth’, *Journal of Mathematical Biology* **45**(2), 125–152.
- Bunimovich-Mendrazitsky, S., Shochat, E. and Stone, L. (2007), ‘Mathematical model of bcg immunotherapy insuperficial bladder cancer’, *Bulletin of Mathematical Biology* **69**(6), 1847–1870.
- Burton, A. (1966), ‘Rate of growth of solid tumors as a problem of diffusion’, *Growth* **30**, 229–244.
- Busini, V., Arosio, P. and Masi, M. (2007), ‘Mechanistic modelling of avascular tumor growth and pharmacokinetics influence—part i’, *Chemical Engineering Science* **62**(7), 1877–1886.

- Byrne, H., Alarcon, T., Owen, M., Webb, S. and Maini, P. (2006), ‘Modelling aspects of cancer dynamics: a review’, *Philosophical Transactions of the Royal Society A: Mathematical, Physical and Engineering Sciences* **364**(1843), 1563–1578.
- Byrne, H. and Drasdo, D. (2009), ‘Individual-based and continuum models of growing cell populations: a comparison’, *Journal of Mathematical Biology* **58**(4), 657–687.
- Byrne, H. M. (1997), ‘The effect of time delays on the dynamics of avascular tumor growth’, *Mathematical Biosciences* **144**(2), 83–117.
- Byrne, H. M. (1999), ‘A weakly nonlinear analysis of a model of avascular solid tumour growth’, *Journal of Mathematical Biology* **39**(1), 59–89.
- Byrne, H. M. (2010), ‘Dissecting cancer through mathematics: from the cell to the animal model’, *Nature Reviews Cancer* **10**(3), 221.
- Byrne, H. M. and Chaplain, M. A. J. (1995), ‘Growth of nonnecrotic tumors in the presence and absence of inhibitors’, *Mathematical Biosciences* **130**(2), 151–181.
- Byrne, H. M. and Chaplain, M. A. J. (1996), ‘Modelling the role of cell-cell adhesion in the growth and development of carcinoma’, *Mathematical and Computer Modelling* **24**(12), 1–17.
- Byrne, H. M. and Chaplain, M. A. J. (1998), ‘Necrosis and apoptosis: distinct cell loss mechanisms in a mathematical model of avascular tumour growth’, *Computational and Mathematical Methods in Medicine* **1**(3), 223 – 235.
- Byrne, H. M. and Gourley, S. A. (1997), ‘The role of growth factors in avascular tumour growth’, *Mathematical and Computer Modelling* **26**(4), 35–55.
- Canal, P., Gamelin, E., Vassal, G. and Robert, J. (1998), ‘Benefits of pharmacological knowledge in the design and monitoring of cancer chemotherapy’, *Pathology and Oncology Research* **4**, 171–178.
- Cappuccio, A., Castiglione, F. and Piccoli, B. (2007), ‘Determination of the optimal therapeutic protocols in cancer immunotherapy’, *Mathematical Biosciences* **209**(1), 1–13.
- Casciari, J. J., Sotirchos, S. V. and Sutherland, R. M. (1988), ‘Glucose diffusivity in multicellular tumor spheroids’, *Cancer Res* **48**(14), 3905–3909.
- Casciari, J. J., Sotirchos, S. V. and Sutherland, R. M. (1992), ‘Mathematical modelling of microenvironment and growth in emt6/ro multicellular tumour spheroids’, *Cell Proliferation* **25**(1), 1–22.
- Castiglione, F. and Piccoli, B. (2006), ‘Optimal control in a model of dendritic cell transfection cancer immunotherapy’, *Bulletin of Mathematical Biology* **68**(2), 255–274.
- Castiglione, F. and Piccoli, B. (2007), ‘Cancer immunotherapy, mathematical modeling and optimal control’, *Journal of Theoretical Biology* **247**(4), 723–732.

- Castiglione, F., Piccoli, B. and ieee (2004), Optimal control in a model of dendritic cell transfection cancer immunotherapy, *in* '43rd IEEE Conference on Decision and Control', San Diego, CA, pp. 585–590.
- Chaplain, M. A. J., Benson, D. L. and Maini, P. K. (1994), 'Nonlinear diffusion of a growth inhibitory factor in multicell spheroids', *Mathematical Biosciences* **121**(1), 1–13.
- Chareyron, S. and Alamir, M. (2009), 'Mixed immunotherapy and chemotherapy of tumors: Feedback design and model updating schemes', *Journal of Theoretical Biology* **258**(3), 444–454.
- Cintron-Arias, A., Banks, H. T., Capaldi, A. and L., L. A. (2009), 'A sensitivity matrix based methodology for inverse problem formulation', *Journal of Inverse and Ill-Posed Problems* **17**, 545–564.
- Danilo, R. and Jose, M. P. (2009), 'An integrated network-based mechanistic model for tumor growth dynamics under drug administration', *Computers in Biology and Medicine* **39**(4), 368–384.
- De Boer, R. J. and Hogeweg, P. (1986), 'Interactions between macrophages and t-lymphocytes: Tumor sneaking through intrinsic to helper t cell dynamics', *Journal of Theoretical Biology* **120**(3), 331–351.
- de Pillis, L. G., Gu, W., Fister, K. R., Head, T., Maples, K., Murugan, A., Neal, T. and Yoshida, K. (2007), 'Chemotherapy for tumors: An analysis of the dynamics and a study of quadratic and linear optimal controls', *Mathematical Biosciences* **209**(1), 292–315.
- de Pillis, L. G., Gu, W. and Radunskaya, A. E. (2006), 'Mixed immunotherapy and chemotherapy of tumors: modeling, applications and biological interpretations', *Journal of Theoretical Biology* **238**(4), 841–862.
- de Pillis, L. G. and Radunskaya, A. (2003), 'The dynamics of an optimally controlled tumor model: A case study', *Mathematical and Computer Modelling* **37**(11), 1221–1244.
- de Pillis, L. G., Radunskaya, A. E. and Wiseman, C. L. (2005), 'A validated mathematical model of cell-mediated immune response to tumor growth', *Cancer Res* **65**(17), 7950–7958.
- de Pillis, L., Renee Fister, K., Gu, W., Collins, C., Daub, M., Gross, D., Moore, J. and Preskill, B. (2009), 'Mathematical model creation for cancer chemo-immunotherapy', *Computational and Mathematical Methods in Medicine: An Interdisciplinary Journal of Mathematical, Theoretical and Clinical Aspects of Medicine* **10**(3), 165 – 184.
- Deakin, A. (1975), 'Model for the growth of a solid in vitro tumour', *Growth* **39**, 159–165.

- Deb, K., Agrawal, S., Pratap, A. and Meyarivan, T. (2000), A fast elitist non-dominated sorting genetic algorithm for multi-objective optimization: Nsga-ii, Parallel Problem Solving from Nature PPSN VI. 6th International Conference. Proceedings (Lecture Notes in Computer Science Vol.1917), Springer-Verlag, Paris, France, pp. 849–58.
- DeBerardinis, R. J., Lum, J. J., Hatzivassiliou, G. and Thompson, C. B. (2008), ‘The biology of cancer: Metabolic reprogramming fuels cell growth and proliferation’, *Cell Metabolism* **7**(1), 11–20.
- Deisboeck, T. S., Zhang, L., Yoon, J. and Costa, J. (2009), ‘In silico cancer modeling: is it ready for prime time?’, *Nat Clin Prac Oncol* **6**(1), 34–42.
- Dhodapkar, M. V., Steinman, R. M., Sapp, M., Desai, H., Fossella, C., Krasovsky, J., Donahoe, S. M., Dunbar, P. R., Cerundolo, V., Nixon, D. F. and Bhardwaj, N. (1999), ‘Rapid generation of broad t-cell immunity in humans after a single injection of mature dendritic cells’, *The Journal of Clinical Investigation* **104**(2), 173–180.
- Drasdo, D., Hoehme, S. and Block, M. (2007), ‘On the role of physics in the growth and pattern formation of multi-cellular systems: What can we learn from individual-cell based models?’, *Journal of Statistical Physics* **128**(1), 287–345.
- Dua, P., Dua, V. and Pistikopoulos, E. N. (2008), ‘Optimal delivery of chemotherapeutic agents in cancer’, *Computers and Chemical Engineering* **32**(1-2), 99–107.
- Dudley, M. E. and Rosenberg, S. A. (2003), ‘Adoptive-cell-transfer therapy for the treatment of patients with cancer’, *Nat Rev Cancer* **3**(9), 666–675.
- Dudley, M. E., Wunderlich, J. R., Robbins, P. F., Yang, J. C., Hwu, P., Schwartzentruber, D. J., Topalian, S. L., Sherry, R., Restifo, N. P., Hubicki, A. M., Robinson, M. R., Raffeld, M., Duray, P., Seipp, C. A., Rogers-Freezer, L., Morton, K. E., Mavroukakis, S. A., White, D. E. and Rosenberg, S. A. (2002), ‘Cancer regression and autoimmunity in patients after clonal repopulation with antitumor lymphocytes’, *Science* **298**(5594), 850–854.
- Durand, R. (1976), ‘Cell cycle kinetics in an in vitro tumor model’, *Cell Proliferation* **9**(5), 403–412.
- Edgar, T., Himmelblau, D. and Lasdon, L. (2001), *Optimization of chemical processes*, McGraw-Hill Chemical engineering series.
- Eisen, M. (1979), *Mathematical models in cell biology and cancer chemotherapy / Martin Eisen*, Lecture notes in biomathematics ; 30, Springer-Verlag, Berlin ; New York .:
- Englezos, P. and Kalogerakis, N. (2001), *Applied parameter estimation for chemical engineers*, Marcel Dekker, New York.
- Folkman, J. and Hochberg, M. (1973), ‘Self-regulation of growth in three dimensions’, *J. Exp. Med.* **138**(4), 745–753.

- Freyer, J. P. (1988), ‘Role of necrosis in regulating the growth saturation of multicellular spheroids’, *Cancer Res* **48**(9), 2432–2439.
- Freyer, J. P. and Sutherland, R. M. (1985), ‘A reduction in the in situ rates of oxygen and glucose consumption of cells in emt6/ro spheroids during growth’, *Journal of cellular physiology* **124**, 516–524.
- Freyer, J. P. and Sutherland, R. M. (1986*a*), ‘Proliferative and clonogenic heterogeneity of cells from emt6/ro multicellular spheroids induced by the glucose and oxygen supply’, *Cancer Res* **46**(7), 3513–3520.
- Freyer, J. P. and Sutherland, R. M. (1986*b*), ‘Regulation of growth saturation and development of necrosis in emt6/ro multicellular spheroids by the glucose and oxygen supply’, *Cancer Res* **46**(7), 3504–3512.
- Friedrich, J., Seidel, C. and Kunz-Schughart, L. A. (2007), Multicellular spheroids: An underestimated tool is catching up again, *in* ‘17th Annual Meeting of the German-Society-of-Cytometry (DGfZ)’, Regensburg, GERMANY, p. 2.
- Gabrilovich, D. I. (2007), ‘Combination of chemotherapy and immunotherapy for cancer: a paradigm revisited’, *The Lancet Oncology* **8**(1), 2–3.
- Gardner, S. N. (2000), ‘A mechanistic, predictive model of dose-response curves for cell cycle phase-specific and nonspecific drugs’, *Cancer Research* **60**(5), 1417–1425.
- Gardner, S. N. (2002), ‘Modeling multi-drug chemotherapy: tailoring treatment to individuals’, *Journal of theoretical biology* **214**, 181–207.
- Gardner, S. N. and Fernandes, M. (2003), ‘New tools for cancer chemotherapy: computational assistance for tailoring treatments’, *Molecular Cancer Therapeutics* **2**(10), 1079–1084.
- Garner, A. L., Lau, Y. Y., Jordan, D. W., Uhler, M. D. and Gilgenbach, R. M. (2006), ‘Implications of a simple mathematical model to cancer cell population dynamics’, *Cell Proliferation* **39**(1), 15–28.
- Gatenby, R. A. (1998), ‘Mathematical models of tumor-host interactions’, *Cancer Journal - France* **11**(6), 289–293.
- Gatenby, R. A. and Gawlinski, E. T. (1996), ‘A reaction-diffusion model of cancer invasion’, *Cancer Research* **56**(24), 5745–5753.
- Gatenby, R. A. and Gawlinski, E. T. (2003), ‘The glycolytic phenotype in carcinogenesis and tumor invasion’, *Cancer Research* **63**(14), 3847–3854.
- Gatenby, R. A., Gawlinski, E. T., Gmitro, A. F., Kaylor, B. and Gillies, R. J. (2006), ‘Acid-mediated tumor invasion: a multidisciplinary study’, *Cancer Research* **66**(10), 5216–5223.
- Ghaffari, A. and Naserifar, N. (2010), ‘Optimal therapeutic protocols in cancer immunotherapy’, *Computers in Biology and Medicine* **40**(3), 261–270.

- Glass, L. (1973), ‘Instability and mitotic patterns in tissue growth’, *Transactions of the ASME. Series G, Journal of Dynamic Systems, Measurement and Control* **95**(3), 324–6.
- Gottfried, E., Kunz-Schughart, L. A., Andreesen, R. and Kreutz, M. (2006), ‘Brave little world - spheroids as an in vitro model to study tumor-immune-cell interactions’, *Cell Cycle* **5**(7), 691–695.
- Greenspan, H. (1972), ‘Models for the growth of a solid tumor by diffusion’, *Studies in Applied Mathematics* **52**, 317–340.
- Hanahan, D. and Weinberg, R. (2000), ‘The hallmarks of cancer’, *Cell* **100**, 57 – 70.
- Harrold, J. M. and Parker, R. S. (2009), ‘Clinically relevant cancer chemotherapy dose scheduling via mixed-integer optimization’, *Computers and Chemical Engineering* **33**(12), 2042–2054.
- Hlatky, L., Sachs, R. and Alpen, E. (1988a), ‘Joint oxygen-glucose deprivation as the cause of necrosis in a tumor analog’, *Journal of Cellular Physiology* **134**(2), 167–178.
- Hlatky, L., Sachs, R. K. and Alpen, E. L. (1988b), ‘Joint oxygen-glucose deprivation as the cause of necrosis in a tumor analog’, *Journal of Cellular Physiology* **134**, 167–168.
- Ho, W. Y., Blattman, J. N., Dossett, M. L., Yee, C. and Greenberg, P. D. (2003), ‘Adoptive immunotherapy: Engineering t cell responses as biologic weapons for tumor mass destruction’, *Cancer Cell* **3**(5), 431–437.
- Holford, N., Ma, S. C. and Ploeger, B. A. (2010), ‘Clinical trial simulation: A review’, *Clin Pharmacol Ther* **88**(2), 166–182.
- Hon, Y. and Evans, W. (1998), ‘Making tdm work to optimize cancer chemotherapy: a multidisciplinary team approach’, *Clinical Chemistry* **44**, 388–400.
- Hooker, A. and Vicini, P. (2005), ‘Simultaneous population optimal design for pharmacokinetics-pharmacodynamic experiments’, *AAPS Journal* **7**(4), E759–E785.
- Hulting, S., Rollins, D. and Bhandari, N. (2006), ‘Optimal experimental design for human thermoregulatory system identification.’, *Chemical Engineering Research and Design* **84**.
- Ichim, C. (2005), ‘Revisiting immunosurveillance and immunostimulation: Implications for cancer immunotherapy’, *Journal of Translational Medicine* **3**(1), 8.
- Iliadis, A. and Barbolosi, D. (2000), ‘Optimizing drug regimens in cancer chemotherapy by an efficacy-toxicity mathematical model’, *Computers and Biomedical Research* **33**(3), 211–226.

REFERENCES

- Jacobs, J., Aarntzen, E., Sibelt, L., Blokx, W., Boullart, A., Gerritsen, M.-J., Hoogerbrugge, P., Figdor, C., Adema, G., Punt, C. and de Vries, I. (2009), ‘Vaccine-specific local t cell reactivity in immunotherapy-associated vitiligo in melanoma patients’, *Cancer Immunology, Immunotherapy* **58**(1), 145–151.
- Jiang, Y., Pjesivac-Grbovic, J., Cantrell, C. and Freyer, J. P. (2005), ‘A multiscale model for avascular tumor growth’, *Biophys. J.* **89**(6), 3884–3894.
- Joshi, B., Wang, X., Banerjee, S., Tian, H., Matzavinos, A. and Chaplain, M. A. J. (2009), ‘On immunotherapies and cancer vaccination protocols: A mathematical modelling approach’, *Journal of Theoretical Biology* **259**(4), 820–827.
- Joyce, A. R. and Palsson, B. O. (2006), ‘The model organism as a system: integrating ‘omics’ data sets’, *Nat Rev Mol Cell Biol* **7**(3), 198–210.
- Kasprzak, E. M. and Lewis, K. E. (2001), ‘Pareto analysis in multiobjective optimization using the collinearity theorem and scaling method’, *Structural and Multidisciplinary Optimization* **22**(3), 208–218.
- Kerr, J. (1971), ‘Shrinkage necrosis: a distinct mode of cellular death’, *journal of pathology* **105**, 13–20.
- Kerr, J., A.H., W. and A.R., C. (1972), ‘Apoptosis: a basic biological phenomenon with wide-ranging implications in tissue kinetics’, *British journal of cancer* **26**, 239–257.
- Khaloozadeh, H., Yazdani, S. and Kamyab, M. (2009), ‘Optimization of breast cancer chemotherapy regimens using a pharmacokinetic/pharmacodynamic model-based design’, *Pharmaceutical Medicine* **23**(1), 11–18 10.2165/013171117-200923010-00004.
- Kim, Y. and Stolarska, M. A. (2007), ‘A hybrid model for tumor spheroid growth in vitro i: Theoretical development and early results’, *Mathematical models and methods in applied sciences* **17**, 1173–1198.
- Kiran, K. L., Jayachandran, D. and Lakshminarayanan, S. (2009), Multi-objective optimization of cancer immuno-chemotherapy, in ‘13th International Conference on Biomedical Engineering’, pp. 1337–1340.
- Kiran, K. L. and Lakshminarayanan, S. (2009), Treatment planning of cancer dendritic cell therapy using multi-objective optimization, in ‘In proceedings of AD-CHEM 2009’, Istanbul, Turkey.
- Kirkpatrick, S., Gelatt, C. D. and Vecchi, M. P. (1983), ‘Optimization by simulated annealing’, *Science* **220**(4598), 671–680.
- Kirschner, D. and Panetta, J. C. (1998), ‘Modeling immunotherapy of the tumor immune interaction’, *Journal of Mathematical Biology* **37**(3), 235–252.
- Kleinsmith, L. (2005), *Principles of cancer biology*, Addison-wesley.

- Kontoravdi, C., Asprey, S., Pistikopoulos, E. and Mantalaris, A. (2005), ‘Application of global sensitivity analysis to determine goals for design of experiments: An example study on antibody-producing cell cultures’, *Biotechnology Progress* **21**, 1128–1135.
- Krantz, W. (2007a), Scaling analysis as a pedagogical tool in teaching transport and reaction processes, in ‘ASEE Annual Conference’.
- Krantz, W. B. (2007b), *Scaling Analysis in Modeling Transport and Reaction Processes: A Systematic Approach to Model Building and the Art of Approximation*, John Wiley & Sons, Hoboken, New Jersey.
- Kunz-Schughart, L. A. (1999), ‘Multicellular tumor spheroids: intermediates between monolayer culture and in vivo tumor’, *Cell Biology International* **23**(3), 157–161.
- Kunz-Schughart, L. A., Kreutz, M. and Knuechel, R. (1998), ‘Multicellular spheroids: a three-dimensional in vitro culture system to study tumour biology’, *International Journal of Experimental Pathology* **79**(1), 1–23.
- Kuznetsov, V. A. and Knott, G. D. (2001), ‘Modeling tumor regrowth and immunotherapy’, *Mathematical and Computer Modelling* **33**(12-13), 1275–1287.
- Kuznetsov, V. A., Makalkin, I. A., Taylor, M. A. and Perelson, A. S. (1994), ‘Non-linear dynamics of immunogenic tumors: Parameter estimation and global bifurcation analysis’, *Bulletin of Mathematical Biology* **56**(2), 295–321.
- Laginha, K., Verwoert, S., Charrois, G. and Allen, T. (2005), ‘Determination of doxorubicin levels in whole tumor and tumor nuclei in murine breast cancer tumors’, *Clinical Cancer Research* **11**, 6944–6949.
- Lake, R. A. and Robinson, B. W. S. (2005), ‘Immunotherapy and chemotherapy - a practical partnership’, *Nat Rev Cancer* **5**(5), 397–405.
- LaRue, K. E. A., Bradbury, E. M. and Freyer, J. P. (1998), ‘Differential regulation of cyclin-dependent kinase inhibitors in monolayer and spheroid cultures of tumorigenic and nontumorigenic fibroblasts’, *Cancer Research* **58**(6), 1305–1314.
- Laszlo Kopper, M. (2001), ‘Tumor cell growth kinetics’, *CME Journal of Gynecologic Oncology* (6), 141–143.
- Ledzewicz, U. and Schttler, H. (2007), ‘Optimal controls for a model with pharmacokinetics maximizing bone marrow in cancer chemotherapy’, *Mathematical Biosciences* **206**(2), 320–342.
- Lee, H. J. and Schiesser, W. E. (2003), *Ordinary and partial differential equation routines in C, C++, Fortran, Java, Maple, and MATLAB*, Chapman & Hall/CRC.
- Li, G., Rabitz, H., Yelvington, P. E., Oluwole, O. O., Bacon, F., Kolb, C. E. and Schoendorf, J. (2010), ‘Global sensitivity analysis for systems with independent and/or correlated inputs’, *The Journal of Physical Chemistry A* **114**, 6022–6032.

- Li, G., Rosenthal, C. and Rabitz, H. (2001), ‘High dimensional model representations’, *The Journal of Physical Chemistry A* **105**(33), 7765–7777.
- Li, G., Wang, S.-W., Rabitz, H., Wang, S. and Jaffe, P. (2002), ‘Global uncertainty assessments by high dimensional model representations (hdmr)’, *Chemical Engineering Science* **57**(21), 4445–4460.
- Li, Z. and Ierapetritou, M. (2008a), ‘Process scheduling under uncertainty: Review and challenges’, *Computers & Chemical Engineering* **32**(4-5), 715–727.
- Li, Z. and Ierapetritou, M. G. (2008b), ‘Reactive scheduling using parametric programming’, *AIChE Journal* **54**(10), 2610–2623.
- Lord, C. and Ashworth, A. (2010), ‘Biology-driven cancer drug development: back to the future’, *BMC Biology* **8**(1), 38.
- Lowengrub, J. S., Frieboes, H. B., Jin, F., Chuang, Y.-L., Li, X., Macklin, P., Wise, S. and Cristini, V. (2010), ‘Nonlinear modelling of cancer: bridging the gap between cells and tumours’, *Nonlinearity* **23**(1), R1–R91.
- Ludewig, B. and Hoffman, M. W., eds (2005), *Adoptive immunotherapy: methods and protocols*, Humana press, Totowa, NJ.
- Mallet, D. G. and De Pillis, L. G. (2006), ‘A cellular automata model of tumor-immune system interactions’, *Journal of Theoretical Biology* **239**(3), 334–350.
- Marino, S., Hogue, I., Ray, C. and Kirschner, D. (2008), ‘A methodology for performing global uncertainty and sensitivity analysis in systems biology’, *Journal of Theoretical Biology* **254**(1), 178–196.
- Martin, R. B. (1992), ‘Optimal control drug scheduling of cancer chemotherapy’, *Automatica* **28**(6), 1113–1123.
- Martins, M. L., Ferreira Jr, S. C. and Vilela, M. J. (2007), ‘Multiscale models for the growth of avascular tumors’, *Physics of Life Reviews* **4**(2), 128–156.
- Maruic, M., Bajzer, e., Vuk-Pavlovic, S. and Freyer, J. (1994), ‘Tumor growth in vivo and as multicellular spheroids compared by mathematical models’, *Bulletin of Mathematical Biology* **56**(4), 617–631.
- Marusic, M., Bajzer, Z., Freyer, J. P. and Vuk-Pavlovic, S. (1994), ‘Analysis of growth of multicellular tumour spheroids by mathematical models’, *Cell Proliferation* **27**(2), 73–94.
- Matveev, A. S. and Savkin, A. V. (2002), ‘Application of optimal control theory to analysis of cancer chemotherapy regimens’, *Systems & Control Letters* **46**(5), 311–321.
- McCall, J., Petrovski, A. and Shakya, S. (2007), Evolutionary algorithms for cancer chemotherapy optimization, in Y. P. Gary B. Fogel, David W. Corne, ed., ‘Computational Intelligence in Bioinformatics’, pp. 263–296.

- McElwain, D. L. S. and Morris, L. E. (1978), ‘Apoptosis as a volume loss mechanism in mathematical models of solid tumor growth’, *Mathematical Biosciences* **39**(1-2), 147–157.
- McElwain, D. L. S. and Ponzio, P. J. (1977), ‘A model for the growth of a solid tumor with non-uniform oxygen consumption’, *Mathematical Biosciences* **35**(3-4), 267–279.
- McKay, M., Beckman, R. and Conover, W. (1979), ‘A comparison of three methods for selecting values of input variables in the analysis of output from a computer code’, *Technometrics* **21**, 239–245.
- Mesri, M., Wall, N. R., Li, J., Kim, R. W. and Altieri, D. C. (2001), ‘Cancer gene therapy using a survivin mutant adenovirus’, *The Journal of Clinical Investigation* **108**(7), 981–990.
- Moreira, J. and Deutsch, A. (2002), ‘Cellular automaton models of tumor development: A critical review’, *Advances in Complex Systems* **5**(2), 247–267.
- Moreno-Sánchez, R., Rodríguez-Enríquez, S., Marn-Hernández, A. and Saavedra, E. (2007), ‘Energy metabolism in tumor cells’, *FEBS Journal* **274**(6), 1393–1418.
- Mosca, E., Alfieri, R., Merelli, I., Viti, F., Calabria, A. and Milanesi, L. (2010), ‘A multilevel data integration resource for breast cancer study’, *BMC Systems Biology* **4**(1), 76.
- Mueller-Klieser, W. (1987), ‘Multicellular spheroids. a review on cellular aggregates in cancer research.’, *Journal of cancer research and clinical oncology* **113**, 101–122.
- Mueller-Klieser, W. (1997), ‘Three-dimensional cell cultures: from molecular mechanisms to clinical applications’, *Am J Physiol Cell Physiol* **273**(4), C1109–1123.
- Mueller-Klieser, W. and Sutherland, R. M. (1982), ‘Oxygen tensions in multicell spheroids of two cell lines’, *British Journal of Cancer* **45**, 256–264.
- Mueller-Klieser, W. and Sutherland, R. M. (1985), ‘Oxygen consumption and oxygen diffusion properties of multicellular spheroids from two cell lines’, *Advances in experimental medicine and biology* **180**, 311.
- Murray, J. (2002), *Mathematical Biology : An Introduction*, Springer, Berlin.
- Murray, J. M. (1990a), ‘Optimal control for a cancer chemotherapy problem with general growth and loss functions’, *Mathematical Biosciences* **98**(2), 273–287.
- Murray, J. M. (1990b), ‘Some optimal control problems in cancer chemotherapy with a toxicity limit’, *Mathematical Biosciences* **100**(1), 49–67.
- Nemhauser, G., Rinnooy Kan, A. H. and Todd, M. J. (1989), *Optimization*, North-Holland.
- Nencioni, A., Grnebach, F., Schmidt, S. M., Müller, M. R., Boy, D., Patrone, F., Ballestrero, A. and Brossart, P. (2008), ‘The use of dendritic cells in cancer immunotherapy’, *Critical Reviews in Oncology/Hematology* **65**(3), 191–199.

- Nof, S. Y. and Parker, R. S. (2009), Automation and control in biomedical systems, in ‘Springer Handbook of Automation’, Springer Berlin Heidelberg, pp. 1361–1378.
- Oswald, J., Marschner, K., Kunz-Schughart, L. A., Schwenzer, B. and Pietzsch, J. (2007), Multicellular tumor spheroids as a model system for the evaluation of pet radiotracer uptake, in ‘20th Annual Congress of the European-Association-of-Nuclear-Medicine’, Copenhagen, DENMARK, pp. S138–S138.
- Panetta, J. C. and Adam, J. (1995), ‘A mathematical model of cycle-specific chemotherapy’, *Mathematical and Computer Modelling* **22**(2), 67–82.
- Panetta, J. C. and Fister, K. R. (2000), ‘Optimal control applied to cell-cycle-specific cancer chemotherapy’, *SIAM Journal on Applied Mathematics* **60**(3), 1059–1072.
- Pappalardo, F., Lollini, P.-L., Castiglione, F. and Motta, S. (2005), ‘Modeling and simulation of cancer immunoprevention vaccine’, *Bioinformatics* **21**(12), 2891–2897.
- Parker, R. S. and Doyle, F. J. (2001), ‘Control-relevant modeling in drug delivery’, *Advanced Drug Delivery Reviews* **48**(2-3), 211–228.
- Perumpanani, A. J. (1996), Malignant and morphogenetic waves, Hilary term, Oxford University.
- Piantadosi, S. (1985), ‘A model of growth with first-order birth and death rates’, *Computers and Biomedical Research* **18**(3), 220–232.
- Piccoli, B. and Castiglione, F. (2006), ‘Optimal vaccine scheduling in cancer immunotherapy’, *Physica A: Statistical Mechanics and its Applications* **370**(2), 672–680.
- Preziosi, L. (2003), *Cancer modelling and simulation*, CRC press.
- Qu, Z., MacLellan, W. and Weiss, J. (2003), ‘Dynamics of the cell cycle: checkpoints, sizers, and timers’, *Biophys J* **85**(6), 3600 – 11.
- Quaranta, V., Rejniak, K. A., Gerlee, P. and Anderson, A. R. A. (2008), ‘Invasion emerges from cancer cell adaptation to competitive microenvironments: Quantitative predictions from multiscale mathematical models’, *Seminars in Cancer Biology* **18**(5), 338–348.
- Quaranta, V., Weaver, A. M., Cummings, P. T. and Anderson, A. R. A. (2005), ‘Mathematical modeling of cancer: The future of prognosis and treatment’, *Clinica Chimica Acta* **357**(2), 173–179.
- Quarteroni, A. (2009), ‘Mathematical models in science and engineering’, *Notices of the American Mathematical Society* **56**, 10–19.
- Rivera, E., Haim Erder, M., Fridman, M., Frye, D. and Hortobagyi, G. (2003), ‘First-cycle absolute neutrophil count can be used to improve chemotherapy-dose delivery and reduce the risk of febrile neutropenia in patients receiving adjuvant therapy: a validation study’, *Breast Cancer Res* **5**, R114 – R120.

- Rodríguez-Enrriquez, S., Gallardo-Prez, J. C., Avils-Salas, A., Marn-Hernández, A., Carreo-Fuentes, L., Maldonado-Lagunas, V. and Moreno-Sánchez, R. (2008), ‘Energy metabolism transition in multi-cellular human tumor spheroids’, *Journal of Cellular Physiology* **216**(1), 189–197.
- Rodrigues, A. and Minceva, M. (2005), ‘Modelling and simulation in chemical engineering: Tools for process innovation’, *Computers & Chemical Engineering* **29**, 1167–1183.
- Rodríguez-Fernández, M. and Banga, J. (2010), ‘Senssb: A software toolbox for the development and sensitivity analysis of systems biology models’, *Bioinformatics* **26**, 1675–1676.
- Rose, P. G. (2005), ‘Pegylated liposomal doxorubicin: Optimizing the dosing schedule in ovarian cancer’, *Oncologist* **10**(3), 205–214.
- Rosenberg, S. A., Restifo, N. P., Yang, J. C., Morgan, R. A. and Dudley, M. E. (2008), ‘Adoptive cell transfer: a clinical path to effective cancer immunotherapy’, *Nat Rev Cancer* **8**(4), 299–308.
- Saltelli, A., Ratto, M., Andres, T., Campolongo, F., Cariboni, J., Gatelli, D., Saisana, M. and Tarantola, S. (2008), *Global sensitivity analysis. The primer*, John Wiley & Sons Ltd.
- Saltelli, A., Tarantola, S. and Chan, K. P. S. (1999), ‘A quantitative model-independent method for global sensitivity analysis of model output’, *Technometrics* **41**(1), 39–56.
- Sanga, S., Frieboes, H. B., Zheng, X., Gatenby, R., Bearer, E. L. and Cristini, V. (2007), ‘Predictive oncology: A review of multidisciplinary, multiscale in silico modeling linking phenotype, morphology and growth’, *NeuroImage* **37**(Supplement 1), S120–S134.
- Sanga, S., Sinek, J. P., Frieboes, H. B., Ferrari, M., Fruehauf, J. P. and Cristini, V. (2006), ‘Mathematical modeling of cancer progression and response to chemotherapy’, *Expert Review of Anticancer Therapy* **6**(10), 1361–1376.
- Schaller, G. and Meyer-Hermann, M. (2006), ‘Continuum versus discrete model: a comparison for multicellular tumour spheroids’, *Philosophical Transactions of the Royal Society A: Mathematical, Physical and Engineering Sciences* **364**(1843), 1443–1464.
- Shampine, L. F. (1994), *Numerical solution of Ordinary Differential Equations*, Chapman & Hall.
- Shepard, D. M., Ferris, M. C., Olivera, G. H. and Mackie, T. R. (1999), ‘Optimizing the delivery of radiation therapy to cancer patients’, *SIAM Review* **41**(4), 721–744.
- Sherratt, J. A. and Chaplain, M. A. J. (2001), ‘A new mathematical model for avascular tumour growth’, *Journal of Mathematical Biology* **43**(4), 291–312.

- Shymko, R. M. and Glass, L. (1976), ‘Cellular and geometric control of tissue growth and mitotic instability’, *Journal of Theoretical Biology* **63**(2), 355–374.
- Silber, H., Nyberg, J., Hooker, A. and Karlsson, M. (2009), ‘Optimization of the intravenous glucose tolerance test in t2dm patients using optimal experimental design’, *Journal of Pharmacokinetics and Pharmacodynamics* **36**(3), 281–295.
- Siu, H., Vitetta, E., May, R. and Uhr, J. (1986), ‘Tumor dormancy. i. regression of bcl1 tumor and induction of a dormant tumor state in mice chimeric at the major histocompatibility complex’, *J Immunol* **137**(4), 1376–1382.
- Smallbone, K., Gavaghan, D. J., Gatenby, R. A. and Maini, P. K. (2005), ‘The role of acidity in solid tumour growth and invasion’, *Journal of Theoretical Biology* **235**(4), 476–484.
- Sobol, I. (2001), ‘Global sensitivity indices for non-linear mathematical models and their monte carlo estimates’, *Mathematics and computers in simulation* **55**, 271–280.
- Stolarska, M. A., Kim, Y. and Othmer, H. G. (2009), ‘Multi-scale models of cell and tissue dynamics’, *Philosophical Transactions of the Royal Society A: Mathematical, Physical and Engineering Sciences* **367**(1902), 3525–3553.
- Stuschke, M. and Pottgen, C. (2010), ‘Chemotherapy: Effectiveness of adjuvant chemotherapy for resected nslc’, *Nat Rev Clin Oncol* **7**, 613–614.
- Sun, C. (2006), Model reduction of systems exhibiting two-time scale behaviour or parametric uncertainty, PhD thesis, Texas A&M University.
- Sun, C. and Hahn, J. (2006), ‘Parameter reduction for stable dynamical systems based on hankel singular values and sensitivity analysis’, *Chemical Engineering Science* **61**(16), 5393–5403.
- Sutherland, R. and Durand, R. (1973), ‘Hypoxic cells in an in vitro tumour model’, *Internation journal of radiation biology* **23**, 235–246.
- Sutherland, R. M., Sordat, B., Bamat, J., Gabbert, H., Bourrat, B. and Mueller-Klieser, W. (1986), ‘Oxygenation and differentiation in multicellular spheroids of human colon carcinoma’, *Cancer Res* **46**, 5320–5329.
- Svane, I. M., Soot, M. L., Buus, S. and Johnsen, H. E. (2003), ‘Clinical application of dendritic cells in cancer vaccination therapy’, *Apmis* **111**(7-8), 818–834.
- Swain, S. M., Whaley, F. S. and Ewer, M. S. (2003), ‘Congestive heart failure in patients treated with doxorubicin’, *Cancer* **97**, 2869 – 2879.
- Swan, G. W. (1986), ‘Cancer chemotherapy: Optimal control using the verhulst-pearl equation’, *Bulletin of Mathematical Biology* **48**(3-4), 381–404.
- Swan, G. W. (1990), ‘Role of optimal control theory in cancer chemotherapy’, *Mathematical Biosciences* **101**(2), 237–284.

- Swan, G. W. (1995), ‘Optimal control of drug administration in cancer chemotherapy’, *Bulletin of Mathematical Biology* **57**(3), 503–504.
- Swierniak, A., Kimmel, M. and Smieja, J. (2009), ‘Mathematical modeling as a tool for planning anticancer therapy’, *European Journal of Pharmacology* **625**(1–3), 108–121.
- Swierniak, A., Polanski, A. and Kimmel, M. (1996), ‘Optimal control problems arising in cell-cycle-specific cancer chemotherapy’, *Cell Proliferation* **29**(3), 117–139.
- Szymanska, Z. (2003), ‘Analysis of immunotherapy models in the context of cancer dynamics’, *Int.J. Appl. Math. Comput. Sci.* **13**(3), 407–418.
- Tamaki, H., Kita, H. and Kobayashi, S. (1996), Multi-objective optimization by genetic algorithms: a review, in ‘Proceedings of IEEE International Conference on Evolutionary Computation’, pp. 517–522.
- Tiina, R., Chapman, S. J. and Philip, K. M. (2007), ‘Mathematical models of avascular tumor growth’, *SIAM Rev.* **49**(2), 179–208.
- Tindall, M. J., Please, C. P. and Peddie, M. J. (2008), ‘Modelling the formation of necrotic regions in avascular tumours’, *Mathematical Biosciences* **211**(1), 34–55.
- Tindall, M. and Please, C. (2007), ‘Modelling the cell cycle and cell movement in multicellular tumour spheroids’, *Bulletin of Mathematical Biology* **69**(4), 1147–1165.
- Tse, S.-M., Liang, Y., Leung, K.-S., Lee, K.-H. and Mok, T. S.-K. (2007), ‘A memetic algorithm for multiple-drug cancer chemotherapy schedule optimization’, *IEEE Transactions on Systems, Man, and Cybernetics, Part B: Cybernetics* **37**(1), 84–91.
- Vaupel, P., Kallinowski, F. and Okunieff, P. (1989), ‘Blood flow, oxygen and nutrient supply, and metabolic microenvironment of human tumors: A review’, *Cancer Research* **49**(23), 6449–6465.
- Venkatasubramanian, R., Henson, M. A. and Forbes, N. S. (2006), ‘Incorporating energy metabolism into a growth model of multicellular tumor spheroids’, *Journal of Theoretical Biology* **242**(2), 440–453.
- Vuylsteke, R. J., Molenkamp, B. G., van Leeuwen, P. A., Meijer, S., Wijnands, P. G., Haanen, J. B., Scheper, R. J. and de Gruijl, T. D. (2006), ‘Tumor-specific cd8+ t cell reactivity in the sentinel lymph node of gm-csf treated stage i melanoma patients is associated with high myeloid dendritic cell content’, *Clinical Cancer Research* **12**(9), 2826–2833.
- Ward, J. P. and King, J. R. (1997), ‘Mathematical modelling of avascular-tumour growth’, *Math Med Biol* **14**(1), 39–69.

REFERENCES

- Weinan, E., Engquist, B., Li, X., Ren, W. and Vanden-Eijnden, E. (2007), ‘Heterogeneous multiscale methods: A review’, *Communications in computational physics* **2**(3), 367–450.
- Witz, I. P. (2009), ‘The tumor microenvironment: The making of a paradigm’, *Cancer Microenvironment* **2** (Suppl 1), S9–S17.
- Xu, C. and Gertner, G. Z. (2008), ‘Uncertainty and sensitivity analysis for models with correlated parameters’, *Reliability Engineering & System Safety* **93**, 1563–1573.
- Zurakowski, R. and Wodarz, D. (2007), ‘Model-driven approaches for in vitro combination therapy using onyx-015 replicating oncolytic adenovirus’, *Journal of Theoretical Biology* **245**(1), 1–8.

Appendix

Example for scaling analysis in Chapter 6

Step 1

$$\frac{dN}{dt} = eC - fN - pNT + \frac{p_N N I}{g_N + I}$$

$$t = 0, N = N_0$$

Step 2 & 3

$$\frac{1}{\alpha_2} \left(\frac{dN}{dt} \right)^* = eC_s C^* - fN_s N^* - pN_s T_s N^* T^* + \frac{p_N N_s N^*}{\left(\frac{g_N}{I_s I^*} + 1 \right)}$$

$$t = 0, N^* = \frac{N_0}{N_s}$$

Step 4

$$\frac{1}{\alpha_2 e C_s} \left(\frac{dN}{dt} \right)^* = C^* - \frac{f N_s}{e C_s} N^* - \frac{p N_s T_s}{e C_s} N^* T^* + \frac{p_N N_s}{e C_s} \frac{N^*}{\left(\frac{g_N}{I_s I^*} + 1 \right)}$$

$$t = 0, N^* = \frac{N_0}{N_s}$$

Step 5

$$\frac{1}{\alpha_2 e C_s} = 1 \Rightarrow \alpha_2 = \frac{1}{e C_s}$$

Similarly, it is done for other model equations. Later other scale factors are found and substituted in the model equations.

Step 6 & 7

$$\left(\frac{dN}{dt} \right)^* = C^* - \Pi_4 N^* - \Pi_5 N^* T^* + \frac{\Pi_6 N^*}{\left(\frac{\Pi_7}{I^*} + 1 \right)}$$

$$\Pi_4 = 1, \Pi_5 = 0.0219, \frac{\Pi_6}{\Pi_7 + I^*} = 0.0228$$

$$t = 0, N^* = \frac{N_0}{N_s} = \frac{N_0 \beta f}{e \alpha}$$

Publications & Presentations

Journal articles

1. Kiran, K.L., Jayachandran, D., and Lakshminarayanan, S. Mathematical modeling of avascular tumor growth based on diffusion of nutrients and its validation, **The Canadian Journal of Chemical Engineering**, 2009, 87, 732-740.
2. Kiran, K.L., and Lakshminarayanan, S. Global sensitivity analysis and model-based reactive scheduling of targeted cancer immunotherapy, **BioSystems**, 2010, 101, 117-26.
3. Kiran, K.L., Lakshminarayanan, S. Application of scaling and sensitivity analysis for tumor-immune model reduction, **Chemical Engineering Science**, 2011, 66, 5164-5172.
4. Kiran, K.L., Lakshminarayanan, S. Dosage optimization of chemotherapy and immunotherapy: In silico analysis using pharmacokinetic-pharmacodynamic and tumor growth models, 2011 (**Under review**).
5. Kiran, K.L., Lakshminarayanan, S. Population based optimal experimental design in cancer diagnosis and chemotherapy, 2011 (**Under review**).

Peer Reviewed Conference Papers

1. Kiran, K.L., Jayachandran, D., and Lakshminarayanan, S. Mechanistic modeling of avascular tumor growth, In proceedings of ADCONIP 2008, Jasper, Canada 2008.
2. Kiran, K.L., Jayachandran, D., and Lakshminarayanan, S. Multi-objective Optimization of Cancer Immuno-Chemotherapy, 13th International Conference on Biomedical Engineering, 2009, pp. 1337-1340.
3. Kiran, K.L., and Lakshminarayanan, S. Treatment planning of cancer dendritic cell therapy using multi-objective optimization, In proceedings of AD-CHEM 2009, Istanbul, Turkey 2009. (**Keynote paper**).
4. Kiran, K.L., Lakshminarayanan, S., Sundaramoorthy, S. Application of model simplification approaches for tumor-immune modeling, In proceedings of COSMA 2009, India, 2009.
5. Kiran, K.L., Kandpal, M., and Lakshminarayanan, S. Characterization of frequently sampled intravenous glucose tolerance test using scaling and sensitivity analysis of MINMOD, The 2010 International Conference on Modelling, Identification and Control (ICMIC), pp. 179-184.
6. Mai chan, L., Kiran, K. L., Lakshminarayanan, S. Data driven strategy for immunotherapy treatment planning, In proceedings of PSE ASIA 2010, Singapore, 2010 .

7. Raghuraj Rao, Kiran, K.L. and Lakshminarayanan, S. PSE techniques in metallurgical industry, In proceedings of PSE ASIA 2010, Singapore, 2010.

Conference - Oral Presentations

1. Kiran, K.L., Jayachandran, D. and Lakshminarayanan, S. Mechanistic modeling of avascular tumor growth, ADCONIP 2008, Jasper, Alberta, Canada.
2. Kiran, K.L., Jayachandran, D. and Lakshminarayanan, S. Multi-objective optimization of cancer immuno-chemotherapy, ICBME 2008, Singapore.
3. Kiran, K.L., Lakshminarayanan, S. Treatment planning of cancer dendritic cell therapy using multi-objective optimization, ADCHEM 2009, Turkey. (**Keynote paper**).
4. Kiran, K.L., Mai Chan, L., Lakshminarayanan, S. Optimization and data driven strategies for robust treatment planning of dendritic cell-interleukin therapy, AIChE Annual Meeting 2009, Nashville.
5. Kiran, K.L., Lakshminarayanan, S., Sundaramoorthy, S. Application of model simplification approaches for tumor-immune modeling, COSMA 2009, NIT Calicut, India.
6. Kiran, K.L., Manoj, K, Lakshminarayanan, S. Characterization of frequently sampled intravenous glucose tolerance test using scaling and sensitivity analysis on MINMOD, ICMIC 2010, Okayama, Japan.
7. Mai chan, L., Kiran, K. L., Lakshminarayanan, S. Data driven strategy for immunotherapy treatment planning, PSE ASIA 2010, Singapore.
8. Raghuraj Rao, Kiran, K.L. and Lakshminarayanan, S. PSE techniques in metallurgical industry, PSE ASIA 2010, Singapore.
9. Kiran, K.L., Loganathan, P., Lakshminarayanan, S. Modeling and analysis of biochemical pathways of glucose metabolism and cell cycle progression, Satellite conference of ICM-2010, Hyderabad, India.
10. Kiran, K.L., Lakshminarayanan, S. Investigation of intracellular cancerous biomarkers: *In silico* analysis, 27th HUGO-IABCR Congress 2010, Genomics, biology and breast cancer treatment, Singapore.

Conference - Poster Presentations

1. Kiran, K.L., Lakshminarayanan, S. Targeted immunotherapy for cancer and its treatment planning using multi-objective optimization, ISPE, Singapore, 2009. (Award winning poster)

CURRICULUM VITAE

NAME: KANCHI LAKSHMI KIRAN Graduate Research Scholar (PhD Student) E5-03-30, Dept. of Chemical & Biomolecular Engg. National University of Singapore Singapore - 117576	Office Phone: (65) 65165802 Hand Phone: (65) 96372987 Fax: (65) 67791936 Email: kanchi@nus.edu.sg, lakshmikirank@gmail.com
---	--

Date of birth: 4th December, 1984

Educational qualifications:

- Doctor of Philosophy, 2007 – 2011
Chemical & Biomolecular Engineering,
National University of Singapore, Singapore
- Bachelor of Engineering, 2002 – 2006
Chemical Engineering,
National institute of technology, Durgapur, India

Technical skills:

Domain: Modeling and simulation, Optimization, Data analysis, Control, Multi-variate statistics, Root cause analysis, Decision making.

Programming Languages: MATLAB, COMSOL, FORTRAN, C

Data mining tools: ACE, MARS, TREENET, Genetic Programming, NetLogo, Anylogic

Current job:

Research engineer, Energy Efficiency Research Center, Singapore Development Center, Yokogawa.

Project works:

PhD Thesis (2007-2011): *Modeling of tumor growth and optimization of therapeutic protocol design*

In this interdisciplinary research, the aim is to “develop supporting tools for oncologists in the implementation of preventive and personalized cancer therapeutic strategies” via the application of Chemical Engineering Principles and Process System Engineering techniques.

Commercial project (2008): *Optimal design of experiments for parameter estimation*

Development of a MATLAB based tool “Model Based Experimental Design (MBOED)” a project sponsored by the Centre for Development of Teaching and Learning (CDTL), NUS. Mini projects

1. *Model based studies of diagnostic protocols of diabetes (2010)*
2. *Process systems engineering in metallurgical process (2010) (in collaboration with Aqua Alloys Pvt. Ltd., India)*
3. *Optimization of radiation therapy for cancer treatment (2007)*

B.E. final year project (2006): *Pneumatic separation of coal particles*

Industrial experience:

1. Vocational training in Vizag Steel Plant, India (2005)
2. Worked as Management Trainee in Associate Cement Companies, India (2006)

Major achievements:

1. Nominated by the Faculty at NUS to participate in the 7th Global Student Forum on Engineering Education, Singapore (2010)
2. Shortlisted for advanced professional degree (APD) event organized by McKinsey & company, Singapore (July, 2010)
3. Won 3rd Prize in International Society for Pharmaceutical Engineering’s student poster competition , Singapore (June, 2010)
4. Won the “Leadership Award” for organizing ChemBiotech’ 09-10 (An international conference on Chemical and Biomolecular Engineering) , Singapore
5. Delivered an invited lecture on “Application of Modeling and Optimization Strategies for Tumor Growth and Development of Therapeutic Interventions ” at Vanderbilt Ingram Cancer Centre, Vanderbilt University, Tennessee (November, 2009)
6. Keynote paper presentation at ADCHEM 2009, Turkey
7. Graduate Research Scholarship from Singapore Government (2007-2011)
8. 96.26 percentile in GATE- Graduate Aptitude Test in Engineering (**Top 5%**), India (2005)
9. 2nd prize in paper presentation in National level tech festival, NIT, Durgapur (2006)
10. Ranked in the **top 1%** in the competitive exam (EAMCET) , India (2002)
11. Mathematics topper in 10th board exams, India (2000)

Responsible roles:

Teaching assistantship

1. Tutorship for Process modeling and numerical simulation (CN 3421) (2007)
2. Training students to learn MATLAB (CN 5010) (2008-2010)
3. Tutor and grader for Data based process characterization (CN 4245R) (2009)

Extra curricular activities

1. Student representative for Engineering Postgraduate Council (2010)
2. Student member of American Institute of Chemical Engineers (2008-2011)
3. International Society for Pharmaceutical Engineering (ISPE), Singapore (2010-2011)
4. President of Graduate Student's Association (2009-10)
5. President, ChemBiotech' 09-10, Singapore
6. Student organizer for the international conference, PSE ASIA, Singapore (2010)
7. ISTE - Indian Society for Technical Education (2002-2006), NIT, Durgapur
8. CHESS- Chemical Engineering Student's Society (2002-2006), NIT, Durgapur
9. CCA- Centre for Cognitive Activities (2002-2006), NIT, Durgapur
10. Representative of Training and Placement Student's Work (2002-2006)

References:

Assoc. Prof. Lakshminarayanan S

Blk E4, 4 Engineering Drive 4, #06-05, Singapore 117576
Department of Chemical & Biomolecular Engineering
National University of Singapore, Singapore
Tel:(65) 65168484 Email: chels@nus.edu.sg

Prof. Farooq Shamsuzzaman

Blk E5, 4 Engineering Drive 4, #02-26, Singapore 117576
Department of Chemical & Biomolecular Engineering
National University of Singapore, Singapore
Tel: (65) 65166545 Email: chesf@nus.edu.sg

Prof. Rangaiah Gade Pandu

Blk E5, 4 Engineering Drive 4, #02-25, Singapore 117576
Department of Chemical & Biomolecular Engineering
National University of Singapore, Singapore
Tel: (65) 65162187 Email: chegpr@nus.edu.sg

Dr. Rao Raghuraj

Vice President-operations

Aqua Alloys Pvt. Ltd.

Sanmati Bldg, Sadashiv Nagar, Belgaum, Karnataka

India - 590 009 Mobile: 9243209569

Email: raoraghuraj@gmail.com